UNIVERSITAT POLITÈCNICA DE VALÈNCIA

Departamento de Máquinas y Motores Térmicos

DOCTORAL THESIS:

"Experimental characterisation of real driving cycles in diesel passenger vehicles under different environmental conditions"

Presented by: D. Fernando Redondo Puelles
Supervised by: Dr. José Manuel Luján Martínez

in fulfillment of the requirements for the degree of

Doctor of Philosophy

Valencia, May 2023

Doctoral Thesis

"Experimental characterisation of real driving cycles in diesel passenger vehicles under different environment conditions"

Presented by: D. Fernando Redondo
Supervised by: Dr. D. José Manuel Luján Martínez

THESIS EXAMINERS

Dr. D. Pablo Fernández-Yáñez Luján
Dr. D. José Martín Herreros Arellano
Dr. D. Xavier Tauzia

DEFENSE COMMITTEE

Chairman: Dr. D. Jaime Martín Díaz
Secretary: Dr. D. Francisco Vera García
Member: Dr. D. José Martín Herreros Arellano

Valencia, May 2023

Abstract

The future of Internal Combustion Engines in the automotive sector seems uncertain, to some extent, due to the recent changes in type approval regulations. Current regulations have considerably reduced the engine pollutant emissions limits, as well as introduced more demanding testing conditions. The introduction of real driving cycles presented a challenging issue for car manufacturers when homologating their vehicles, since the traditional and undemanding New European Driving Cycle (NEDC) certification cycle has been replaced by more severe cycles such as World Light-Duty Test Cycle (WLTC) and Real Driving Emissions (RDE).

This study, in the first place, presents a methodology for implementing RDE cycles in an engine test bench. Even knowing that the essence of RDE regulation is to assess actual driving conditions, reproducing RDE cycles in a test bench is of great interest since, the controlled and reproducible conditions that can be achieved in a laboratory lead to valuable information to understand engine behaviour in real driving conditions, and therefore contribute to engine development. This document applies the most recent European Community regulation and sets the essential steps to carry out an RDE cycle in an engine test bench.

Secondly, as the feasibility of a test bench to perform RDE cycles has been proven, different RDE cycles have been performed under different dynamic solicitations and external conditions such as ambient or intake air temperatures. After that, the pollutant's emission and fuel mass consumption were analysed with the aim of characterising RDE cycles and conditions.

Furthermore, a comparison of RDE test emissions and fuel consumption versus those obtained from steady-state tests has been carried out, where very small discrepancies were found.

Keywords: RDE; Pollutants; Engines; Regulation; Test bench

Resumen

El futuro de los Motores de Combustión Interna en el sector de la automoción parece incierto, en cierta medida, debido a los cambios recientes en las normativas de homologación. Las regulaciones actuales han reducido considerablemente los límites de emisiones contaminantes , así como también han introducido pruebas más exigentes. La introducción de ciclos de conducción reales supuso un reto para los fabricantes de automóviles a la hora de homologar sus vehículos, ya que el tradicional y poco exigente ciclo de certificación del New European Driving Cycle (NEDC) ha sido sustituido por ciclos más severos como el World Light-Duty Test Cycle (WLTC) y Real Driving Emissions (RDE).

Este estudio, en primer lugar, presenta una metodología para implementar ciclos RDE en un banco de ensayos de motores. Aun sabiendo que la esencia de la regulación RDE es evaluar las condiciones reales de conducción, reproducir los ciclos RDE en un banco de pruebas es de gran interés ya que las condiciones controladas y reproducibles que se pueden lograr en un laboratorio aportan información valiosa para entender el comportamiento del motor en conducción real, y por lo tanto contribuyen al desarrollo del motor. Este documento aplica la normativa más reciente de la Comunidad Europea y establece los pasos imprescindibles para realizar un ciclo RDE en un banco de pruebas de motores.

En segundo lugar, gracias a que se ha demostrado la viabilidad de una sala de pruebas para realizar ciclos RDE, se han realizado diferentes ciclos RDE bajo diferentes solicitaciones dinámicas y condiciones externas como temperatura ambiente o temperatura del aire de admisión. Posteriormente, se analizó la emisión de contaminantes y el consumo de combustible con el fin de caracterizar los ciclos y condiciones de RDE.

Además, se ha llevado a cabo una comparación de las emisiones y el consumo de combustible de las pruebas RDE frente a las obtenidas en las pruebas de estado estacionario, donde se encontraron discrepancias bastante bajas.

Resum

El futur dels Motors de Combustió Interna al sector de l'automoció sembla incert, en certa mesura, a causa dels canvis recents a les normatives d'homologació. Les regulacions actuals han reduït considerablement els límits d'emissions contaminants i també han introduït proves més exigents. La introducció de cicles de conducció reals va suposar un repte per als fabricants d'automòbils a l'hora d'homologar els seus vehicles, ja que el tradicional i poc exigent cicle de certificació del New European Driving Cycle (NEDC) ha estat substituït per cicles més severs com el World Light-Duty Test Cycle (WLTC) i Real Driving Emissions (RDE).

Aquest estudi, en primer lloc, presenta una metodologia per implementar cicles RDE a un banc d'assajos de motors. Tot i saber que l'essència de la regulació RDE és avaluar les condicions reals de conducció, reproduir els cicles RDE en un banc de proves és de gran interès ja que les condicions controlades i reproduïbles que es poden aconseguir en un laboratori aporten informació valuosa per entendre el comportament del motor en conducció real, i per tant contribueixen al desenvolupament del motor. Aquest document aplica la normativa més recent de la Comunitat Europea i estableix els passos imprescindibles per fer un cicle RDE en un banc de proves de motors.

En segon lloc, gràcies al fet que s'ha demostrat la viabilitat d'una sala de proves per fer cicles RDE, s'han realitzat diferents cicles RDE sota diferents sol · licitacions dinàmiques i condicions externes com ara temperatura ambient o temperatura de l'aire d'admissió. Posteriorment, es va analitzar l'emissió de contaminants i el consum de combustible per tal de caracteritzar els cicles i les condicions de RDE.

A més, s'ha dut a terme una comparació de les emissions i el consum de combustible de les proves RDE davant de les obtingudes a les proves d'estat estacionari, on es van trobar discrepàncies força baixes.

List of publications

This thesis is based on the work contained in the following papers:

[1] J. M. Luján, V. Bermudez, B. Pla, and F. Redondo. "Engine test bench feasibility for the study and research of real driving cycles: Pollutant emissions uncertainty characterization". *International Journal of Engine Research* 0(0) (2021), p. 0. DOI: 10.1177/14680874211007999

[2] J. M. Luján, H. Climent, S. Ruiz, and F. Redondo. "Analysis of pollutant emissions and fuel consumption, during real driving cycles in different intake temperature scenarios". *Proceedings of the Institution of Mechanical Engineers, Part D: Journal of Automobile Engineering* 0(0) (2022), p. 0. DOI: 10.1177/09544070221078402

[3] J. M. Luján, P. Piqueras, J. de la Morena, and F. Redondo. "Experimental Characterization of Real Driving Cycles in a Light-Duty Diesel Engine under Different Dynamic Conditions". *Applied Sciences* 12(5) (2022). DOI: 10.3390/app12052472

Division of work between authors

The work leading up to this thesis was done in collaboration with other researchers.

Acknowledgments

In the first place, I wish to thank Dr. José Manuel Luján Martínez for sharing his great knowledge, and for his patience and guidance through the sinuous path that has been this thesis.

Of course, to my parents for the values and education that you have given to me, your advice and big support, and my sister that always had been there when I have needed it since I started my university career.

And, thanks to Ale for your constant love, optimism, and support, knowing how to cheer me up in bad times. Without you I am completely sure that it would not have been possible.

Valencia, 2023.

"Life is too short to do the things you don't love doing."

Bruce Dickinson.

Contents

List of Tables

List of Figures

List of symbols

Latin characters

A	Frontal area	m^2
F_{Aero}	Aerodynamic resistance force	N
$F_{Rolling}$	Rolling resistance force	N
g	Gravity acceleration	m/s^2
i	nº of combustion per revolution and cylinder in a for stroke engine	
kw	Wet-dry correction factor	
L	Measurig length	m
M	Mass	kg
MM	Molecular weight	$kg \cdot mol^{-1}$
N	Opacity	%
n	Engine speed	rpm
P	Power	kW
$P2$	Oulet compressor pressure	bar
$P2'$	Oulet WCAC pressure	bar
$P3$	Inlet turbine pressure	bar
R^2	Coefficient of determination. R-squared	
$T2'$	Outlet WCAC temperature	$°C$
$T2''$	Intake manifold temperature	$°C$
$T3$	Inlet turbine temperature	$°C$
v	Vehicle speed	km/h
$Vol.eff$	Volumetric efficiency	%
z	Numbers of cylinders	

Greek characters

α	Road grade	°
ϵ	Error relative	%
μ	Rolling coefficient	%
ρ	Density	$kg \cdot m^{-3}$
σ	Standard deviation	

Acronyms

AFR	Air-Fuel Ratio
AMF	Air Mass Flow
AQI	Air Quality Index
CF	Conformity Factor
CI	Compression ignition
CO	Carbon Monoxide
CO_2	Carbon Dioxide
CVS	Constant Volume Sampler
DOC	Diesel Oxidation Catalyst
DPF	Diesel Particulate Filter
ECU	Engine Control Unit
EEA	European Environment Agency
ECU	Engine Control Unit
EGR	Exhaust Gas Recirculation
FMF	Fuel Mass Flow
GHG	Greenhouse Gases
GPS	Global positioning system
HCLD	Heated Chemiluminescent Detector
HFID	Heated Flame Ionization Detector
HP	High Pressure
ICCT	Internacional Council on Clean Transportation
IEA	Internation Energy Agency
JRC	Joint Research Centre-Institute for Energy
LNT	Lean NO_X Trap
LP	Low Pressure
MAW	Mobil Average Windows
NEDC	New European Driving Cycle
NID	Nondispersive Infrared Detector
NIST	National Institute of Standards and Technology
NMVOC	Non-Methane Volatile Organic Compounds
NO_2	Nitrogen Dioxide
NO_X	Nitrogen Oxides
NTE	Not To Exceed
O_3	Ozone
OICA	International Organization of Motor Vehicle Manufacturers
PB	Power Binning
PEMS	Portable Emissions Measurement System

PI	Provocated Ignition
PM	Particulate Mass
RDE	Real Driving Emissions
RF	Result Evaluation Factor
SCR	Selective Catalyst Reductor
SO_2	Sulphur Dioxide
SO_X	Sulphur Oxides
THC	Total Hydrocarbons
UN	United Nations
WCAC	Water Charge Air Cooler
WHO	World Health Organization
WLTC	World Light-Duty Test Cycle

Chapter 1

Introduction

Contents

1.1 Motivation

The world's light-duty vehicle fleet has considerably increased during the last decades. Currently, there are more than 1.2 billion vehicles in the world, according to the International Organization of Motor Vehicle Manufacturers (OICA) http://www.oica.net/category/vehiclesin-use/). Adding that the world population could be increased to more than 11 billion in 2100, according to the United Nations (UN) [4], and the development of countries such as China and India (Global Economic Prospects, World Bank Group) [5], the number of vehicles will continue rising.

Most of these vehicles are equipped with internal combustion engines that use fossil fuels as their primary energy source. In addition, despite the number of electric vehicles has increased in recent years, achieving a share of 5.1 million in the world according to the International Energy Agency (IEA)[6], they only represent 0.4% of the total. Furthermore, the internal combustion engines will have significant importance in the ecological transition in the following decades, improving their efficiency and incorporating hybrid solutions [7].

Currently, one of the biggest concerns in the world is air quality. Many of the largest cities have implanted different regulations, especially to ban the circulation of older vehicles and reduce as much as possible pollutant emissions. These restrictions were applied due to poor air quality, as reported in 2019 by the European Environment Agency (EEA) [8]. The 2020 report [9] points to significant reductions in emissions of air pollutants, particularly from road transport, aviation and international shipping but mainly due to the lockdown actions introduced by most of the European countries to reduce transmission of COVID-19. The EEA considers air quality through the parameter known as Air Quality Index (AQI) (https://www.eea.europa.eu/themes/air/air-quality-index). To calculate this parameter, it is necessary to consider the hourly concentrations of the polluting substances as ozone (O_3), particulate mass (PM), carbon monoxide (CO), sulfur dioxide (SO_2), and nitrogen dioxide (NO_2).

Actually, according to EEA [9], road transport is not the main and only responsible for air pollution, as shown in the figure 1.1. (Percentages shown in the figure belong to emission contribution from road transport).

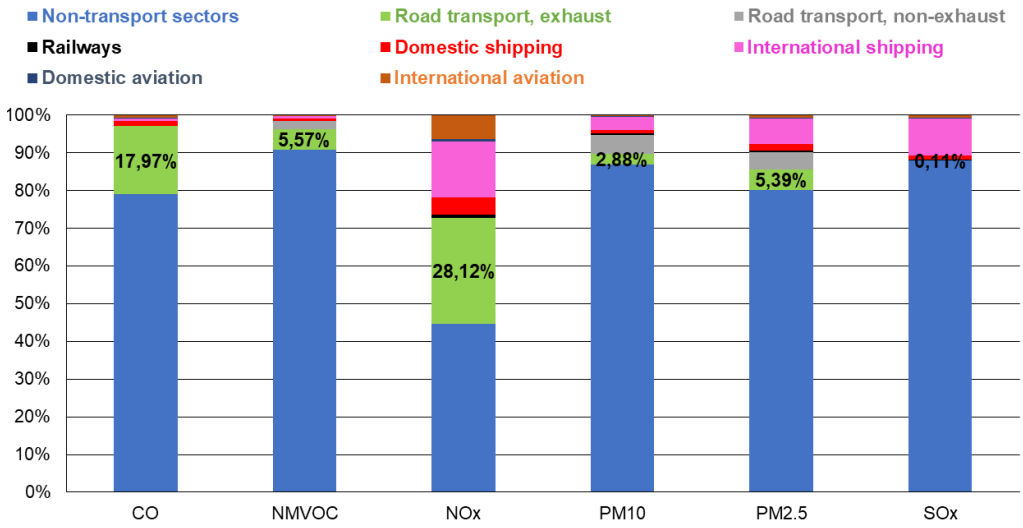

Figure 1.1: Pollutants emissions contribution of each sector. *CO*, Non-methane volatile organic compounds (NMVOC), Nitrogen oxides (NO_X), Particle matter smaller than 2.5μm (PM_{10}), Particle matter smaller than 2.5μm ($PM_{2.5}$) and Sulphur oxides (SO_X).

Furthermore, as stated by the EEA source, [10], air pollutants emissions trends from transport are downward, as shown in the figure 1.2.

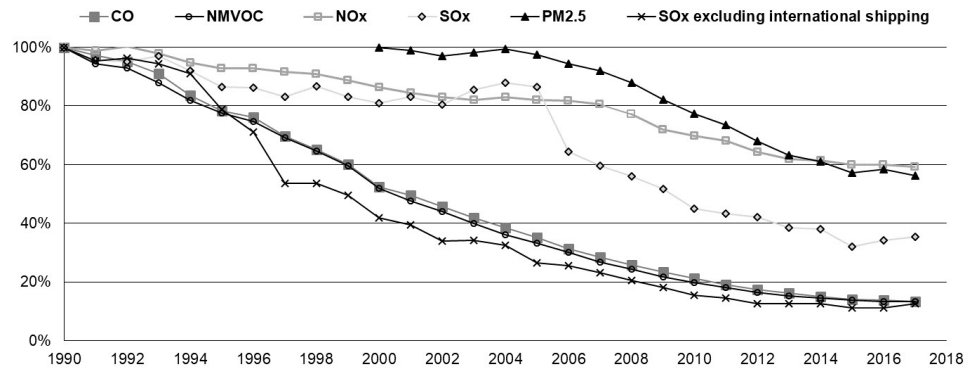

Figure 1.2: Trend pollutant emissions from transport. CO, NMVOC, NO_X, SO_X, $PM_{2.5}$

This reduction is attributable to substantial anti-pollution regulations that have taken place during the last years. However, the previous European regulations have not managed to preserve good air quality, as some studies point out [11] [12]. In addition, vehicles increase their polluting emissions as their age and mileage increase [13].

Nowadays, car manufacturers' efforts are principally focused on decreasing pollutant emissions through different actives, and passives systems [14] [15].

Besides this, there is the problem of greenhouse gas emissions culprits of climate change. Nowadays, the world is facing the impact of climate change, being the last six years the warmest on record [16]. To achieve the challenges proposed in the climate change conference held in Paris 2015 [17], the concept of carbon footprint is of great importance, especially for greenhouse gasses (GHG) emissions management [18]. Significant developments in renewable energies [19] have been done to reduce GHG emissions, although additional efforts are required from critical sectors like transportation.

GHG emissions have no boundaries. In other words, the entire planet is affected if they are emitted in any part of the world. Internal combustion engines that work with fossil or hydrocarbon fuels, during the combustion, emit Carbon Dioxide (CO_2) gases as equation 1.1 shows. In sum, more fuel consumption involves more CO_2 emissions.

$$C_nH_{2n+2} + O_2 \rightarrow CO_2 + H_2O \tag{1.1}$$

CO_2 emission comes from total transport representing a 24% in 2019 according to the International Energy Agency (IEA) [20]. Road vehicles like cars, trucks, buses and, two and three-wheelers contribute to nearly three-quarters of transport CO_2 emissions, which involves around 18% of the total CO_2 emissions. In this regard, the European Union has established stringent standards, reflected in the 443/2009 [21] regulation. This directive specifies that the EU fleet-wide average emission target for new cars must be 95gCO2/km from 2021. Later on, the European Union decided to reduce this limit by an additional 15% from 2025 and 37.5% from 2030 through regulation 2019/631 [22].

Moreover, the well-known trade-off between NO_X and CO_2 emissions represents a significant inconvenience when using different pollutant emissions control as Exhaust Gases Recirculation (EGR) systems impair the combus-

tion process or aftertreatment systems, increasing engine backpressure and subsequently pumping losses. Nowadays, car manufacturers have made their utmost efforts to reduce pollutant emissions and improve the engine's performance. They are pretty complex to fulfil both purposes since, often, the improvement of one makes the others worse.

The spark ignition engine can reduce their gaseous pollutant emissions with a unique device, the three-way catalytic converter. However, the issue with diesel engines is harder to solve. In this engine, Total Hydrocarbons (THC) and CO emissions can be reduced with the diesel oxidation catalyst, commonly used in this kind of engine. Particulates can also be reduced through combustion systems improvement, mainly with sophisticated injection systems. In addition, diesel engines are equipped with particulate filters.

Nevertheless, NO_X emissions are hard to solve. Although EGR systems are fully implemented in diesel engines reducing significantly NO_X emissions at the combustion chamber, exhaust NO_X emissions are still important. Two different technologies, Lean NO_X Trap (LNT) and Selective Catalyst Reduction (SCR), are currently used to reduce NO_X emissions.

In the second half of the twentieth century, the research community pointed out the negative impacts of the engine's exhaust gases. These gases affect humans and the environment. The adverse effects are greatly appreciated in big cities with traffic jam problems. Poor air quality is a big issue for human health. It is estimated that approximately 3% of cardiopulmonary and 5% of lung cancer deaths are attributable to PM globally, according to the World Health Organization (WHO) [23]. The first regulation restricting the emissions of pollutant gases was established in California in the 60s[24]. Years later, the first pollutant emissions regulation for vehicles appeared in Europe, known as EURO 1 regulation [25]. Its first version was introduced in 1992 by delimiting the emissions of NO_X, THC, CO, and PM. To certify that the limits of each one of these substances had been accomplished, the NEDC type approval cycle was established in 2000 [26].

This cycle has to be performed in a rolling test cell facility. Over the years, the limits of each of these substances have been reduced [27], with the final purpose that car manufacturers design engines committed to the environment and human health. The fulfilment of these limits was verified with the NEDC. However, the NEDC became questioned years later since, it is an undemanding cycle for current engines and vehicles, whose power and

performance have increased over the years. Consequently, the type approval emissions have been strongly reduced during the last years, as can be observed in the table 1.1, whereas real driving emissions have decreased only by 40% on average between Euro3 and Euro6 [28]. In other words, real driving emissions are substantially higher than emissions under type approval conditions, with variable factors from 4 to 10 times depending on the source [29].

	Date	CO **[g/km]**	NO_X **[g/km]**	PM **[g/km]**	$THC + NO_X$ **[g/km]**
Euro 1	Jul-92	2.72	-	0.14	0.97
Euro 2	Jan-96	1	-	0.08	0.9
Euro 3	Jan-00	0.64	0.5	0.1	0.56
Euro 4	Jan-05	0.5	0.25	0.05	0.3
Euro 5	Sep-09	0.5	0.18	0.05	0.23
Euro 6	Sep-14	0.5	0.08	0.05	0.17
Reduction from Euro1 to Euro6*		-81.6%	-84%	-64.3%	-82.5%

Table 1.1: Pollutant vehicle emissions from Euro 1 to the last Euro 6. *In the case of NO_X, since, the first limit was established (Euro 3).

This situation was known by the European Union a long time ago, and there are reports, such as the report drawn up by the Joint Research Centre-Institute for Energy (JRC), an Institute depending on the European Commission [30]. Other reports elaborated by independent organizations such as the International Council on Clean Transportation (ICCT) [31] and [32] arrive to similar conclusions.

These issues were revealed after the "diesel gate" scandal [33], finding out that most of the vehicles, not only Volkswagen cars, widely surpassed the emission limits the regulation imposed when driving in the street. Consequently, NO_X and particle concentrations are higher than recommended, especially in big cities subject to dense traffic [8]. To solve it during the following years, the vehicle manufacturers and owners had to suffer several costs to deal with and repair this issue [34].

In this respect, the European Commission drafted a report about the automobile emissions measurement, finding significant differences between emis-

sions in the NEDC and road emissions, blaming manufacturers for this fact [35].

To cope with this situation, the European Commission recently established a relevant modification concerning evaluating pollutant emissions limits. This modification consists of the implantation of two news cycles, WLTC and RDE, described for the first time in the regulation in 2016 [36]. The WLTC is performed in a chassis dynamometer, as well as NEDC, but with different characteristics and requirements [37] [38].

The WLTC was obtained from "real world" driving data [39], and its conditions are more demanding than NEDC [40], not only due to the higher duration but also to the higher power needed to follow the speed profile as a consequence of more aggressive accelerations and a higher percentage of the cycle with high speeds. These requirements extend the engine operating map, giving emission information in a wider operation zone including high load conditions[41] [42], where the emissions can widely differ [43].

On the other hand, the European Regulation [36] introduced the RDE as a method to assess vehicle emissions during real driving conditions. In order to register pollutant emissions, a Portable Emissions Measure System (PEMS) must be used [44] [45].

The RDE regulation establishes many conditions and restrictions to perform a valid RDE cycle. However, different cycle alternatives and routes are infinite. Those cycles can have diverse dynamic conditions with the same car, and therefore different pollutant emissions and fuel consumption can be obtained, which affects when the homologation of the vehicle is carried out.

Due to the complexity of RDE cycles that establishes the regulation with all the restrictions and guidelines, performing valid RDE cycles may be an arduous task, since, during the conduct of the test, it may be aborted due to deviations from the admitted range in the operating conditions or even, after finishing it, when the data will be processed, realise that the cycle is not valid.

1.2 Background

Several fields of study have been explored for considering a full view of a study carried out in this work. The highlighted investigations are described next.

Nowadays, research works optimise different control systems and strategies that minimise the fuel consumption and emissions of the engines in transient evolutions. In general, these strategies are applied to the precisely defined cycles as the WLTC, reaching very satisfactory results that, in many cases, are validated with tests in experimental laboratory facilities (rolling test benches or engine test cells) [46, 47]. There are also many publications in which these results are obtained by simulation, which entails a substantial cost reduction compared to physical vehicle testing [48] [49] [50].

However, it is not easy to carry out these validations for real driving situations, where it is necessary to reproduce specific engine operating conditions on the road. Another problem is the lack of repeatability found on road cycles. If the driver changes, significant dynamical differences can be found [51]. Even if on-road cycles try to be repeated with the same driver and conditions, issues can spoil the test (Diesel particulate filter (DPF) regeneration, traffic jams...). Testing on-road cycles, even following the same route, has great NOx emissions dispersion [52], with final emissions differences higher than 24% [53]. Furthermore, PEMS has smaller precision than stationary laboratory equipment [54]. Consequently, transporting the RDE conditions to an engine test bench could greatly help engine calibration and research and development tasks [55].

1.3 Objetives

Reproducing RDE cycles under controlled conditions in the laboratory is a challenge that the different research groups have considered [56]. An option to mitigate the repeatability problem is to transfer the dynamic conditions obtained in an RDE cycle done on road with a PEMS to an engine test bench, so although finally, it is necessary to perform the RDE on-road, reproducing its conditions to a test bench could help to many developments works [57].

Implementing these real driving conditions in an engine test bench environment is possible thanks to the software's capacity to simulate driving conditions. So, reproducing the RDE test in an engine test bench allows to, after comparing the obtained results with those in the real route, take profit of the test bench higher instrumentation and control capabilities to get accurate results that assess the performance of the engine and allow to carry out specific studies aimed to improve the engine performance in this particular

route.

After that, comparatives, or many parametric studies in the same RDE cycle, can be done without being affected by traffic and climatology conditions or driving behaviour. Using this methodology, studies aimed at reducing pollutants emissions and fuel consumption can be entirely performed with accuracy guarantees. For instance, implementing new driving behaviour strategies, engine control, trying different engine components, bodyworks with better drag coefficient or climatic conditions studies, tasks are already done in WLTC, and NEDC cycles [58].

This thesis's first objective is to analyse the RDE regulation and the characteristics of this type of cycle to study the viability later and assess the uncertainty of transporting and performing RDE cycles with its complex features in an internal combustion engine test bench.

Test benches have been traditionally used to test engines under several stationary or transient conditions. Still, works on determining the variability of measurements before complete RDE cycles have not been found in the literature. These cycles, due to their long duration, as well as their range of use of the engine, and the numerous and rapid transient evolutions to which the engine is subjected, force the engines to behave in a non-repetitive way (mainly due to non-repetitive control actions of systems such as turbocharger, EGR or injection systems). So, it has been considered to quantify and limit these discrepancies to rigorously determine the improvements that can be obtained from the engines, due to the changes in their components or control strategies.

To make this possible, the repeatability and reproducibility of real-world conditions, such as RDE cycles in an engine test bench, have been studied. Hence, it is also crucial to consider the accuracy and uncertainty of all the measurement systems used.

The analysis of RDE cycles will help to assess the uncertainty in the main variables measured in the engine test bench, such as pressures, temperatures, mass flows, pollutant emissions, etc., in a driving cycle. All the improvements that could have been found in the research work carried out in the test cell, will be finally confirmed on the route.

A second objective is to analyse different RDE cycles with different dynamic solicitations and driver behaviour and check how engine efficiency and polluting emissions are affected. Furthermore, an analysis of the polluting

emissions from the RDE tests versus those extracted from steady-state tests was carried out.

The last objective of the thesis is to study the influence of intake manifold and ambient temperatures on pollutant emissions and fuel consumption in a diesel engine under RDE conditions. The intake manifold temperature change could be produced for two different reasons, first, due to an improvement in the efficiency of the Water Charger Air Cooler (WCAC), whose aim is to lower the intake air temperature upstream of the combustion chamber, to grow air density and thus increase air mass flow, the other reasonable reason that can explain a change in the intake temperature would be a different ambient temperature, a fact that will be more studied in more detail thanks to the installation of the engine in a climatic test bench. The analysis under different ambient temperature scenarios involves incurring extended regulation conditions, where the European regulation changes since, the engine can drastically change its behaviour and polluting emissions.

1.4 Thesis outline

Considering this introduction as Chapter 1, subsequent chapters are organised as follows.

In the first place, the current RDE regulation is described in Chapter 2. After that, the engine test bench feasibility for the research and study of real driving cycles will be proved.

The pollutant emission uncertainty characterisation of RDE is analysed in Chapter 3.

In Chapter 4, the different RDE cycles will be analysed under different dynamics solicitations and driver behaviours, where it can be affirmed how very different RDE cycles can be considered valid and significant polluting emissions dispersion can be found.

Chapter 5 reports a study where different RDE tests were carried out under different air intake and ambient temperatures, where the polluting emissions and fuel consumption are analysed, and how the European regulation influences the accounting of emissions.

Finally, the findings and contributions, as well as limitations and suggestions for future studies, are summarised in Chapter 6 of the thesis.

Chapter 1 Bibliography

[4] *World population prospects*. Vol. volume II. demographic profiles, 2019 (cit. on p. 2).

[5] *World Bank Group*. 2020 (cit. on p. 2).

[6] *Global EV Outlook 2019*. 2019 (cit. on p. 2).

[7] R. D. Reitz et al. "IJER editorial: The future of the internal combustion engine". *International Journal of Engine Research* 21(1) (2020), pp. 3–10. DOI: 10.1177/1468087419877990 (cit. on p. 2).

[8] EEA. *Air quality in Europe—2019 report*. 2019 (cit. on pp. 2, 6).

[9] A. Ortiz and C. Guerreiro. *Air Quality in Europe - 2020 report*. Nov. 2020. DOI: 10.2800/786656 (cit. on p. 2).

[10] *National emissions reported to the Convention on Long-range Transboundary Air Pollution (LRTAP Convention)*. 2020 (cit. on p. 3).

[11] N. Hooftman, M. Messagie, J. Van Mierlo, and T. Coosemans. "A review of the European passenger car regulations – Real driving emissions vs local air quality". *Renewable and Sustainable Energy Reviews* 86 (2018), pp. 1–21. ISSN: 1364-0321. DOI: https://doi.org/10.1016/j.rser.2018.01.012. URL: https://www.sciencedirect.com/science/article/pii/S1364032118300182 (cit. on p. 4).

[12] G. P. Chossière, R. Malina, F. Allroggen, S. D. Eastham, R. L. Speth, and S. R. Barrett. "Country- and manufacturer-level attribution of air quality impacts due to excess NOx emissions from diesel passenger vehicles in Europe". *Atmospheric Environment* 189 (2018), pp. 89–97. ISSN: 1352-2310. DOI: https://doi.org/10.1016/j.atmosenv.2018.06.047. URL: https://www.sciencedirect.com/science/article/pii/S1352231018304382 (cit. on p. 4).

[13] L. Hao, Z. Zhao, H. Yin, J. Wang, L. Li, W. Lu, Y. Ge, and Åke Sjödin. "Study of durability of diesel vehicle emissions performance based on real driving emission measurement". *Chemosphere* 297 (2022), p. 134171. ISSN: 0045-6535. DOI: https://doi.org/10.1016/j.chemosphere.2022.134171. URL: https://www.sciencedirect.com/science/article/pii/S0045653522006646 (cit. on p. 4).

[14] M. Lapuerta, Ángel Ramos, D. Fernández-Rodríguez, and I. González-García. "High-pressure versus low-pressure exhaust gas recirculation in a Euro 6 diesel engine with lean-NOx trap: Effectiveness to reduce NOx emissions". *International Journal of Engine Research* 20(1) (2019), pp. 155–163. DOI: 10.1177/1468087418817447. eprint: https://doi.org/10.1177/1468087418817447. URL: https://doi.org/10.1177/1468087418817447 (cit. on p. 4).

[15] A. van Niekerk, B. Drew, N. Larsen, and P. Kay. "Impact of low NOx strategies on holistic emission reduction from a CI engine over transient conditions". *International Journal of Engine Research* 22(11) (2021), pp. 3286–3299. DOI: 10.1177/1468087420973887. eprint: https://doi.org/10.1177/1468087420973887. URL: https://doi.org/10.1177/1468087420973887 (cit. on p. 4).

[16] *Provisional Report. World Meteorological Organization (WMO).* 2020 (cit. on p. 4).

[17] *Center for Climate and Energy Solutions. Outcomes of the UN climate change conference in Paris. In: 21st session of the conference of the parties to the United Nations framework convention on climate change (COP 21).* 2015 (cit. on p. 4).

[18] P. D. A. M. and P. J.S. "The Development of Motor Vehicle Exhaust Emission Standards in California.Carbon footprint: current methods of estimation." *Environ Monit Assess* 178 (2011), pp. 135–160. DOI: https://doi.org/10.1007/s10661-010-1678-y (cit. on p. 4).

[19] *Energy Technology Perspectives 2014.* 2014. URL: https://www.iea.org/reports/energy-technology-perspectives-2014 (cit. on p. 4).

[20] *Global EV Outlook 2019.* Paris, 2019. URL: https://www.iea.org/reports/global-ev-outlook-2019 (cit. on p. 4).

[21] *Regulation (EC) No 443/2009 of the European Parliament and of the Council of 23 April 2009 setting emission performance standards for new passenger cars as part of the Community's integrated approach to reduce CO 2 emissions from light-duty vehicles.* 2009. URL: http://data.europa.eu/eli/reg/2009/443/oj (cit. on p. 4).

[22] *Regulation (EU) 2019/631 of the European Parliament and of the Council of 17 April 2019 setting CO2 emission performance standards for new passenger cars and for new light commercial vehicles, and repeal-*

ing Regulations (EC) No 443/2009 and (EU) No 510/2011. 2019. URL: http://data.europa.eu/eli/reg/2019/631/oj (cit. on p. 4).

[23] *Health effects of particulate matter*. 2013 (cit. on p. 5).

[24] J. A. Maga and G. C. Hass. "The Development of Motor Vehicle Exhaust Emission Standards in California". *Journal of the Air Pollution Control Association* 10(5) (1960), pp. 393–414. DOI: 10.1080/00022470.1960.10467949 (cit. on p. 5).

[25] *Council Directive 91/441/EEC of 26 June 1991 amending Directive 70/220/EEC on the approximation of the laws of the Member States relating to measures to be taken against air pollution by emissions from motor vehicles*. 1991 (cit. on p. 5).

[26] *Directive 98/69/EC of the European Parliament and of the Council of 13 October 1998 relating to measures to be taken against air pollution by emissions from motor vehicles and amending Council Directive 70/220/EEC*. 1998 (cit. on p. 5).

[27] G. Fontaras and P. Dilara. "The evolution of European passenger car characteristics 2000–2010 and its effects on real-world CO2 emissions and CO2 reduction policy". *Energy Policy* 49 (2012). Special Section: Fuel Poverty Comes of Age: Commemorating 21 Years of Research and Policy, pp. 719–730. ISSN: 0301-4215. DOI: https://doi.org/10.1016/j.enpol.2012.07.021 (cit. on p. 5).

[28] M. Weiss, P. Bonnel, R. Hummel, U. Manfredi, R. Colombo, G. Lanappe, P. Lelijour, and M. Sculati. "Analyzing on-road emissions of light-duty vehicles with Portable Emissions Measurement Systems (PEMS)". *JRC Scientific and Technical Reports* (2011) (cit. on p. 6).

[29] L. Pelkmans and P. Debal. "Comparison of on-road emissions with emissions measured on chassis dynamometer test cycles". *Transportation Research Part D: Transport and Environment* 11(4) (2006), pp. 233–241. ISSN: 1361-9209. DOI: https://doi.org/10.1016/j.trd.2006.04.001 (cit. on p. 6).

[30] R. Suarez Bertoa, M. Astorga-Llorens, V. Franco, Z. Kregar, V. Valverde Morales, M. Clairotte, J. Pavlovic, and B. Giechaskiel. "On-road vehicle emissions beyond RDE conditions, EUR 29905 EN". *Publications Office of the European Union* (2011). DOI: 10.2760/214318 (cit. on p. 6).

[31] V. Franco, F. P. Sánchez, J. German, and P. Mock. "Real-world exhaust emissions from modern diesel cars". *communications* 49(30) (2014), pp. 847129–102 (cit. on p. 6).

[32] U. Tietge, P. Mock, N. Zacharof, and V. Franco. "Real-world fuel consumption of popular European passenger car models". *The international council of clean transportation (ICCT)* (2015) (cit. on p. 6).

[33] *Diesel gate: Who? What? How?* September, 2016. URL: //www.transportenvironment.org/sites/te/files/2016_09_Dieselgate_report_who_what_how_FINAL_0.pdf (cit. on p. 6).

[34] F. Baumgärtner and P. Letmathe. "External costs of the Dieselgate – Peccadillo or substantial consequences?" *Transportation Research Part D: Transport and Environment* 87 (2020), p. 102501. ISSN: 1361-9209. DOI: https://doi.org/10.1016/j.trd.2020.102501. URL: https://www.sciencedirect.com/science/article/pii/S136192092030688X (cit. on p. 6).

[35] *REPORT on the inquiry into emission measurements in the automotive sector(2016/2215(INI)) Committee of Inquiry into Emission Measurements in the Automotive Sector*. A8-0049/2017, 2017 (cit. on p. 7).

[36] *COMMISSION REGULATION (EU) 2016/427 of 10 March 2016 amending Regulation (EC) No 692/2008 as regards emissions from light passenger and commercial vehicles (Euro 6)*. 2016. URL: https://eur-lex.europa.eu/legal-content/EN/TXT/PDF/?uri=CELEX:32016R0427 (cit. on pp. 7, 20, 50, 134).

[37] N. Ligterink, P. van Mensch, and R. Cuelenaere. "NEDC - WLTP comparative testing" (Oct. 2016). DOI: 10.13140/RG.2.2.19039.66723 (cit. on p. 7).

[38] P Bielaczyc, A Szczotka, and J Woodburn. "Carbon dioxide emissions and fuel consumption from passenger cars tested over the NEDC and WLTC – an overview and experimental results from market-representative vehicles". *IOP Conference Series: Earth and Environmental Science* 214 (2019), p. 012136. DOI: 10.1088/1755-1315/214/1/012136. URL: https://doi.org/10.1088/1755-1315/214/1/012136 (cit. on p. 7).

[39] M. Tutuianu, P. Bonnel, B. Ciuffo, T. Haniu, N. Ichikawa, A. Marotta, J. Pavlovic, and H. Steven. "Development of the World-wide harmonized Light duty Test Cycle (WLTC) and a possible pathway for its introduction in the European legislation". *Transportation Research*

Part D: Transport and Environment 40 (2015), pp. 61–75. ISSN: 1361-9209. DOI: https://doi.org/10.1016/j.trd.2015.07.011. URL: https://www.sciencedirect.com/science/article/pii/S1361920915001030 (cit. on p. 7).

[40] H. Lee and K. Lee. "Comparative Evaluation of the Effect of Vehicle Parameters on Fuel Consumption under NEDC and WLTP". *Energies* 13(16) (2020). ISSN: 1996-1073. DOI: 10.3390/en13164245. URL: https://www.mdpi.com/1996-1073/13/16/4245 (cit. on p. 7).

[41] A. Ramos, J. Muñoz, F. Andrés, and O. Armas. "NOx emissions from diesel light duty vehicle tested under NEDC and real-word driving conditions". *Transportation Research Part D: Transport and Environment* 63 (2018), pp. 37–48. ISSN: 1361-9209. DOI: https://doi.org/10.1016/j.trd.2018.04.018. URL: https://www.sciencedirect.com/science/article/pii/S1361920918301767 (cit. on p. 7).

[42] J. Pielecha, A. Merkisz-Guranowska, and I. Jacyna-Gołda. "A New Ecological Research – Real Driving Emissions". *Journal of Kones* 21 (May 2014), pp. 259–265. DOI: 10.5604/12314005.1133902 (cit. on p. 7).

[43] P. Bielaczyc, J. Woodburn, J. Merkisz, and J. Pielecha. "Analysis of Emission Factors in RDE Tests As Well as in NEDC and WLTC Chassis Dynamometer Tests" (2016). ISSN: 0148-7191. DOI: https://doi.org/10.4271/2016-01-0980. URL: https://doi.org/10.4271/2016-01-0980 (cit. on p. 7).

[44] (Cit. on p. 7).

[45] A Clenci, V Sălan, R Niculescu, V Iorga-Simăn, and C Zaharia. "Assessment of real driving emissions via portable emission measurement system". *IOP Conference Series: Materials Science and Engineering* 252 (2017), p. 012084. DOI: 10.1088/1757-899x/252/1/012084. URL: https://doi.org/10.1088/1757-899x/252/1/012084 (cit. on p. 7).

[46] G. Vagnoni, M. Eisenbarth, J. Andert, G. Sammito, J. Schaub, M. Reke, and M. Kiausch. "Smart rule-based diesel engine control strategies by means of predictive driving information". *International Journal of Engine Research* 20(10) (2019), pp. 1047–1058. DOI: 10.1177/1468087419835696 (cit. on p. 8).

[47] J. Manuel Lujan, B. Pla, P. Bares, and V. Pandey. "Adaptive calibration of Diesel engine injection for minimising fuel consumption with constrained NO x emissions in actual driving missions". *International Journal of Engine Research* (2020), p. 1468087420918800 (cit. on p. 8).

[48] J. Krammer and A. Nahtigal. "Model Based Assessment of Real-Driving Emissions - A Variation Study on Design and Operation Parameter" (2019). ISSN: 0148-7191. DOI: https://doi.org/10.4271/2019-26-0241. URL: https://doi.org/10.4271/2019-26-0241 (cit. on p. 8).

[49] J. Andert, F. Xia, S. Klein, D. Guse, R. Savelsberg, R. Tharmakulasingam, M. Thewes, and J. Scharf. "Road-to-rig-to-desktop: Virtual development using real-time engine modelling and powertrain co-simulation". *International Journal of Engine Research* 20(7) (2019), pp. 686–695. DOI: 10.1177/1468087418767221 (cit. on p. 8).

[50] F. Payri, J. Martín, F. J. Arnau, and S. Artham. "Analysis of temperature and altitude effects on the Global Energy Balance during WLTC". *International Journal of Engine Research* 0(0) (2021), p. 14680874211034292. DOI: 10.1177/14680874211034292. eprint: https://doi.org/10.1177/14680874211034292. URL: https://doi.org/10.1177/14680874211034292 (cit. on p. 8).

[51] T. Bodisco and A. Zare. "Practicalities and driving dynamics of a real driving emissions (RDE) Euro 6 regulation homologation test". *Energies* 12(12) (2019), p. 2306 (cit. on pp. 8, 53, 56).

[52] J. Czerwinski, P. Comte, Y. Zimmerli, and F. Reutimann. "Testing emissions of passenger cars in laboratory and on-road (PEMS, RDE)". *Combustion Engines* 55 (2016) (cit. on pp. 8, 53).

[53] G. Triantafyllopoulos, D. Katsaounis, D. Karamitros, L. Ntziachristos, and Z. Samaras. "Experimental assessment of the potential to decrease diesel NOx emissions beyond minimum requirements for Euro 6 Real Drive Emissions (RDE) compliance". *Science of the Total Environment* 618 (2018), pp. 1400–1407 (cit. on pp. 8, 53).

[54] R. Varella, B. Giechaskiel, L. Sousa, and G. Duarte. "Comparison of portable emissions measurement systems (PEMS) with laboratory grade equipment". *Applied Sciences* 8(9) (2018), p. 1633 (cit. on pp. 8, 56).

[55] J. Claßen et al. "Statistically supported real driving emission calibration: Using cycle generation to provide vehicle-specific and statistically representative test scenarios for Euro 7". *International Journal of Engine Research* 21(10) (2020), pp. 1783–1799. DOI: 10.1177/1468087420935221. URL: https://doi.org/10.1177/1468087420935221 (cit. on p. 8).

[56] J. Claßen, S. Pischinger, S. Krysmon, S. Sterlepper, F. Dorscheidt, M. Doucet, C. Reuber, M. Görgen, J. Scharf, M. Nijs, et al. "Statistically supported real driving emission calibration: Using cycle generation to provide vehicle-specific and statistically representative test scenarios for Euro 7". *International Journal of Engine Research* 21(10) (2020), pp. 1783–1799 (cit. on p. 8).

[57] P. Roberts, A. Mason, A. Headley, L. Bates, S. Whelan, and K. Tabata. "RDE Plus - A Road to Rig Development Methodology for Whole Vehicle RDE Compliance: Road to Engine Perspective" (2021). ISSN: 0148-7191. DOI: https://doi.org/10.4271/2021-01-1223. URL: https://doi.org/10.4271/2021-01-1223 (cit. on p. 8).

[58] J. M. Luján, H. Climent, S. Ruiz, and A. Moratal. "Influence of ambient temperature on diesel engine raw pollutants and fuel consumption in different driving cycles". *International Journal of Engine Research* 20(8-9) (2019), pp. 877–888 (cit. on p. 9).

Chapter 2

RDE European Regulation

Contents

2.1 Introduction

The European RDE regulation appeared for the first time in the 2016/427 regulation [36] in March 2016. The implementation of this RDE regulation has as its main objective to equate the emissions obtained in the type approval tests, with those obtained in real driving conditions [59].

Compared with previous regulations and homologation cycles, the most disruptive factor was that the RDE must be carried out on the road instead of in a chassis dynamometer. Another big difference is that the previous cycles were perfectly defined. However, RDE cycle routes are entirely open to the user's choice. The regulation marks an extensive and complex requirements guide to perform a valid RDE cycle [60], but even so, the possibilities of different cycles and routes are uncountable [61].

In the beginning, two different validation methodologies coexisted to evaluate pollutant emissions, Mobil Average Windows (MAW) and Power Binning (PB) [62]. In 2017, with 1151/2017 [63] and later on in 2018, with 1832/2018 regulations [64], the European Commission made some changes in the methodology since, the adoption of two different methods (MAW and PB) led to incoherent results and often invalid tests[65]. In particular, the application of the two methods shows noticeable differences in the emission rates ranging from 10% to 45% depending on the considered pollutant [66]. After that, PB was removed, and MAW was modified, and due to incoherent results[67], MAW is no more used for emissions calculation, but it is needed to certify the validity of the cycle. In addition, the emissions during the cold start period that before were not considered shall be included in the evaluation of the results due to their significant contribution to the total emissions [68] [69] and that can seriously pose threats to human health. Additionally, a new concept known as Result evaluation Factor (RF) was introduced to calculate the final emissions, which tries to equalise the emissions of more or less dynamic cycles.

2.2 RDE regulation

The main characteristic of the RDE cycles is that they must have three different vehicle speed zones, concretely, urban, rural and motorway. Furthermore, currently, the regulation establishes a vast list of guidelines which are grouped

in the three steps listed below, where different conditions must be completed to consider a cycle valid.

STEP A:

- Climatological conditions.
- Altitude.
- Dynamic route requirements.

STEP B:

- Relative position acceleration (RPA).
- The 95^{th} percentile of the product of vehicle speed and acceleration (va[95]).
- Cumulative altitude gain.

STEP C:

- MAW.

Step A assesses that the driving cycle is carried out respecting limits on ambient, altitude, and overall route conditions of each zone (Urban, rural and motorway) such as time, kilometres covered, mean vehicle speeds..etc. The regulation establishes a minimum and maximum threshold for every criterion, and if one of these is not fulfilled, the cycle will not be valid. Table 2.1 presents a resume of the parameters that must be fulfilled.

		Min value	Max value
Route characteristics			
Duration	min	90	120
Altitude	m a.s.l.	0	700
Temperature	°C	0	30
Altitude difference (Start-End)	m a.s.l.		100
Urban zone			
Distance	km	16	-
Distance proportion	%	29	44
Stop time (idle)	%	6	30
Longer stop	%	-	80
Average speed	km/h	15	30
Rural zone			
Distance	km	16	-
Distance proportion	%	23	43
Motorway zone			
Distance	km	16	-
Distance proportion	%	23	43
Time speed >100 km/h	min	5	-

Table 2.1: RDE route requirements

Step B introduces the calculation of two parameters to regulate the driving cycle dynamics. The first one, the RPA, is an average acceleration calculated for each zone. Equation 2.1 shows how to calculate it where k=urban, rural or motorway.

$$RPA_k(\frac{m}{s^2}) = \sum(\triangle t * (v * a_{pos})_k)/d_k \tag{2.1}$$

Where:

- v = Instantaneous vehicle speed.
- a_{pos} = Instantaneuos positive acceleration.

- d = Distance covered in each zone.

This RPA value must be above the following calculated thresholds, based on the average speed in each cycle zone (urban, rural and motorway).

If $\bar{v_k} \leq 94,05$ km/h and $RPA_k < (-0.0016 * \bar{v_k} + 0,1755)$ is fulfilled, the trip is invalid.

If $\bar{v_k} > 94,05$ km/h and $RPA_k < 0.025$ is fulfilled, the trip is invalid.

The second parameter, va[95], is the 95th percentile of the product of vehicle speed and positive acceleration (only when the instantaneous acceleration is higher than 0,1 m/s^2) for urban, rural, and motorway driving. In this case, it must be less than another threshold, which also depends on the average speed in each zone which has to be calculated as follows.

If $\bar{v_k} \leq 74,6$ km/h and $va[95]_k > (0.136 * \bar{v_k} + 14.44)$ is fulfilled, the trip is invalid.

If $\bar{v_k} > 74,6$ km/h and $va[95]_k > (-0.097 * \bar{v_k} + 31.635)$ is fulfilled, the trip is invalid.

Furthermore, in this step, the cumulative altitude gain is also calculated. It should be lower than 1200m/100km to avoid routes with large negative slopes, which would mean lower fuel consumption and emissions.

The last step, step C, consists of the calculations of MAW. First, to carry out this step, a WLTC must be performed in order to obtain a CO_2. Reference mass value consisting of half of the CO_2 mass emitted by the vehicle during the test. Finally, averaged emissions and engine speed at low, medium, and extra-high zones are calculated from WLTC data. Once the average values are obtained, a reference CO_2 curve can be calculated.

The CO_2 mass reference is used to calculate the average windows used for RDE cycle analysis. They use a sampling frequency of 1Hz, CO_2, and emissions will be cumulated until they reach the CO_2 reference. During this period, the average speed in km/h and the average specific emissions of CO_2 in g/km was calculated and obtained in the first window. The following window will start a second later than the first the same calculation will be done until the cycle is over. And finally, the test is valid when it comprises at least 50% of the urban, rural, and motorway windows within the tolerances defined by

the CO_2 characteristic curve.

If the three steps have been met successfully, the emissions calculation can be done as described in appendices 4 and 6 of the regulation[64]. In order to do that, the RF obtained from the CO_2 emissions ratio of RDE and WLTC needs to be used. This RF factor reduces the RDE emissions if the performed RDE cycle has higher CO_2 specific emissions than those obtained in the WLTC. It is applied throughout the entire route and in the rural zone. Once it is applied, in order to obtain the type approval conformity report, total and rural specific emissions have to be under the limits of Euro 6 regulation. Nevertheless, due to developing a vehicle to meet the regulation limits in a wide range of driving conditions proposed by RDE has a massive impact on all the aspects of the powertrain development, Conformity Factors (CF) were introduced to relax, at least temporarily, the emissions limits. In this way, Not to Exceed (NTE) limits for RDE are according to equation 2.2.

Table 2.2 shows Euro 6 limits of NO_X, THC, $HCNM$ (Non-methane Hydrocarbons), CO, PN (Particulate Number), and PM.

$$NTE_{pollutant} = CF_{pollutant} * Euro\,6_{pollutant} \tag{2.2}$$

EURO 6													
NOX		**THC + NOX**		**THC**		**HCNM**		**CO**		**PN**		**PM**	
mg/km		mg/km		mg/km		mg/km		mg/km		#/km		mg/km	
PI	CI	PI	CI	PI	CI	PI	CI	PI	CI	PI	CI	PI	CI
60	80	-	170	100	-	68	-	1000	500	6E11	6E11	4,5	4,5

Table 2.2: Euro 6 limits. PI = Provocated Ignition. CI=Compression Ignition

Initially, in the Euro 6d-temporary, it was stipulated a CF of 2.1 for NO_X emissions, which was cut down to 1.43 in the final Euro 6d. The CF for PN is 1.5. These reductions complicate even more the regulation fulfilment for the car manufacturers.

After applying the first RDE regulations, the European Commission realised that the spectrum of different cycles and final emission values could be vast, so it implemented two correction factors.

In the first place, it coined the denomination of extended conditions. The extended conditions occur in specific temperature or altitude ranges, concretely between -7°C to 0°C and from 30°C to 35°C and regarding altitudes between 700 and 1300 m.a.s.l. Once the RDE cycle or all of it enters into extended conditions, the polluting emissions during the time that these conditions exist should be divided by 1.6, excepting CO_2.

In the second place, the European Commission introduced the RF to equate emissions of different RDE cycles. This factor is calculated as the ratio between the CO_2 emissions measured during the RDE test and the WLTC test in grams per kilometre.

To calculate the RF, specific CO_2 in grams per kilometre of the RDE cycle and WLTC are needed. Having these two values, the ratio between both emissions is obtained as shown in the equation 2.3, where k is equal to Urban or Total.

$$r_k = \frac{m_{CO2_{RDE},K}}{m_{CO2_{WLTC},K}} \tag{2.3}$$

After obtaining this ratio, the next step is to obtain the RF. It is obtained through the table 2.3.

When:	**RF value (depending on r_k value) is equal to:**	**Where:**
$If: r_k < RF_{L1}$	$RF_k = 1$	
$If: RF_{L1} < r_k > RF_{L2}$	$RF_k = a_1 * r_k + b_1$	$a_1 = \frac{RF_{L2}-1}{[RF_{L2}*(RF_{L1}-}$ $b_1 = 1 - a_1 * RI$
$If: r_k < RF_{L2}$	$RF_k = \frac{1}{r_k}$	

Table 2.3: RF calculation

The current values of the parameters RF_{L1} and RF_{L2} are as follows:

- $RF_{L1} = 1.30$
- $RF_{L2} = 1.50$

Figure 2.1 shows the RF values once the equations of the table 2.3, and the values of the parameters RF_{L1} and RF_{L2}.

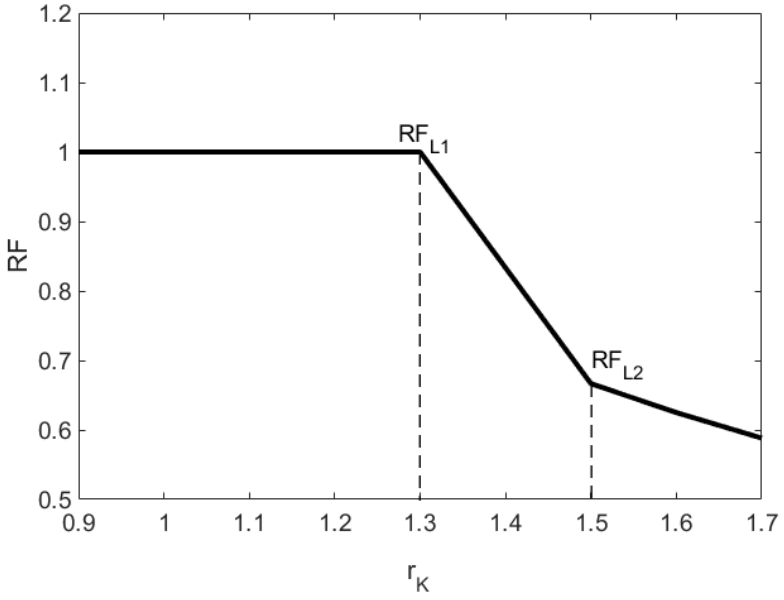

Figure 2.1: European RDE conformity factor (RF).

As can be observed, the RF is reduced as this ratio rises. The RF is always less than or equal to unity and serves to equalise emissions between low, normal or very aggressive cycles.

Finally, once the polluting emissions were obtained, it has to be checked if the cycle entered extended conditions. The division of 1.6 has to be applied in the specific periods where this occurs.

Secondly, to obtain the final emission of all the polluting emissions of the complete RDE trip and the urban part, equation 2.4 has to be used, where k is equal to Urban or Total.

$$M_{RDE,k} = m_{RDE,k} * RF_k \tag{2.4}$$

The tested vehicle could be certified with these results, checking if every

polluting emission is below the current limits established by the European regulation.

2.3 Conclussions

After carrying out a comprehensive analysis of the European RDE regulation, in the first place, it is possible to affirm that it establishes several guidelines and restrictions to limit as far as possible the characteristics of a valid RDE cycle.

However, despite the many guidelines for performing an RDE cycle, multiple factors can spoil it due to the complexity of carrying out these cycles on road. Factors such as temperature, traffic conditions, aftertreatment regenerations, and especially the driver behaviour that has to follow the guidelines of this cycle in the different zones of the cycle and for between 90 and 120 minutes, make it complex to perform RDE cycles on road.

The regulation tries in the first place to specially define the characteristics of the route with the guidelines and limits established in STEP A.

STEP B delimits the driver behaviour, providing maximum and minimum limits in two parameters known as RPA and va[95] obtained through dynamic cycle parameters like vehicle speeds and accelerations.

The engine solicitations are stipulated in STEP C through the calculation of the MAWs. Thanks to the curve obtained from the WLTC and the maximum and minimum limits, this step narrows the zones where the engine must work in the different zones of the cycle since, the MAWs are associated with specific CO_2 emissions and vehicle speed. Specific CO_2 emissions are linked with the engine efficiency, so it forces to carry out a cycle with specific dynamic solicitations and that the engine runs under high load zones, contrary to what happened in the NEDC, that it happened in the WLTC, whence the MAW is based on this cycle.

Nevertheless, the possibilities of different RDE cycles are endless, notwithstanding the European regulation gives a plethora of guidelines and instructions. These cycles can have very different dynamic characteristics, and diverse driver behaviours can perform them.

Furthermore, not only the route characteristics and the driver behaviour affect the results. External agents such as ambient temperature, pressure or, wind have to be considered since, they can considerably affect polluting emissions, and fuel consumption. So diverse results can be obtained for a given vehicle and route, thus increasing the results dispersion of these cycles.

Chapter 2 Bibliography

[36] *COMMISSION REGULATION (EU) 2016/427 of 10 March 2016 amending Regulation (EC) No 692/2008 as regards emissions from light passenger and commercial vehicles (Euro 6).* 2016. URL: https://eur-lex.europa.eu/legal-content/EN/TXT/PDF/?uri=CELEX:32016R0427 (cit. on pp. 7, 20, 50, 134).

[59] R. Suarez-Bertoa, V. Valverde, M. Clairotte, J. Pavlovic, B. Giechaskiel, V. Franco, Z. Kregar, and C. Astorga. "On-road emissions of passenger cars beyond the boundary conditions of the real-driving emissions test". *Environmental Research* 176 (2019), p. 108572. ISSN: 0013-9351. DOI: https://doi.org/10.1016/j.envres.2019.108572. URL: https://www.sciencedirect.com/science/article/pii/S001393511930369X (cit. on p. 20).

[60] Z. A and B. P. "Real Driving Emissions Regulation". (KJ-NA-30123-EN-N (online),KJ-NA-30123-EN-E) (2020). ISSN: 1831-9424 (online),1831-9424. DOI: 10.2760/176284(online),10.2760/531926 (cit. on p. 20).

[61] E. Commission, J. R. Centre, V Franco, J Pavlovic, R Suarez-Bertoa, C Astorga, M Clairotte, B Giechaskiel, V Valverde, and Z Kregar. *On-road vehicle emissions beyond RDE conditions : experimental assessment addressing EU Real-Driving Emission (RDE).* Publications Office, 2019. DOI: doi/10.2760/683267 (cit. on p. 20).

[62] M. Weiss, P. Bonnel, J. Kühlwein, A. Provenza, U. Lambrecht, S. Alessandrini, M. Carriero, R. Colombo, F. Forni, G. Lanappe, et al. "Will Euro 6 reduce the NOx emissions of new diesel cars?–Insights from on-road tests with Portable Emissions Measurement Systems (PEMS)". *Atmospheric Environment* 62 (2012), pp. 657–665 (cit. on p. 20).

[63] *COMMISSION REGULATION (EU) 2017/1151 of 1 June 2017 supplementing Regulation (EC) No 715/2007 of the European Parliament and of the Council on type-approval of motor vehicles with respect to emissions from light passenger and commercial vehicles (Euro 5 and Euro 6) and on access to vehicle repair and maintenance information, amending Directive 2007/46/EC of the European Parliament and of the Council, Commission Regulation (EC) No 692/2008 and Commission Regulation (EU) No 1230/2012 and repealing Commission Regulation (EC) No 692/2008.* 2017. URL: https://eur-lex.europa.eu/legal-content/EN/TXT/?uri=celex\%3A32017R1151 (cit. on p. 20).

[64] *COMMISSION REGULATION (EU) 2018/1832 of 5 November 2018 amending Directive 2007/46/EC of the European Parliament and of the Council, Commission Regulation (EC) No 692/2008 and Commission Regulation (EU) 2017/1151 for the purpose of improving the emission type approval tests and procedures for light passenger and commercial vehicles, including those for in-service conformity and real-driving emissions and introducing devices for monitoring the consumption of fuel and electric energy.* 2018. URL: https://eur-lex.europa.eu/legal-content/EN/TXT/HTML/?uri=CELEX:32018R1832\&from=EN (cit. on pp. 20, 24, 40, 56, 99).

[65] M. V. Prati, G. Meccariello, L. Della Ragione, and M. A. Costagliola. *Real driving emissions of a light-duty vehicle in Naples. Influence of road grade.* Tech. rep. SAE Technical Paper, 2015 (cit. on p. 20).

[66] J. M. Luján, V. Bermúdez, V. Dolz, and J. Monsalve-Serrano. "An assessment of the real-world driving gaseous emissions from a Euro 6 light-duty diesel vehicle using a portable emissions measurement system (PEMS)". *Atmospheric Environment* 174 (2018), pp. 112–121 (cit. on pp. 20, 35, 58).

[67] R. A. Varella, J. P. Ribau, P. C. Baptista, L. Sousa, and G. O. Duarte. "Novel approach for connecting real driving emissions to the European vehicle laboratorial certification test procedure". *Environmental Science and Pollution Research* 26(34) (2019), pp. 35163–35182 (cit. on p. 20).

[68] B. Du, L. Zhang, Y. Geng, Y. Zhang, H. Xu, and G. Xiang. "Testing and evaluation of cold-start emissions in a real driving emissions test". *Transportation Research Part D: Transport and Environment* 86 (2020), p. 102447. ISSN: 1361-9209. DOI: https://doi.org/10.1016/j.trd.2020.102447. URL: https://www.sciencedirect.com/science/article/pii/S1361920920306349 (cit. on p. 20).

[69] L. Chen, B. Du, L. Zhang, J. Han, B. Chen, X. Zhang, Y. Li, and J. Zhang. "Analysis of real-driving emissions from light-duty gasoline vehicles: A comparison of different evaluation methods with considering cold-start emissions". *Atmospheric Pollution Research* 12(5) (2021), p. 101065. ISSN: 1309-1042. DOI: https://doi.org/10.1016/j.apr.2021.101065. URL: https://www.sciencedirect.com/science/article/pii/S1309104221001318 (cit. on p. 20).

Chapter 3

Engine test bench characterisation

Contents

3.1 Introduction

Reproducing RDE cycles under controlled conditions in the laboratory is a challenge considered by different research groups [70]. An option to mitigate the repeatability problem is to transfer the dynamic conditions obtained in an RDE cycle done on road with a PEMS to an engine test bench, so although finally, it is necessary to perform the RDE on road, reproducing its conditions to a test bench could help to many developments works.

Implementing these real driving conditions in an engine test bench environment is possible thanks to the software's capacity to simulate driving conditions. So, reproducing the RDE test in an engine test bench allows to, after comparing the obtained results with those in the real route, taking profit of the test bench's higher instrumentation and control capabilities to get accurate results that assess the performance of the engine and allow to carry out specific studies aimed to improve the engine performance in this particular route.

Using this methodology, studies focused on reducing pollutants emissions, and fuel consumption can be entirely performed with accuracy guarantees. For instance, implementing new driving behaviour strategies, engine control, trying different engine components, bodyworks with better drag coefficient or climatic conditions studies, tasks are already done in WLTC, and NEDC cycles [71].

This section aims to study the viability and assess the uncertainty of performing RDE cycles in an internal combustion engine test bench.

3.2 Methodology

In order to calculate the instantaneous force to move the vehicle at each instant of time, equations 3.1 and 3.2 were applied, where ρ is the air density, v is the vehicle speed, g is the gravity acceleration, α road grade.

Where F_{Aero} is the aerodynamic resistance force, Cx is the aerodynamic transversal coefficient, A is the vehicle section, ρ is the air density, and v is the vehicle speed. And $F_{Rolling}$ is the rolling resistance force, where μ is the rolling coefficient, M the vehicle mass, g the gravity acceleration, and α the

road grade. The values of the different coefficients can be found in table 3.3.

$$F_{aero} = Cx * A * \frac{\rho}{2} * v^2 \tag{3.1}$$

$$F_{rolling} = \mu * M * g * cos(\alpha) \tag{3.2}$$

The required power,P_{engine}, to be supplied by the engine was calculated according to Equation 3.3, where a corresponds to the instantaneous vehicle acceleration:

$$P_{engine} = v * [(M * a) + F_{Aero} + F_{Rolling}] \tag{3.3}$$

3.2.1 Engines and Simulated Vehicles

Two engines were used to implement RDE cycles in an engine test bench. Table 3.1 shows its main characteristics.

		Engine A	**Engine B**
Regulation		Euro 5	Euro 6
Fuel		Diesel	Diesel
Aspiration		Turbocharged	Turbocharged
Engine capacity	*cm3*	1598	2180
Max. Power	*kW*	96	126
Max. Torque	*Nm*	320	400
EGR system		HP and LP	HP
Aftertreatment system		DPF and DOC	DPF, DOC and SCR

Table 3.1: Engines characteristics

Both aftertreatment systems were composed of a Diesel Oxidation Catalyst (DOC) responsible for oxidising THC and CO and a DPF to bate the PM emissions. Considering that the DPF requires periodic regenerations, a specific cleaning procedure was performed between two consecutive cycles.

This strategy complemented the passive oxidation promoted by cerium dioxide added to the fuel.

In the case of engine B, a SCR to reduce NO_X emissions was integrated into the exhaust line. Nevertheless, the AdBlue injection was deactivated in all tests. Therefore, although the gas analyser was placed downstream of the aftertreatment system, raw NO_X emissions were monitored. Both engines have EGR systems, in case of engine A, it has High and Low Pressure (HP and LP) systems, however, engine B only has the HP system. The engines A and B layout and pressure, temperature, and polluting sensors installed in it are shown in figures 3.1 and 3.2 respectively.

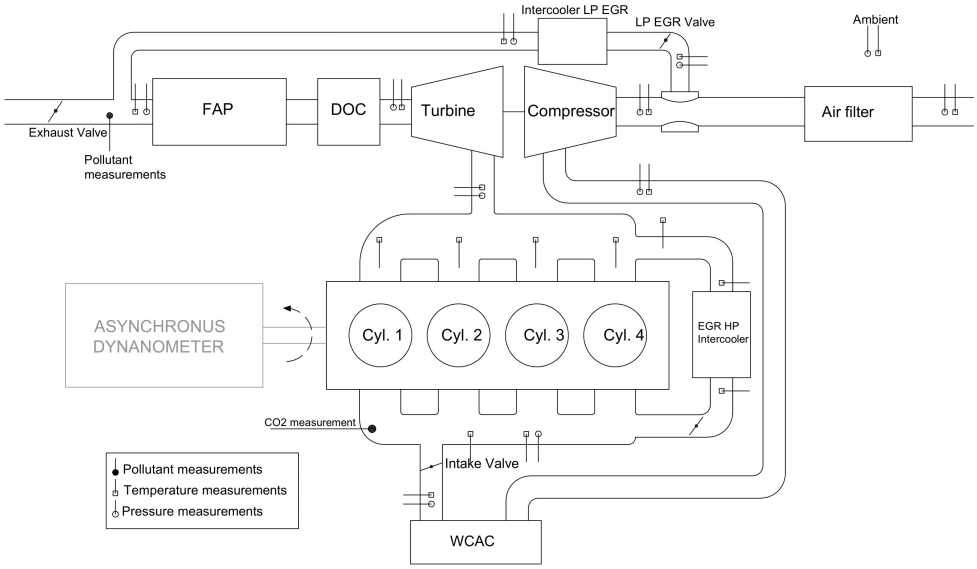

Figure 3.1: Engine A layout.

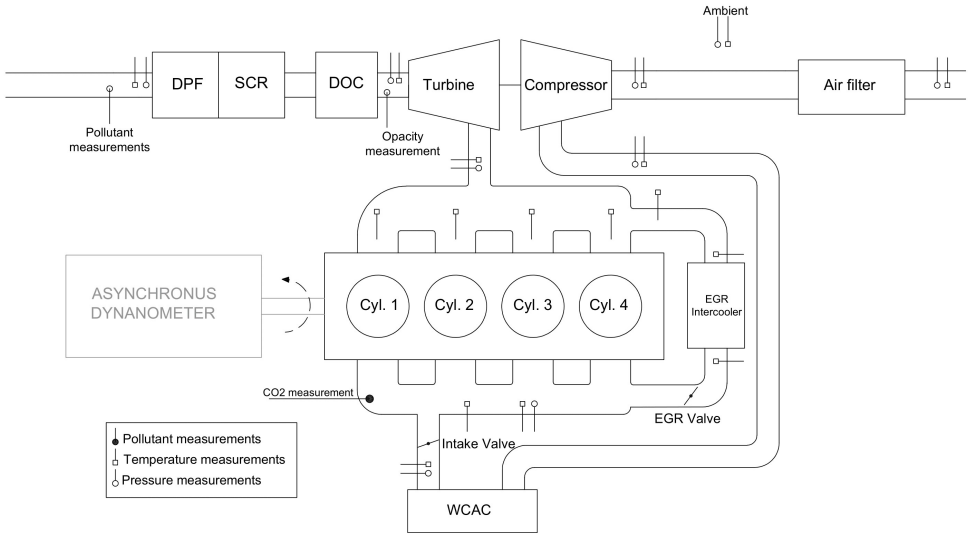

Figure 3.2: Engine B layout.

The acquisition frequency was always 1Hz (as RDE regulation imposes) for all the pollutant emissions, dynamic variables, temperatures, pressures, and mass flows.

The dynamic characteristics of a cycle previously performed on road were obtained [66], and in the case of engine A, the vehicle simulated in the test bench was the same used on road (a passenger car). To perform RDE cycles in engine B, the chosen simulated vehicle was a van since, as commercially corresponds to the tested engine. In order to perform the simulations, many different vehicle and gearbox characteristics need to be introduced into the simulation software. Data of these parameters are shown in table 3.3.

		Vehicle A	**Vehicle B**
Tires code		195/60 R16	225/70 R15
Vehicle mass (M)	*kg*	1581	2731
Frontal area (A)	m^2	2.8	3.95
Drag coefficient (Cx)		0.3	0.335
Rolling coefficient (μ)		0.03	0.032
Nº of gears:		6	6
1st	*Vehicle speed (km/h at 1000rpm)*	8.69	6.79
2nd		16.42	12.96
3rd		25.42	21.20
4th		37.77	31.80
5th		48.79	41.62
6st		57.32	47.33

Table 3.2: Vehicle characteristics

3.2.2 Engine Test Bench

The test bench hosts the engine, together with the following facilities:

- **Horiba SCHENK DYNAS3 asynchronous dynamometer** , which imposed the engine's brake by simulating the corresponding resistance force along with the real driving cycles. The resistance force applied by the brake is considered aerodynamic, friction, and inertia forces that would be exerted on the vehicle.
- **Watlow type K thermocouples. Range: -200°C to 1270°C**
- **Kistler 4045A5 piezoresistive pressure sensors. Range: 0 to 5bar)**
- **Horiba MEXA-7000 gas analyser:** , which measured volumetric concentrations of O_2, THC, NO_X, CO_2, and CO at the exhaust tailpipe. To estimate the EGR rate, CO_2 concentration was also registered at the intake manifold downstream of the EGR junction.
- **AVL 439 opacimeter,**to measure the exhaust gases opacity.

Measuring principles, ranges and uncertainties for each one of the substances are listed in table 3.3. Uncertainty-1 is expressed in relative values, while Uncertainty-2 shows absolute values.

Pollutant	**Measuring principle**	**Range-1**	**Uncertainty-1**	**Range-2**	**Uncertainty-2**
CO	*NID*	0-1250ppm	2%	1250-5000ppm	25ppm
CO_2	NID	0-10%	2%	10%-20%	0.2vol%
NO_X	HCLD	0-250ppm	2%	250-5000ppm	5ppm
THC	HFID	0-250ppm	2%	0-50000ppm	5ppm

Table 3.3: Pollutant emissions measuring principles, ranges and uncertainties of Horiba Mexa-7000. NID: Nondispersive Infrared Detector; HCLD: Heated Chemiluminescent Detector; HFID: Heated Flame Ionization Detector.

From polluting volumetric concentrations of NO_X, THC and CO, the mass flow emissions were calculated using equation 3.4.

$$Pollutant[g/s] = \frac{MM_{pollutant}}{MM_{air}} * (Pollutant[ppm] * kw)/10000 * (AMF + FMF) \tag{3.4}$$

- MM= Molecular weight.
- $Pollutant$= Dry volumetric concentration measured by the pollutant emissions analyser.
- kw= Wet-dry correction factor. In the case of THC, dry-wet correction is equal to 1 since, the analyser measures them in wet conditions.
- AMF= Air mass flow.
- FMF=Fuel mass flow.

And in the case of CO_2, mass flow emissions are calculated using the equation 3.5:

$$CO_2[g/s] = \frac{MM_{CO_2}}{MM_{air}} * CO_2[\%] * kw * (AMF + FMF) \tag{3.5}$$

To obtain the particulate mass, with the opacity can be calculated the soot density [72] through equation 3.6.

$$\rho_{soot}(mg/m^3) = 7.5353 + 235.23[k] - 176.45[k]^2 \tag{3.6}$$

And k is calculated with the equation 3.7:

$$k = \frac{-ln(1 - \frac{N}{100})}{L} \tag{3.7}$$

Where:

- L=Measuring length.
- N=Opacity (%).

After calculating the soot density, it is possible to obtain the PM mass flow through the exhaust mass flow.

3.2.3 RDE validation

In order to set the RDE cycle conditions in a test bench, a specific cycle was used as the baseline. This cycle on road was performed in Valencia, Spain. The required data to implement an RDE cycle in the cell was collected by Global Positioning System (GPS) and PEMS installed in the vehicle. The figures 3.3 and 3.4 show vehicle speed and power versus time for the cycle performed on road and the cycle performed on the test benches.

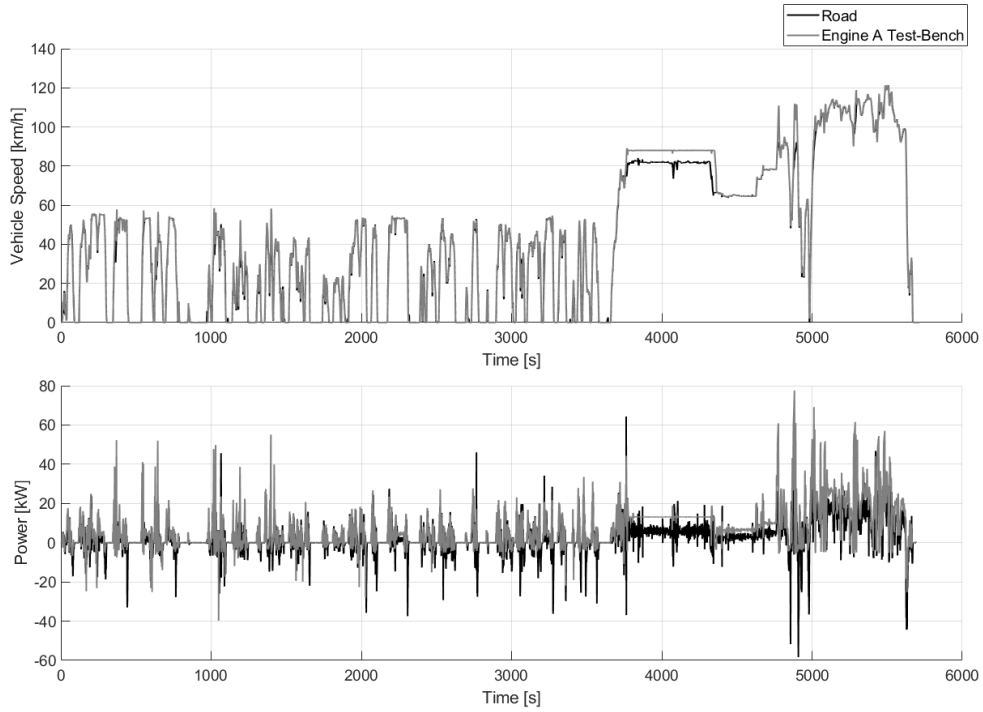

Figure 3.3: RDE on road, versus RDE engine A in the test bench.

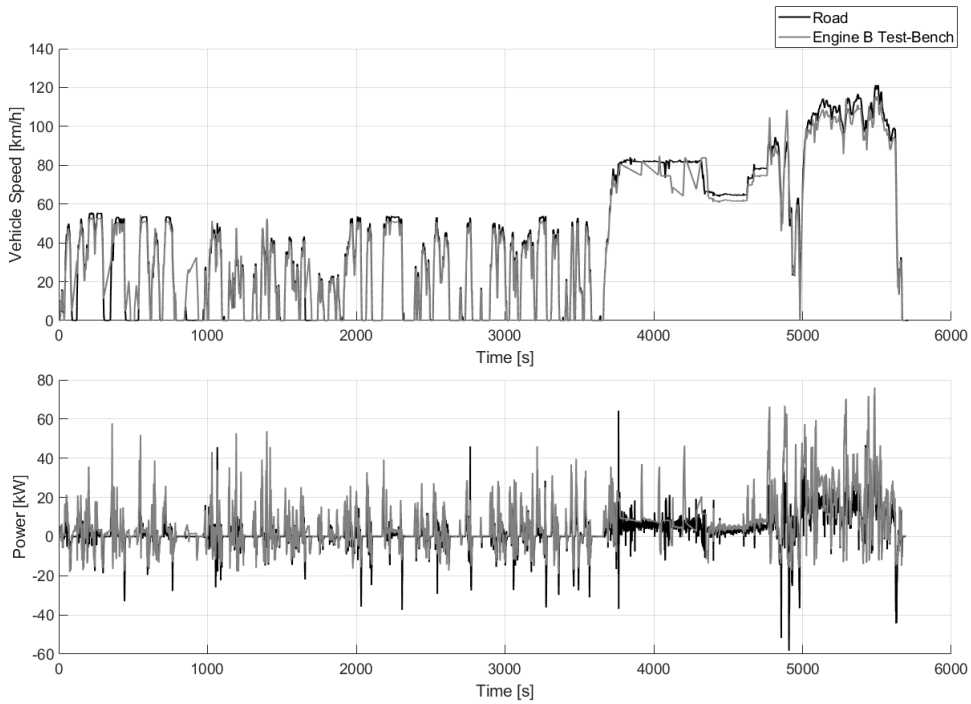

Figure 3.4: RDE on road, versus RDE engine B in the test bench.

As it can be observed, neither the power nor the speed obtained on the test benches perfectly coincides with those obtained on the road. These deviations are due to various reasons. Firstly, both engines had to modify the RDE vehicle speed profile. In the case of engine A, on the left side of the figure 3.3, the vehicle speed changes in a specific section to adapt the RDE cycle to the ewest regulation [64] since, the cycle performed on road does not comply with it, and it would be an invalid cycle.

Secondly, engine A differs from the engine used on road, so their behaviour and efficiency vary.

In the case of engine B, the vehicle speed profile had to be adapted to the engine's characteristics and, more specifically, to those of vehicle B simulated in this engine.

This RDE cycle is divided into urban, rural, and motorway zones. Tables 3.4 and, 3.5 show the characteristics of the cycles performer in engines A and

B.

		Urban	**Rural**	**Motorway**
Average speed	km/h	21.98	79.97	117.49
Time	s	3906	1142	622
Distance	km	23.57	25.29	20.36

Table 3.4: RDE engine Acharacteristics

		Urban	**Rural**	**Motorway**
Average speed	km/h	22.22	76.44	102.50
Time	s	3906	1142	622
Distance	km	24.30	23.43	17.72

Table 3.5: RDE engine B characteristics

Before dealing with the result analysis, it has to be verified that the RDE cycle is valid. This chapter only analyses the cycle performed in engine A since, engine B is widely analysed in Chapter 4.

The three steps previously commented on in chapter 2 were checked to verify if it is a valid cycle. The right column in table 3.6 indicates the obtained values of the specific RDE that was analysed. These restrictions are applied to the three zones, and it can be observed that all the parameters are within specifications.

Step A:

		Min Value	Max Value	Obtained Value
Route Requirements				
Duration	min	90	120	95
Altitude	m.a.s.l	0	700	6
Temperature	°C	0	30	20
Altitude difference(Start-End)	m	0	100	0
Urban Zone				
Distance	km	16	-	23.85
Distance Proportion	%	29	44	34.30
Stop time (iddle)	%	6	30	29
Longer stop	%	-	80	10.21
Average speed	km/h	15	30	21.76
Rural zone				
Distance	km	16	-	25.37
Distance proportion	%	23	43	36.50
Motorway zone				
Distance	km	16	-	20.30
Distance proportion	%	23	43	29.20
Time speed >100km/h	min	5	-	8.96

Table 3.6: RDE constraints and obtained values.

Step B:
Crossed marks in figure 3.5 represent the specific values of va[95] and RPA. It can also be confirmed that the performed cycle is valid as the values are below and under their thresholds, respectively. The cumulative altitude gain is 0 since, road gradient simulation was not incorporated into the test.

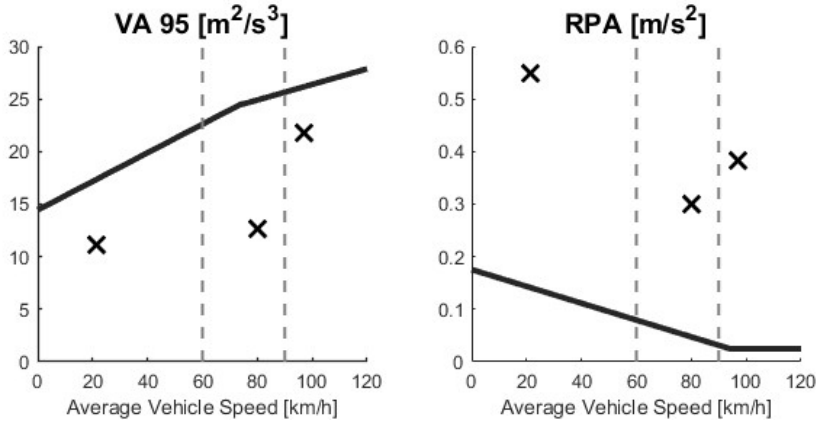

Figure 3.5: va[95] and RPA.

Step C:

Step C, which corresponds to the MAWs, is completely validated since, at least 50% of the windows are included inside the tolerances, as figure3.6 shows.

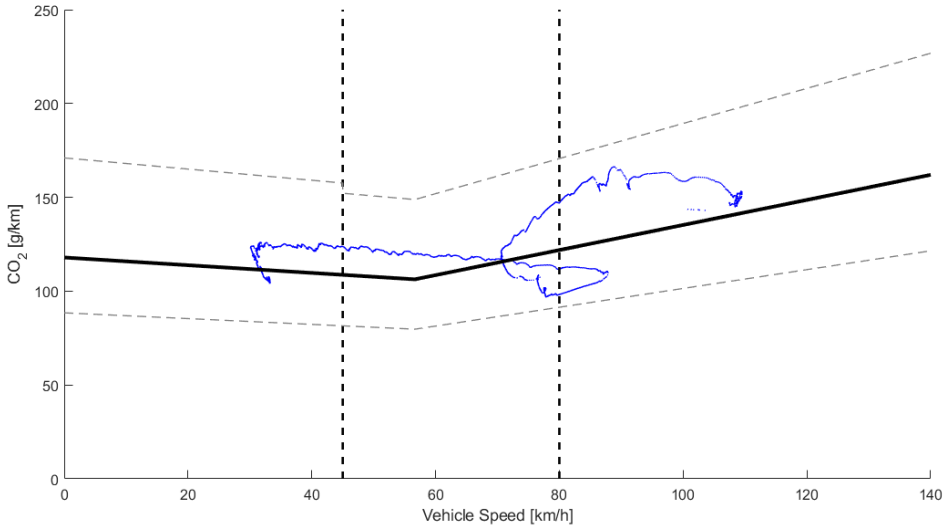

Figure 3.6: CO2 curve, tolerances and MAWs obtained.

Six repetitions of RDE were carried out in the test cell. The table 3.7 shows some cycle characteristics.

		RDE
Average power	kW	7.07
Max power	kW	55.21
Average load	%	7.36
High load	%	57.51

Table 3.7: Main RDE characteristics.

In order to obtain the uncertainty of the data, once the RDE cycle was implemented on the test cell, the selected RDE cycle was repeated six times. Apart from torque, speed, mass flows, temperature, and pressure measurements, the tailpipe type approval pollutant emissions were registered, except for the particulate number and particulate mass, which were not measured. CO_2 emissions are also considered an indication of fuel consumption. Figure 3.7 shows instantaneous emissions measured of NO_X and CO_2.

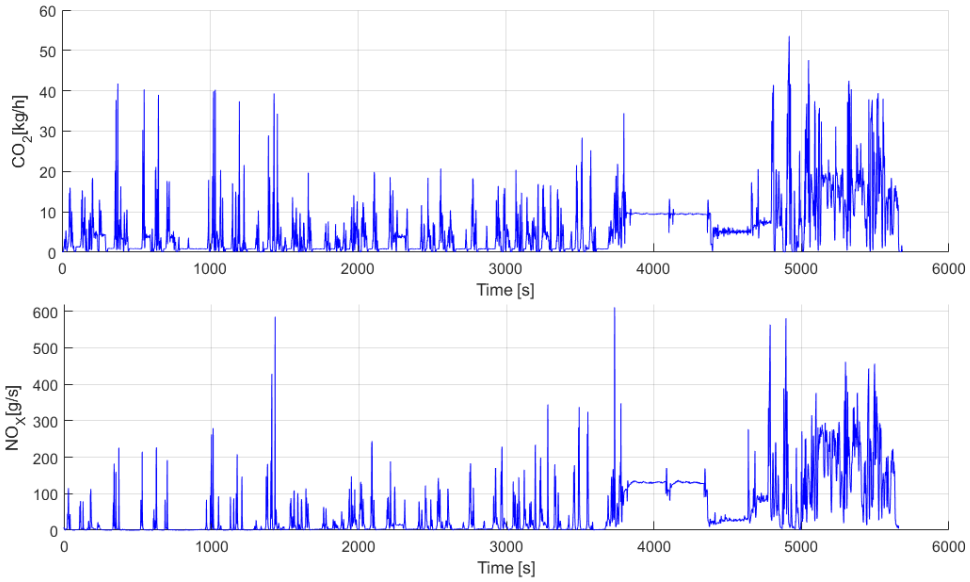

Figure 3.7: Instantaneous NO_X and CO_2 emissions.

Figure 3.8 presents pollutant emissions of each of the six repetitions. These are divided into urban, rural and motorway zones, and also the total cycle

emissions have been plotted.

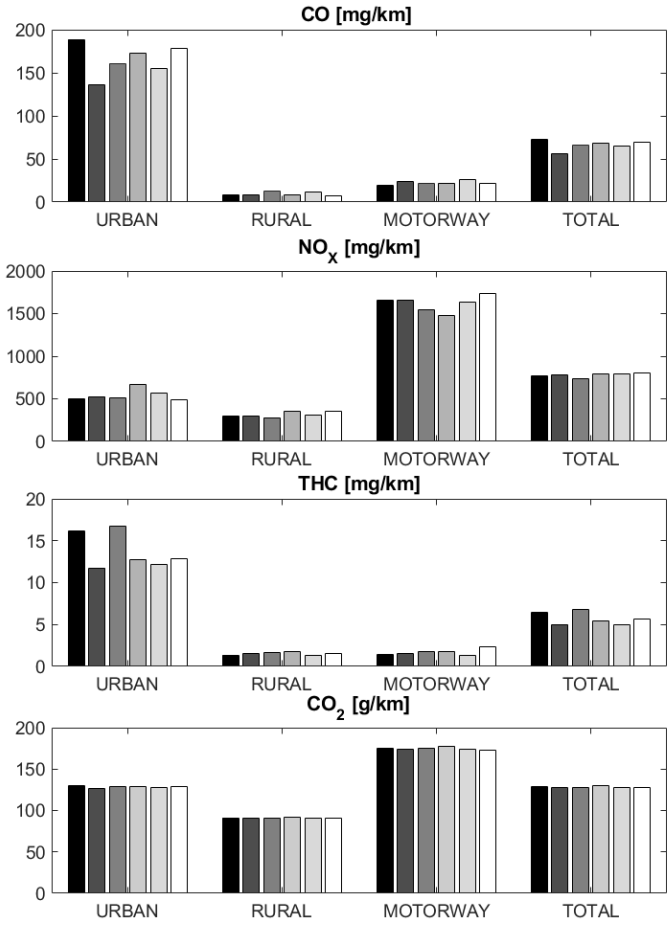

Figure 3.8: Final pollutant emission measured

As figure 3.8 shows, minimal differences between each repetition were obtained regardless of the cycle analysed. These data will be used in the following section to calculate the uncertainty of the measurements.

3.2.4 Statistical Analisis

This section presents the dispersion analysis in the results obtained in several repetitions of the tested driving cycles. Repeatability is defined by the National Institute of Standards and Technology (NIST) Guidelines for Evaluating and Expressing as [73]: *"Closeness of the agreement between the results of successive measurements of the same measurand carried out under the same conditions of measurement"*. Repeatability may be expressed quantitatively in terms of the dispersion characteristics of the results. The following conditions are needed to evaluate repeatability:

- The same measurement procedure.
- The same observer.
- The same measuring instrument was used under the same conditions.
- The same location.
- Repetition over a short period.

In order to identify anomalous results, the proposed methodology is split into two parts. The first part calculates the weighted average of the relative error of test variables. The relative error ϵ is weighted using the instantaneous variable measurement magnitude. The mathematical expression is shown in the equation 3.8, where the relative error is calculated using a Riemann sum.

$$\epsilon = \frac{\int_0^T \bar{\beta} * \bar{x}(t))dt}{\int_0^T \bar{x}(t)dt} \approx \frac{\sum_{i=0}^{i=n} \bar{\beta}(t) * \bar{x_i}}{\sum_{i=0}^{i=n} \bar{x_i}} \tag{3.8}$$

Where beta is the instantaneous average relative error of each variable, x means the instantaneous measured average of each parameter, and n is the number of data points in a test. Both were obtained from the average of several repetitions of the equivalent tests. The sampling frequency is 1Hz (as imposed by the RDE regulation).

β is calculated as the equation 3.9 shows.

$$\bar{\beta} = \frac{1}{m} * \int_{j=0}^{j=m} \alpha_j \tag{3.9}$$

Parameter m means the number of test repetitions. Parameter α is the instantaneous relative error of each test repetition that can be calculated with the equation 3.10:

$$\alpha_j = \frac{|x_j - \bar{x}|}{\bar{x}} \tag{3.10}$$

Where $\bar{x}$ is the parameter under study at the j test repetition. By combining equation 3.9 and 3.10, equation 3.11 can be obtained:

$$\epsilon = \frac{\frac{1}{m}\sum_{i=0}^{i=n}\sum_{i=0}^{i=m}|x_{i,j} - \bar{x_i}|}{\sum_{i=0}^{i=n}\bar{x_i}} \tag{3.11}$$

This error calculation is a modification of the original definition of the Symmetric Mean Average Percentage Error (SMAPE) defined by Flores [74]. It shows how great the dispersion of the tests is.

In order to analyse the accuracy and uncertainty of the tests, the evolution of the following variables will be considered: Speed, Torque, Vehicle Speed, fuel mass flow, exhaust mass flow, boost pressure, and turbine outlet temperature, during RDE tests, using the equation 3.11.

	Error [%]
Exhaust mass flow	7.67
Speed	0.90
Torque	10.05
Vehicle speed	0.92
Fuel mass flow	14.45
Boost pressure	1.89
Outlet temperature turbine	1.84

Table 3.8: RDE errors.

As table 3.8 shows, excepting exhaust mass flow, torque, and mass fuel flow, the other errors are below 5%. In the cases where errors are high, it is partially explained due to high variations of these variables in short time period. These errors are due to the differences between the measurement systems frequency and the acquisition frecuency. The acquisition frequency

applied was 1Hz, and these variables can suffer relative high variations in a second.

However, very small relative errors are obtained when the calculation is applied to the global values of the cycle. If the relative error is applied to the final mean values, very small values are obtained. It can be seen in table 3.9 where the relative errors are shown.

	Relative Error		
RDE	**Exhaust mass flow [%]**	**Torque [%]**	**Fuel mass flow [%]**
1	1.273	0.356	0.163
2	4.630	0.688	0.179
3	0.704	0.395	0.124
4	2.632	0.296	0.157
5	1.409	0.352	0.042
6	1.387	0.594	0.334

Table 3.9: RDE relative errors.

Once these previous variables were analysed, the second part consists of analysing the pollutant emission measurement. A specific analysis methodology was used since, emissions naturally show higher dispersion than the previously analysed variables. This analysis is based on the cumulated emissions of each repetition. After quantifying them, the standard deviation was calculated using the equation 3.12:

$$\sigma = \sqrt{\frac{\sum_{i=1}^{i=1}(\bar{x} - x(i))^2}{m-1}} \tag{3.12}$$

where m is the sample size, $\bar{x}$ is the pollutant average, and $x(i)$ are the values of each repetition.

A 95% of confidence interval was considered as the equation 3.13 shows, where m is the sample size, and t_{m-1} depends on the sample size, in this case, is six and, according to a Student-t distribution is 2.57.

$$CI95\% = Average \pm t_{m-1} * \frac{\sigma}{\sqrt{m}} \tag{3.13}$$

Table 3.10 presents the data obtained from the cumulated pollutant emissions after six repetitions of the same cycle.

	CO	NO_X	THC	CO_2
	[g/cycle]	[g/cycle]	[g/cycle]	[kg/cycle]
Average	4.578	53.701	0.396	8.881
Median	4.627	54.130	0.385	8.863
Range	1.150	4.946	0.125	0.181
σ	0.359	1.602	0.041	0.061

Table 3.10: RDE statistical analysis.

The following errors were obtained:

- CO = 4.578 ± 0.376 g/cycle = 4.578 ± 8.23 % g/cycle
- NO_X = 53.701 ± 1.681 g/cycle = 53.701 ± 3.13% g/cycle
- THC= 0.396 ± 0.043 g/cycle = 0.396 ± 10.88% g/cycle
- CO_2 = 8.881 ± 0.064 kg/cycle= 8.880 ± 0.72% kg/cycle

Considering a 95% confidence interval, CO_2 andNO_X emissions uncertainty enter within the uncertainty of the measurement system. The highest error percentage is in the THC for the WLTC cycle. Also, CO, the error is relatively high. It is mainly due to the particularity of those substances, which are produced mostly during cold starts. At these moments, the aftertreatment system may be in a different state. Therefore it can work having other efficiencies since, the temperature of the test cell is not accurately controlled. Also, as shown in the results, THC emissions are very low compared to other emissions. So, slight variations can lead to significant percentage differences. For this reason, the interpretation of THC emissions should not be given too much importance when analysing the results.

Making a deeper analysis and focusing only on test bench measurement feasibility, in table 3.11, the polluting emissions produced during engine warming-up were not taken into account since, during this period is when the engine in two different tests can have a different behaviour produced by a control

strategy change based on the engine coolant temperature. This engine's particular feature is that it uses EGR HP during cold starts. When the coolant temperature rises to a setpoint temperature, it switches to EGR LP to avoid condensation in the compressor inlet. This temperature can be reached at different times, making it harder for the cycles to compare. In this study, the first 5 minutes were considered warming-up, as the European regulation imposes [36] as the maximum. After the first 5 minutes, the coolant setpoint temperature was reached in the six tests, which involves the same control strategy during the rest of the cycle in all the tests.

	CO	NO_X	THC	CO_2
	[g/cycle]	[g/cycle]	[g/cycle]	[kg/cycle]
Average	3.614	52.506	0.302	8.532
Median	3.608	54.633	0.301	8.512
Range	0.602	3.763	0.061	0.165
σ	0.177	1.285	0.015	0.057

Table 3.11: RDE statistical analysis without a warming-up period.

Applying the values of the table 3.11, the following errors with a 95% of confidence interval were obtained.

- CO = 3.614 ± 0.186 g/cycle = 3.614 ± 5.15 % g/cycle
- NO_X = 52.506 ± 1.348 g/cycle = 52.506 ± 2.57% g/cycle
- THC= 0.302 ± 0.015 g/cycle = 0.302 ± 5.18% g/cycle
- CO_2 = 8.532 ± 0.060 kg/cycle= 8.532 ± 0.70% kg/cycle

As can be observed, there are error reductions in the four substances. Table 3.12 shows these reductions.

	CO	NO_X	THC	CO_2
Complete Cycle	8.23%	3.13%	10.88%	0.72%
W/O Warming-up	5.15%	2.57%	5.18%	0.70%
Error Reduction	-37.41%	-17.99%	-52.39%	-2.53%

Table 3.12: Pollutant uncertainty and error reduction without warming-up.

Looking at the table 3.12, significant improvements were obtained overall in the CO and THC, pollutants that are mainly produced during the warming-up period. This analysis helps to make a deeper characterisation of the test cell measurement capacity, which was proven to carry out the RDE test without hindrance.

Another methodology to verify the repeatability would be using the current tolerances for the PEMS validation method established in the European Regulation. This consists of measuring the emissions in a WLTC cycle, utilising a PEMS and a Constant Volume Sampler (CVS), and obtaining a difference between the two that is at least less than one of the two following tolerances:

- Absolute tolerance.
- Relative tolerance if this relative tolerance is greater than the absolute tolerance.

Table 3.13 presents the tolerances and the maximum difference between the values obtained in RDE. The bold numbers represent the situations when the obtained uncertainty is under the limit of the PEMS validation method, and it can be confirmed as at least one of the two are within the range of absolute or relative tolerances.

	Permissible absolute tolerance	**Result**	**Permissible relative tolerance**	**Result**
	mg/km	mg/km	%	%
CO	150	**9.97**	15	15.07
NO_X	15	44,49	15	**5.73**
THC	15	**1.08**	15	18.93
CO_2	10,000	**1556.69**	10	**1.20**

Table 3.13: Comparison between errors obtained and PEMS regulative tolerances.

3.3 Conclussions

The feasibility of an engine test cell for reproducing the real driving conditions was analysed. The test cell control software implemented an RDE cycle using an engine test bench, simulating a standard passenger car. Once the cycle was repeated several times, data corresponding to the engine operating together with pollutant emissions was statistically treated.

The errors obtained from the statistical study are minimal, significantly, when eliminating the effect generated by the warming-up control period that would cause a greater dispersion.

In the case of an RDE cycle with a duration of 96 minutes, small errors were calculated. On one hand, in the case of NO_X emissions, the error is 3.13% in Nitrogen Oxides which takes on particular importance, considering the importance that NO_X emissions have in the regulation (especially for diesel engines). On the other hand, the CO_2 dispersion is even lower, which would help in crucial studies to reduce it since, it is linked with fuel consumption and whose reduction is a key factor in fighting against climatic change and the greenhouse effect.

CO and THC emissions behave similarly, with the highest uncertainties being found in these substances. But these emissions are not a concern for vehicle manufacturers due to the high efficiency of oxidation catalysts incorporated in all vehicles, complying with the regulations without significant problems. The uncertainties obtained are pretty small compared to RDE carried out on

the road, where significant differences can be found. Even in some cases, these cycles cannot be considered due to their high variability or because they do not comply with the regulation, as shown in some abovementioned research papers [51, 52, 53].

Therefore, it is of great interest to carry out these types of cycles in a test cell to compare them. Using this methodology, multiple studies could be done as parametric studies modifying driving behaviour or engine controls, aftertreatment systems, engine components, etc... The uncertainty obtained in these tests can quantify the eventual reduction of polluting substances that may occur solely due to the engine modifications.

Chapter 3 Bibliography

[36] *COMMISSION REGULATION (EU) 2016/427 of 10 March 2016 amending Regulation (EC) No 692/2008 as regards emissions from light passenger and commercial vehicles (Euro 6).* 2016. URL: https://eur-lex.europa.eu/legal-content/EN/TXT/PDF/?uri=CELEX:32016R0427 (cit. on pp. 7, 20, 50, 134).

[51] T. Bodisco and A. Zare. "Practicalities and driving dynamics of a real driving emissions (RDE) Euro 6 regulation homologation test". *Energies* 12(12) (2019), p. 2306 (cit. on pp. 8, 53, 56).

[52] J. Czerwinski, P. Comte, Y. Zimmerli, and F. Reutimann. "Testing emissions of passenger cars in laboratory and on-road (PEMS, RDE)". *Combustion Engines* 55 (2016) (cit. on pp. 8, 53).

[53] G. Triantafyllopoulos, D. Katsaounis, D. Karamitros, L. Ntziachristos, and Z. Samaras. "Experimental assessment of the potential to decrease diesel NOx emissions beyond minimum requirements for Euro 6 Real Drive Emissions (RDE) compliance". *Science of the Total Environment* 618 (2018), pp. 1400–1407 (cit. on pp. 8, 53).

[64] *COMMISSION REGULATION (EU) 2018/1832 of 5 November 2018 amending Directive 2007/46/EC of the European Parliament and of the Council, Commission Regulation (EC) No 692/2008 and Commission Regulation (EU) 2017/1151 for the purpose of improving the emission type approval tests and procedures for light passenger and commercial vehicles, including those for in-service conformity and real-driving emissions and introducing devices for monitoring the consumption of*

fuel and electric energy. 2018. URL: https://eur-lex.europa.eu/legal-content/EN/TXT/HTML/?uri=CELEX:32018R1832\&from=EN (cit. on pp. 20, 24, 40, 56, 99).

[66] J. M. Luján, V. Bermúdez, V. Dolz, and J. Monsalve-Serrano. "An assessment of the real-world driving gaseous emissions from a Euro 6 light-duty diesel vehicle using a portable emissions measurement system (PEMS)". *Atmospheric Environment* 174 (2018), pp. 112–121 (cit. on pp. 20, 35, 58).

[70] J. Claßen et al. "Statistically supported real driving emission calibration: Using cycle generation to provide vehicle-specific and statistically representative test scenarios for Euro 7". *International Journal of Engine Research* 21(10) (2020), pp. 1783–1799. DOI: 10.1177/1468087420935221 (cit. on p. 32).

[71] J. M. Luján, H. Climent, S. Ruiz, and A. Moratal. "Influence of ambient temperature on diesel engine raw pollutants and fuel consumption in different driving cycles". *International Journal of Engine Research* 20(8-9) (2019), pp. 877–888. DOI: 10.1177/1468087418792353 (cit. on p. 32).

[72] D. Campos Navarro. *Estudio de las emisiones de escape en motores de combustión interna alternativos utilizando diferentes sistemas de control de contaminantes*. Universidad Politecnica de Valencia. Departamento de Máquinas y Mo-tores Térmicos, 2016 (cit. on p. 38).

[73] B. N. Taylor and C. E. Kuyatt. "Guidelines for evaluating and expressing the uncertainty of NIST measurement results" (1994) (cit. on p. 46).

[74] B. E. Flores. "A pragmatic view of accuracy measurement in forecasting". *Omega* 14(2) (1986), pp. 93–98. URL: https://ideas.repec.org/a/eee/jomega/v14y1986i2p93-98.html (cit. on pp. 47, 83).

Chapter 4

RDE dynamic assessment

Contents

4.1 Introduction

The newest RDE regulation [64], as was described in Chapter 2, dictates a series of guidelines for carrying out the tests. These guidelines try to resemble cycles to normal and real driving conditions [75] as its name indicates, and these conditions have a significant influence on the polluting emissions [76].

The cycle would be considered invalid if any of the requirements were not fulfilled. Although the regulation is very extensive and detailed, the number of possible different cycles is infinite, so different tests can have an important dispersion in terms of pollutant, and CO_2 emissions [77][78]. Therefore traffic [79] and weather conditions, altitude [80], route typology, road grade or slope [81] and driver behaviour [82] [83][84] have a great influence on the cycle results [51][85][86][87], even repeating the same trip, large differences between different cycles can be found [88]. Also, some studies combine experimental on-road data with numerical analysis to assess the impact of the Stop/Start system, vehicle mass, drag coefficient, and different aftertreatment system layouts [89].

In this chapter, the methodology explained in Chapter 3 is applied, which consists of performing real driving cycles on an engine test bench since, as the tests were performed under highly controlled operating conditions, the intrinsic engine response can be analysed with greater reliability since, the uncertainties caused by traffic, temperature, or driver behaviour are eliminated [1]. It can be possible to find similar studies in literature carried out aimed at improving the reproduction of the flow conditions on the road and to be able to perform cycles on a chassis dyno [90][91][92]. Furthermore, it is added that although PEMSs are being improved [93][94], they have smaller accuracy than a stationary system (CVS) [54] [95].

In this section, six cycles were analysed. Cycles that fulfil the actual RDE regulation but have different dynamic solicitations. The methodology above was always applied, and the registered test data was rigorously examined. The first one replicates an on-road cycle and will be used for baseline comparison. A second one was designed combining several WLTC dynamic phases. The last four were defined using a computational tool considering different dynamic conditions. Concretely with the previous two cycles, a study analysing two other driver behaviours were also performed, which could not be carried out on road in a consistent and repeatable manner. The data from the cycles

above were analysed in detail to relate cycle dynamics and engine operation.

Additionally, a comparative study of different recorded variables and CO_2 and NO_X emissions obtained from the RDE tests and the steady-state results from the engine map was performed considering the engine speed, torque or throttle during the cycles. It would help to anticipate the emissions that a cycle may have [96], to predict the instantaneous emissions on board [97] [98] or improve the measurement of them [99].

4.2 Matherial and methods

4.2.1 Methodology

To create the RDE cycle characteristics, a computational tool were developed. Thanks to this tool, it is possible to design RDE cycles with different durations, dynamic features, and driver behaviours that can later be transported to the engine test bench to analyse how these parameters affect fuel consumption and polluting emissions.

Furthermore, after performing a steady-state engine study and obtaining engine maps of several variables, different results of the cycles are compared with the results obtained by interpolation with the engine maps. It helps to understand the behaviour of the engine during the transient conditions of the RDE cycles and if these conditions are similar or not to steady-state conditions.

4.2.2 Test bench and engine

In order to be able to compare real cycles accurately, an engine test bench was employed to reproduce the conditions of every proposed test. In this way, the inherent uncertainties of on-road tests are eliminated, and a common framework for comparison is established. In this study, the engine and vehicle B were used in the hole study, and both configurations, engines and vehicles A and B, were only used in the section 4.4.2 where the cycles are compared with the results from steady-state tests.

4.3 RDE cycles description

Although the quantity of possible RDE cycles is infinite, there are some procedures to build valid RDEs [100]. In this section, six different cycles to evaluate the engine's emissions and consumption in other driving conditions are defined. All cycles met the needs required by the current Euro 6d regulation to be considered valid. Given the vast number of cycles that can fulfil the requirements, these were chosen in such a way that, maintaining similar typologies, the effect produced by the specific modifications implemented in each were comparable.

In this study, the maximum engine speed was set along with the gear shifting, representing different driver behaviours under the standard field of diesel engines. Table 4.1 shows the maximum engine speed at which the shifting sequence occurs for each RDE cycle.

	RDE 1-5	RDE 6
1st	3400	2900
2nd	3300	2800
3rd	3200	2700
4th	3100	2700
5th	3000	2650
6st	-	-

Table 4.1: Maximum engine speed limits for each gear.

4.3.1 RDE 1

This cycle was obtained from on-road driving in Valencia (Spain) [66]. Using the data obtained from this test, it was possible to transfer its characteristics to the engine test bench. In particular, a vehicle model was used to calculate the instantaneous effective torque and engine speed considering the vehicle speed profile, the vehicle, gearbox characteristics, and the driver behaviour. These two parameters were used as inputs in the engine test cell.

4.3.2 RDE 2

The second cycle performed was obtained by combining different WLTC segments to meet RDE requirements. WLTC represents real driving conditions, although it must be performed in a chassis dynamometer. It is expected that WLTC will also be used in the next Euro 7 regulation as CO_2 emission certification.

In this case, WLTC phases in which the vehicle speed is less than 60km/h were used to generate the urban zone, phases with vehicle speed between 60 and 90km/h were applied to build the rural zone, and phases characterised by vehicle speeds over 90km/h were considered to define the motorway zone. As WLTC is much shorter than the RDE cycles, several WLTC parts were mixed and repeated. After obtaining the speed profile, it was combined with the remaining data related to the vehicle, gearbox, and driver to get the required torque and engine speed to meet the instantaneous vehicle speed setpoint.

4.3.3 RDE 3,4,5 and 6

The last four cycles were obtained using a computational tool with MATLAB. It was designed to generate RDE cycles. This function selects different speed profile phases with different vehicle speeds and accelerations. To fulfil the regulatory requirements these phases fulfil standard real driving drivings. As a result, cycles with different dynamic demands, durations, and other characteristics were obtained. The user can choose the number of times every phase, characterised by different engine load conditions, is repeated in the software. Consequently, depending on the number of dynamic phases, the cycle generated is more or less loaded. After the cycle is generated, torque and engine speed were finally determined in the same way as the previous cycles.

All the cycles presented a specific repetition pattern in the route. In the urban zone, it could be like repeating the same circuit in a particular city, provided that the conditions of traffic, driving behaviour, and traffic lights do not affect it. This approach was also applied in the rural and motorway areas, where the same conditions could be reproduced on a highway without traffic, and the driver replicated the speed conditions imposed. Using this tool, different routes, driver behaviours, etc., can be examined, reducing economic costs and uncertainties from on-road testing.

- **RDE 3:** This cycle presented the lowest duration but the highest average vehicle speed in every zone. This cycle was also characterised by a similar proportion of high and low loads.
- **RDE 4:** In this case, the previous RDE 3 was taken as a reference. The objective of this RDE 4 was to generate a more dynamic cycle in the rural zone. This cycle was also less loaded, being the average vehicle speeds in urban and motorways zones lower than in RDE 3.
- **RDE 5:** The objective of this cycle was to generate a less loaded and dynamic cycle than the previous ones. In order to do that, phases with low dynamic demands were chosen. As observed in figure 4.1, the differences in vehicle speed were reduced for the rural and motorway zones compared to other cycles.
- **RDE 6:** This last cycle was obtained with the same vehicle profile as RDE 5, with the driver's behaviour as the only difference. In this case, the gear shifting sequence was modified to obtain a lower engine speed profile.

The RDE vehicle speed profiles are shown in 4.1.

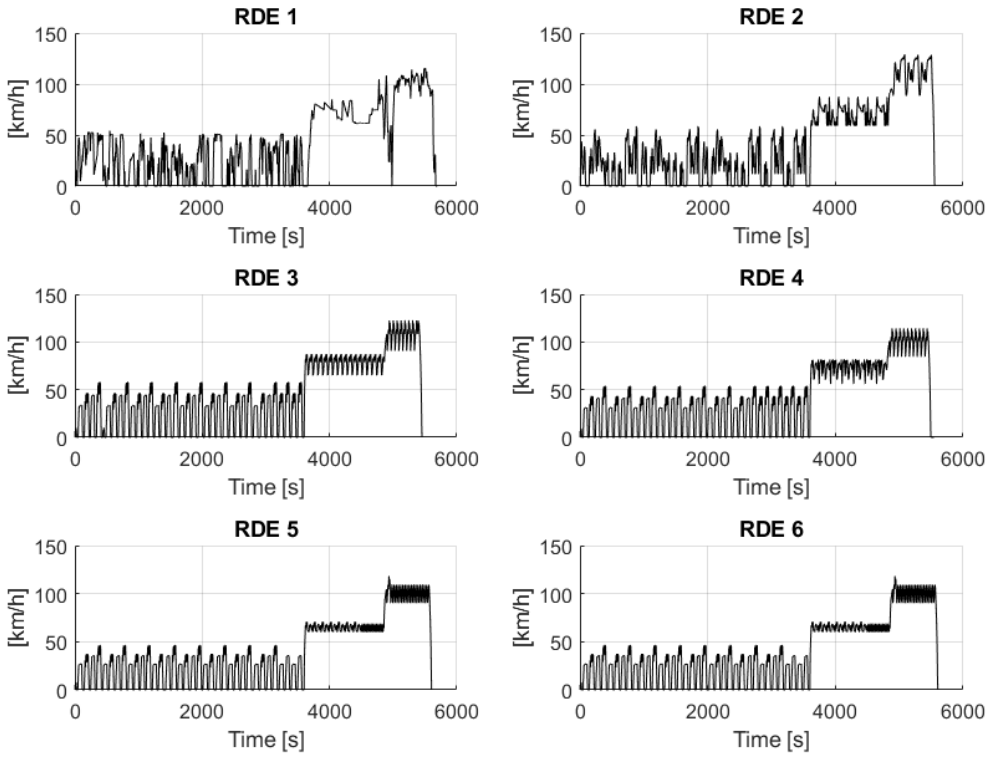

Figure 4.1: RDE cycles vehicle speed profiles.

Figure 4.1 shows noticeable differences between RDEs 1 and 2 compared to RDEs 3 to 6, despite the patterns of the urban, rural, and motorway zones being similar. The main difference is that cycles 3 to 6 are composed of a limited set of vehicle speed transitions repeated along each cycle area, making them significantly more repeatable in an engine test bench environment.

Table lists the characteristics of every cycle described above. It also shows the minimum and maximum thresholds of the different parameters established by the regulation, finding all of them accomplished by the designed RDEs.

		Min value	Max value	RDE 1	RDE 2	RDE 3	RDE 4	RDE 5&6
Route characteristics								
Duration	min	90	120	94.9	92.58	90.9	92.33	93.4
Altitude	m a.s.l.	0	700	6	6	6	6	6
Temperature	°C	0	30	20	20	20	20	20
Altitude difference (Start-End)	m		100	0	0	0	0	0
Urban zone								
Distance	km	16	-	24.1	21.59	25.87	24.86	24.19
Distance proportion	%	29	44	36.48	32.86	36.38	34.54	36.71
Stop time (iddle)	%	6	30	28.87	28.94	27.67	28.74	29.24
Longer stop	%	-	80	7.25	5.67	4.08	4.23	4.05
Average speed	km/h	15	30	22.4	20.93	25.67	24.2	23.96
Rural zone								
Distance	km	16	-	24.25	23.64	27.89	26.61	22.31
Distance proportion	%	23	43	36.71	35.98	39.22	36.97	33.86
Motorway zone								
Distance	km	16	-	17.71	20.47	17.36	20.5	19.39
Distance proportion	%	23	43	26.81	35.98	39.22	36.97	33.86
Time speed >100 km/h	min	5	-	6.85	8.95	7.37	6.88	6.17

Table 4.2: RDE cycles characteristics.

To fulfil the RDE regulation, it is also necessary to carry out the calculation of two parameters. Firstly, RPA is an average acceleration calculated for urban, rural, and motorway zones that must be above the regulated minimum value as a function of vehicle speed. Secondly, the so-called parameter va[95], which corresponds to the 95^{th} percentile of multiplying the positive acceleration times the vehicle speed, provided that the positive acceleration is higher than 0.1 m/s^2 and must be below the regulated limit. The va[95] must also be calculated for the three RDE phases.

Figure 4.2 shows the fulfilment of the va[95] and RPA criteria for all the proposed RDE cycles despite a wide dispersion between them. In particular, higher RPA and va[95] point out a more loaded cycle.

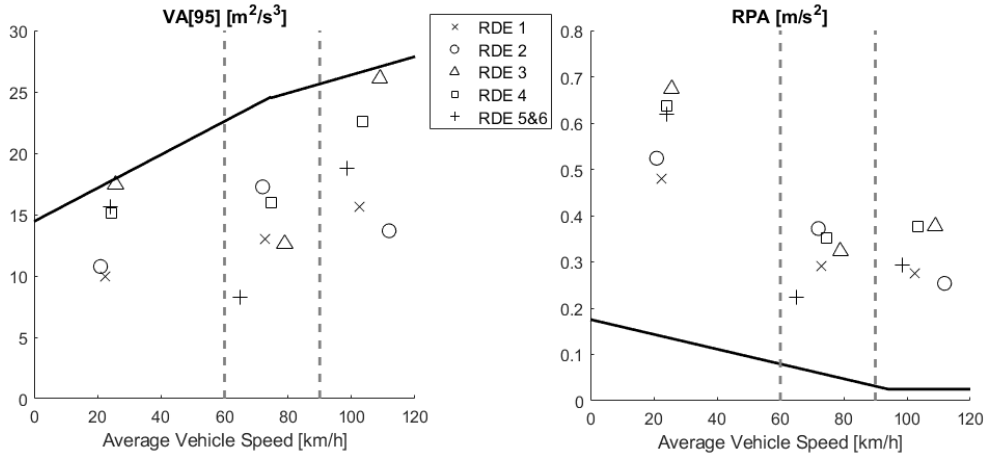

Figure 4.2: va[95] and RPA values in each driving zone for the proposed RDE cycle.

As shown in the figure 4.2, the dispersion between the values gives an idea of how different the cycles are, and it will be confirmed below, that all are equally valid.

The last calculation corresponds to the Moving Averaging Window (MAW). The calculation starts from a previously performed WLTC, which obtains the so-called CO_2 reference mass, defined as half of the CO_2 mass emitted by the vehicle during this WLTC reference test. The CO_2 reference mass is used to calculate the MAW as follows: CO_2 emissions are cumulated from the beginning of the RDE test (having a sampling frequency of 1 Hz) until reaching the

CO_2 mass reference. The average speed and the average specific emissions of CO_2 in g/km in this period permit the definition of the first window. After resetting the CO_2 count to zero, the following window will start a second later and continue with the same calculation method until the end of the cycle.

The RDE cycle is only considered valid when at least 50% of urban, rural, and motorway windows are within the tolerances defined by regulation calculated through the CO_2 characteristic curve.

Figure 4.3 shows the MAWs of the cycles under study, and as can be observed, all cycles have at least 50% of MAWs within the tolerances of the CO_2 curve for every driving zone.

The sixth RDE may seem invalid at first glance because many windows are below the lower limit. Nevertheless, it has 57% within tolerances of the urban zone and 58% of the rural zone, thus complying with the requirements of RDE.

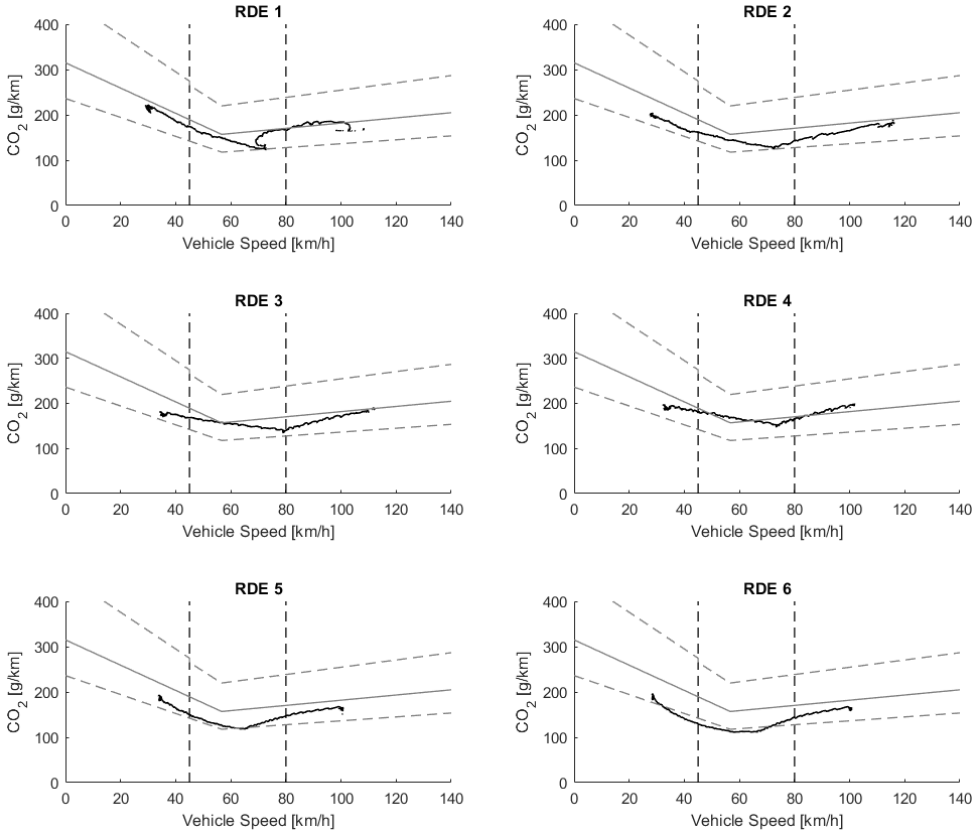

Figure 4.3: CO_2 curve, tolerances, and MAWs obtained of cycles RDE 1, RDE 2, RDE 3, RDE 4, RDE 5, RDE 6.

4.4 Results

In this section, an analysis of the dynamic characteristics of the RDE cycles and emissions was carried out.

4.4.1 RDE tests.

The analysis of cycles was done by looking at the distribution of the dynamic variables [101]. This analysis divides the vehicle speed, torque, engine speed,

and power into five segments. Figure 4.4 shows the distribution frequency of these parameters for each RDE cycle.

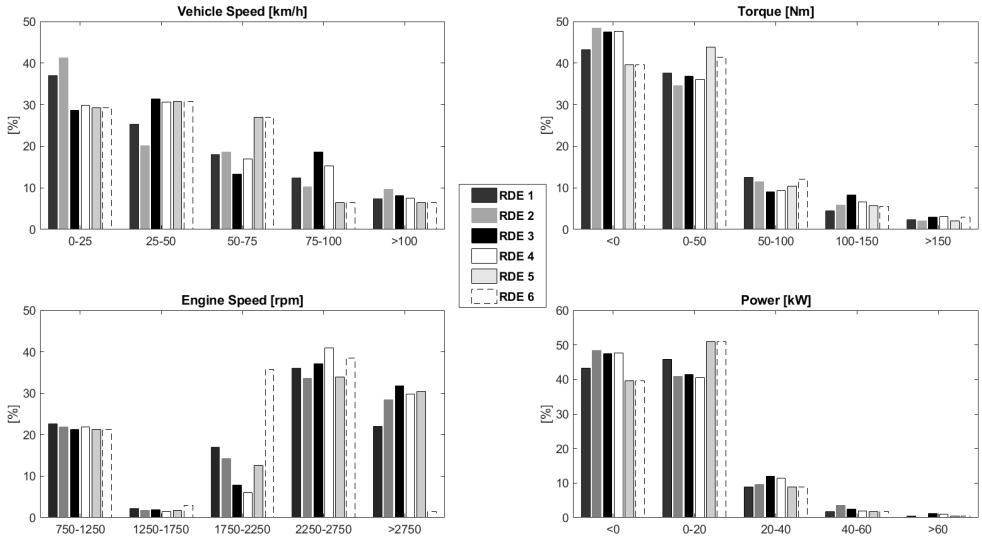

Figure 4.4: Distribution of vehicle velocity, torque, engine Speed, and power.

Regarding vehicle speed, the groups were divided into intervals of 25km/h to 100 km/h and one more for speeds higher than 100 km/h. The engine torque was also divided into groups of 50 Nm. The engine speed was split into groups of 500 rpm and, finally, the power in groups of 20 kW. The events in which the power and torque were less than zero corresponded to circumstances when the engine was dragging, or the driver was braking.

At first sight, the cycles show a great dispersion between each other and consider that all of them are valid, evidencing that a wide variety of cycles fit the regulation. In the case of RDEs 5 and 6, considering that the vehicle speed and power distribution were identical (as defined), the different driver behaviour led to various engine operating conditions in terms of torque, engine speed, and pedal position. Figure 4.4 shows that RDE 6 had much fewer points in the strip of greater than 2750 rpm since, driver behaviour was programmed with the aim of making the gearshift before, avoiding high engine speed. This action could be representative of the down speeding technique [102], which is

a current trend where the goal is that the engine works at high performance, reducing consumption and, as far as possible, pollutant emissions.

Additionally, to make a deeper analysis, the cycles were divided into 13 bins depending on vehicle speed and power. Table 4.3 shows the conditions of those bins.

			Power [kW]				
			-	>0	>20	>40	>60
			≤ 0	≤ 20	≤ 40	≤60	-
Dragging			*Bin 0*	-	-	-	-
Vehicle Speed [km/h]	=0(Idle)		*Bin 1*	-	-	-	-
	>0	<60	-	*Bin 2*	*Bin 5*	*Bin 8*	*Bin 11*
	≥ 60	<90	-	*Bin 3*	*Bin 6*	*Bin 9*	*Bin 12*
	≥ 90	-	-	*Bin 4*	*Bin 7*	*Bin 10*	*Bin 13*

Table 4.3: Division of the test into different bins depending on vehicle speed and power.

Figure 4.5 shows the results of the 13 bins applied to the 6 RDE cycles. It can be seen that the dispersion between these cycles increases in the higher power region (bin 8 on-wards). As an example, RDE 2 cycle does not present any values in bins 8, 11, and 12, which denotes that the power was below 40 kW in the urban area. It can also be observed in RDE 2 bin 13, corresponding to the maximum motorway power fraction, the time proportion was the lowest, corresponding to few accelerations and steadier driving. Another interesting aspect is that RDE 1 was the only one that went into all bins, implying that this test would make the engine work in more diverse operating conditions than the others.

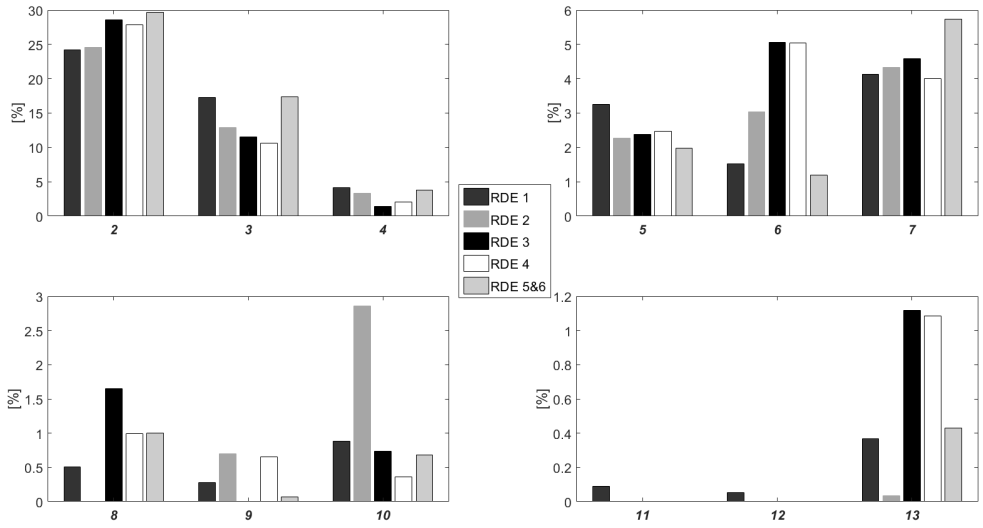

Figure 4.5: Bin proportions from 2 to 13 of each cycle.

Looking at RDEs 3 and 4 and the bins that represent the urban area (3, 6, 9, and 12), the values of bins 3 and 6 are very similar. However, bin 9 of the RDE 3 is equal to zero, but 0.64% in RDE 4, which involves that more considerable power was reached in this cycle in the urban zone due to a higher dynamic solicitation. RPA and VA[95] values also point it out, with RDE 4 above RDE 3, as observed in Figure 4.2.

Finally, RDEs 5 and 6 were generated to avoid aggressive driving. It is especially noticeable in the motorway zone, where the highest values are in bin 7 (low power zone), whilst bins 10 and 13 are less representative.

Figure 4.6 shows the specific emissions in grams per kilometer of NO_X, CO, THC, and CO_2. Tests were performed without urea injection, so NO_X emissions exceeded the regulatory limit. On the other hand, THC and CO fulfil the type-approval limits after being oxidised in the DOC.

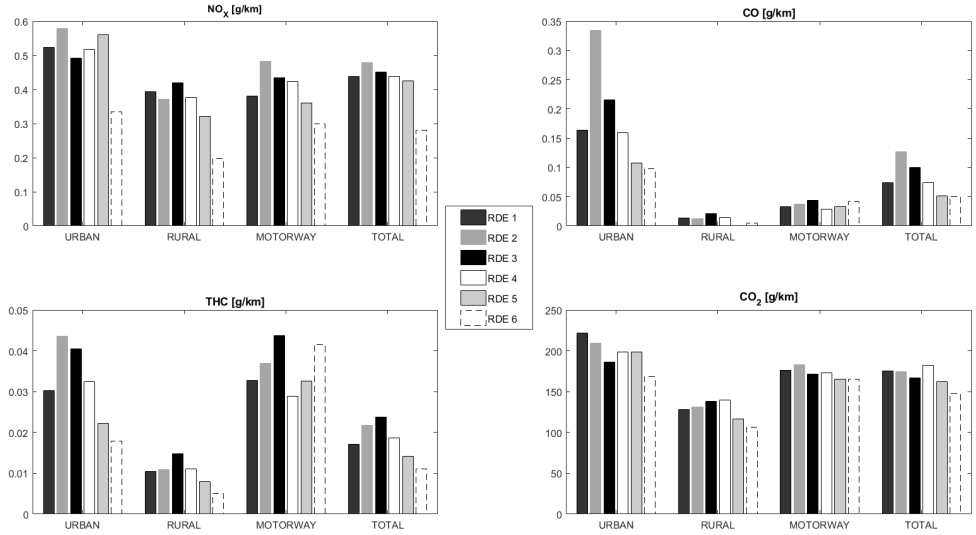

Figure 4.6: Pollutant emissions.

	NO_X	THC	CO	CO_2
	[g/km]			
RDE 1	0.4378	0.0170	0.0738	175.28
RDE 2	0.4778	0.0217	0.1268	174.29
RDE 3	0.4508	0.0234	0.0978	164.15
RDE 4	0.4384	0.0174	0.0685	169.73
RDE 5	0.4241	0.0142	0.0515	162.27
RDE 6	0.2799	0.0110	0.0501	147.34

Table 4.4: RDE pollutants emissions per kilometre.

Figure 4.6 shows a significant dispersion between pollutant emissions. In the case of , NO_X emissions, leaving RDE 6 aside (the driver behaviour was modified), the differences reached up to 17.39% in an urban zone, 30.88% in the rural zone, and 27.10% in the motorway. The total specific emissions showed the maximum difference of 12.74% between RDEs 2 and 5.

THC and CO strongly depended on the engine and aftertreatment temperatures. RDEs 5 and 6, the less-loaded cycles, showed the lowest THC

emissions.

THC and CO emissions are produced due to incomplete combustion under two main circumstances, first when the engine works in cold conditions and second in case of phases with high load or high EGR rates where lambda was even below 1. RDE 2 produced the highest CO emissions, mainly due to the significant contribution in the urban area. This cycle had the lowest urban and total distances, which increased specific emissions per kilometre due to the higher impact of the engine warm-up phase. The other cycles did not show significant differences.

There were also significant differences in the case of CO_2 emissions, with RDEs 1 and 2 producing the highest emissions. The most crucial difference between RDEs 3 and 4 was the average vehicle speed reduction, which implied an increase in fuel consumption. RDE 5 resulted in the lowest CO_2 emission among the cycles with the same driver behaviour (RDE 1 to RDE 5).

RDE 1 was the most representative of real driving since it was directly extracted from a cycle performed on-road. Comparing RDEs 1 and 2, where the results are similar, contributes to the state that a WLTC presents similar dynamic conditions as an RDE cycle since, CO_2 and NO_X emissions showed analogous values.

The comparison between RDEs 5 and 6 led to characterising the effect of the different driver behaviour in the same trip and vehicle speed profile. In the case of RDE 6, NO_X emissions were reduced by 34% compared to RDE 5. Similar reductions were obtained for THC, CO whilst CO_2 emissions were decreased by 9.2%.

The required engine power to reach a certain vehicle speed in a cycle is obtained from the engine speed and torque. Due to the engine speed was reduced in the case of the RDE 6 by varying the shifting procedure, the torque was increased. Figure 4.7 shows the effective engine torque as a function of engine speed for RDEs 5 and 6. RDE 6 dots are closer to the top left corner (high torque and low engine speed).

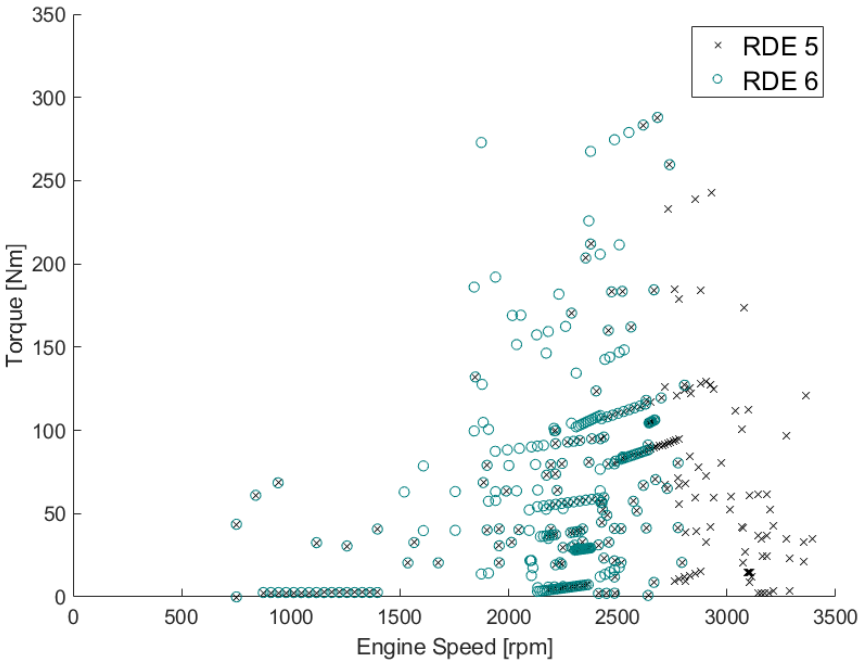

Figure 4.7: RDE 5 and RDE 6 engine map comparison.

According to the driver behaviour, in the case of RDE 5, the engine speed reached higher values while more loaded conditions were characteristic in RDE 6. Figure 4.8 shows three different fractions of RDE 5 and 6 cycles during urban, rural, and motorway driving, where the differences in CO_2 and NO_X emissions can be observed.

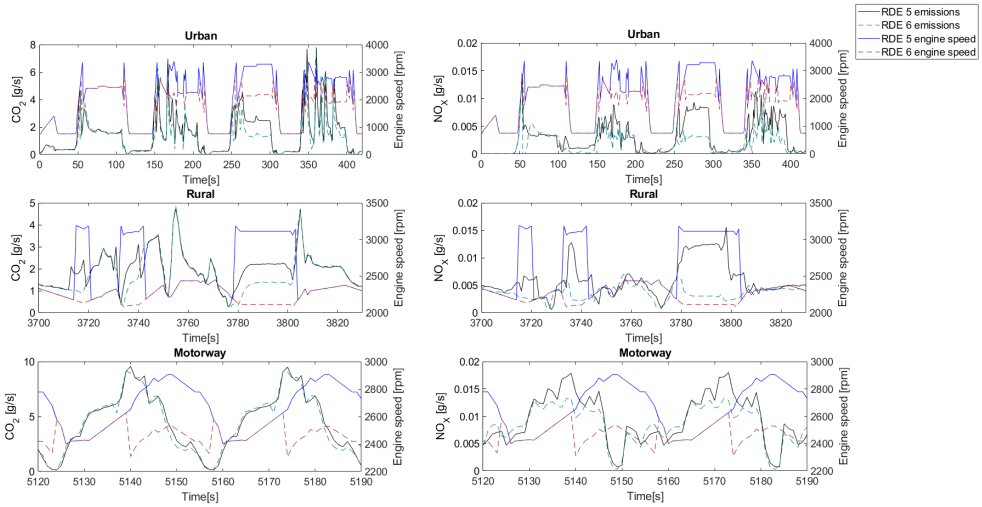

Figure 4.8: Comparison of NO_X, NO_X emissions, and engine speed between RDEs 5 and 6.

Figure 4.8 illustrates emission differences in some specific portions of RDEs 5 and 6 where the engine speed changed. These differences are mainly noticed in urban and rural zones, where the engine speed disparity was more significant. In the case of CO_2 emissions, benefits were obtained in RDE 6, implying a more efficient driving mode at higher loads, with a reduction of 9.20%. Regarding pollutant emissions, this driving behaviour also involved relevant reductions, as shown in Figure 4.6. In the case of NO_X emissions, a non-negligible decrease of 34.01% was obtained.

4.4.2 Tests results versus map results

Additionally, both engines used in this document were widely characterised. In order to do that, several points in the steady-state were measured in all possible engine operating zones.

After these steady-state tests, a comparison of different recorded data between points obtained in these tests and points extracted from RDE was carried out. This analysis will apport the results deviation of the cycles with the steady-state points.

Based on these deviations, the results of an RDE cycle could be estimated without the need to carry out a test, only knowing the driving speed profile and the driver behaviour, in order to know the dynamic requests of the engine.

The main characteristics of both engines where the comparison was performed, were previously listed in Chapter 3 in the table 3.1.

The steady-state studies have several points, concretely the mapping tests of engine A, the range is from 850 to 2850 every 250rpm combined with torque increments of 40Nm from 10 to 250Nm, which is a total of 7 torque levels * 8 engine speed levels + iddle point = 57 points.

The figures 4.9 and 4.10 show the result of this study, regarding CO_2 and NO_X emissions.

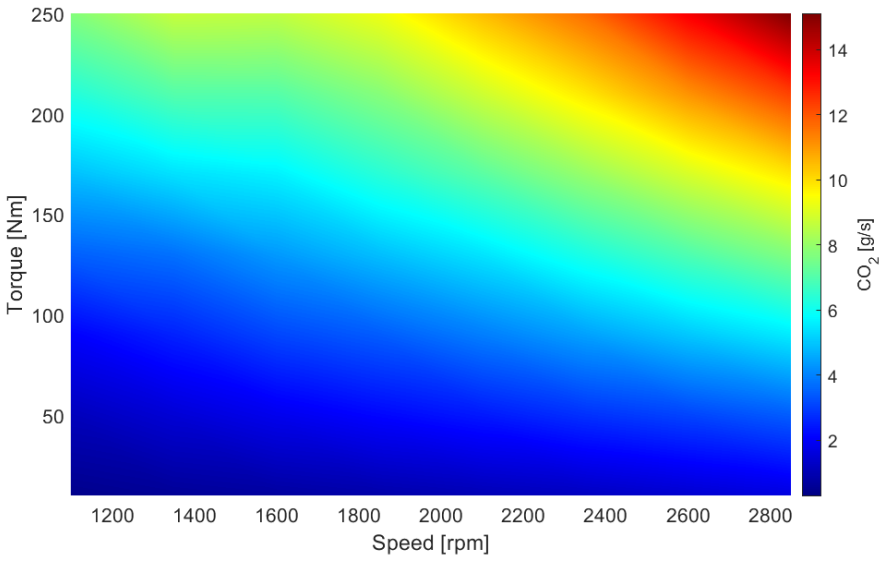

Figure 4.9: CO_2 engine A map study.

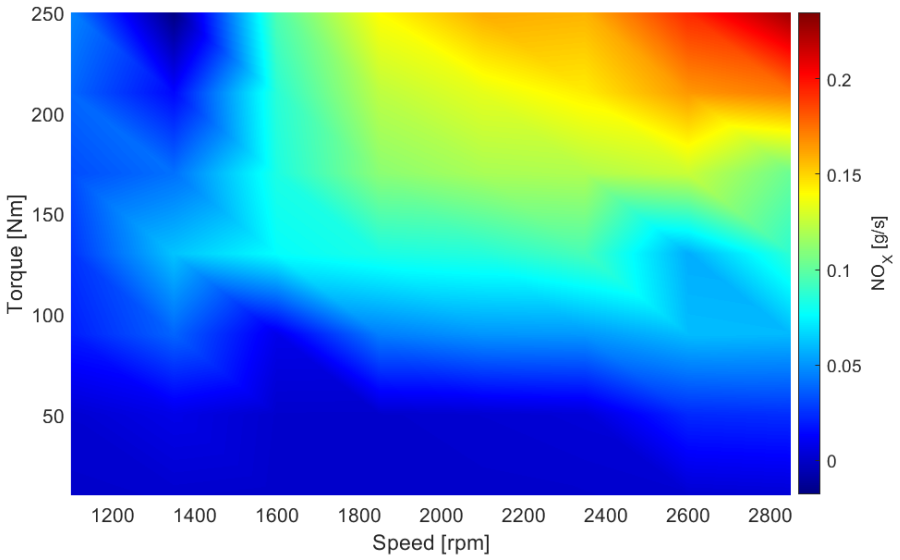

Figure 4.10: NO_X engine A map study.

In the case of engine B, a more exhaustive analysis was carried out, and the methodology has changed. The engine map was split with the throttle position instead of the torque. The points are ranged from 1000 rpm to 3500 rpm every 100 rpm, combined with 0 to 100% of throttle increments of 10%, and also the 15% throttle level, which means 12 throttle levels x 25 engine speed levels, + iddle point = 301 points, and as in engine A, the figures 4.11 and 4.12 show the CO_2 and NO_X emissions of the engine B.

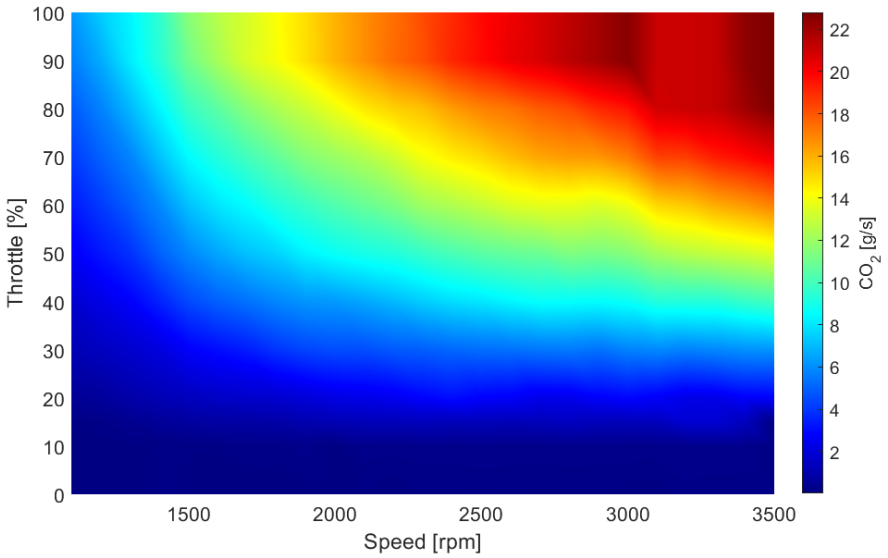

Figure 4.11: CO_2 engine B map study.

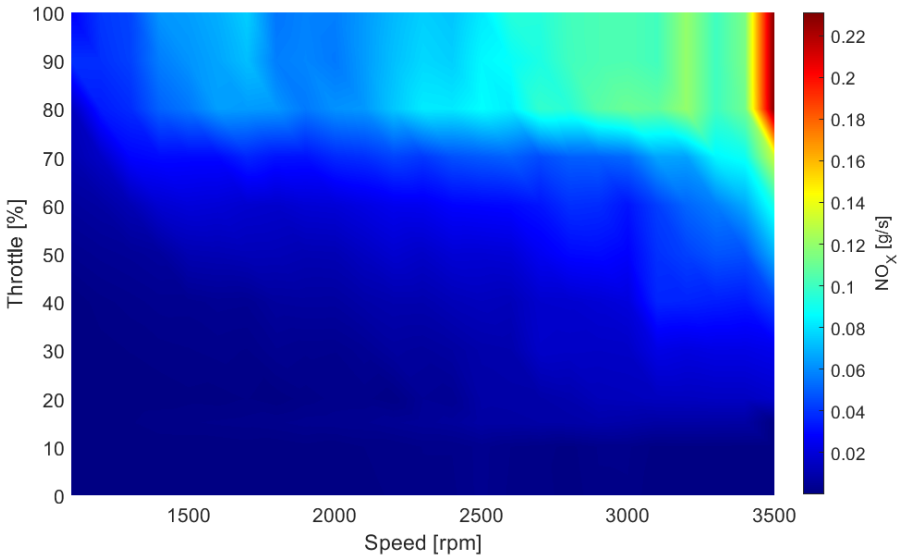

Figure 4.12: NO_X engine B map study.

Thanks to this study, it is possible to estimate different parameters such as temperatures, pressures, valve positions, starts of injections..etc. And also pollutant emissions in all the engine operation zones.

The CO_2 and NO_X map emissions are represented in Figure 4.13. Dots also represent the operating area of RDE 1 on the contour plots, which are devoted to CO_2 and NO_X emissions. As observed in Figure 4.13, the maximum CO_2 emission was located in the top right corner, while the minimum was at the bottom left. However, Figure 4.13 shows how NO_X emissions were mainly influenced by the EGR rate, which is different depending on the operative engine conditions, although it can be affirmed that the higher load and speed the NO_X emissions increase.

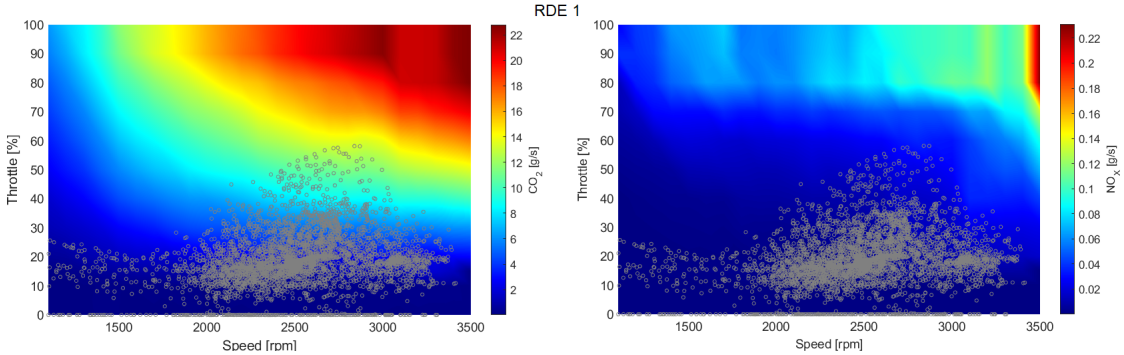

Figure 4.13: CO_2 [g/s] and NO_X [g/s] emission from engine maps (color scale) and those obtained from the tested cycle (dots).

After performing the engine mapping study under steady-state conditions, a comparative analysis of CO_2 and NO_X with emissions from the RDE tests. In order to do that, as regulation imposes, the RDE cycles were recorded with a frequency of 1Hz. Using the engine speed and the torque or throttle position every second, it is possible to get this point into the map, which will be surrounded by four points, and through linear interpolation, the desired value is obtained, the figure 4.14 shows this process. In the first place, the RDE point is plotted on the map, later two points up and down of the map are generated, taking into account its proximity to the contiguous points, and finally, with these two points, and repeating the process, it is possible to obtain the value of this RDE point for all variables for which there is a stationary map.

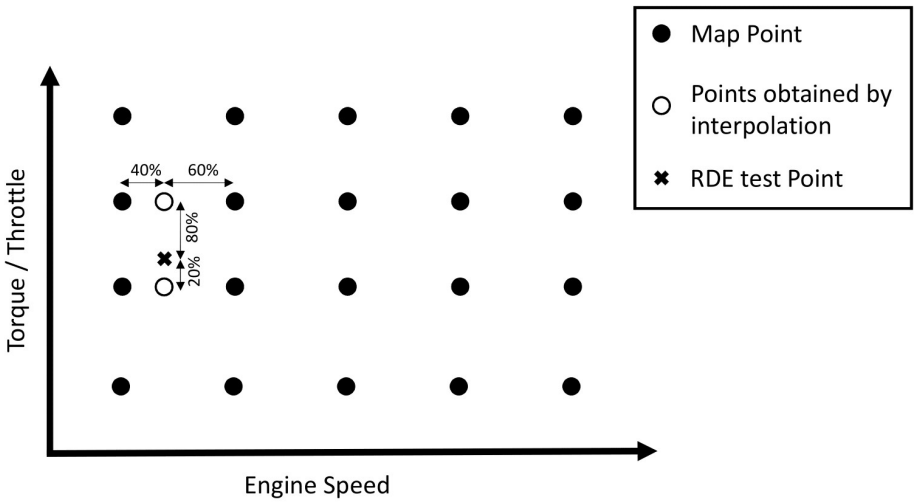

Figure 4.14: Interpolation map process.

This study were performed in engine A and engine B, with their respective vehicle simulations. The main and significant objective of this comparison is to get the discrepancies in total emissions, when they are obtained from a real cycle or when they are calculated through steady-state points.

In the first place, there are represented the CO_2 and NO_X emissions of engine A in figures 4.15 and 4.16 respectively.

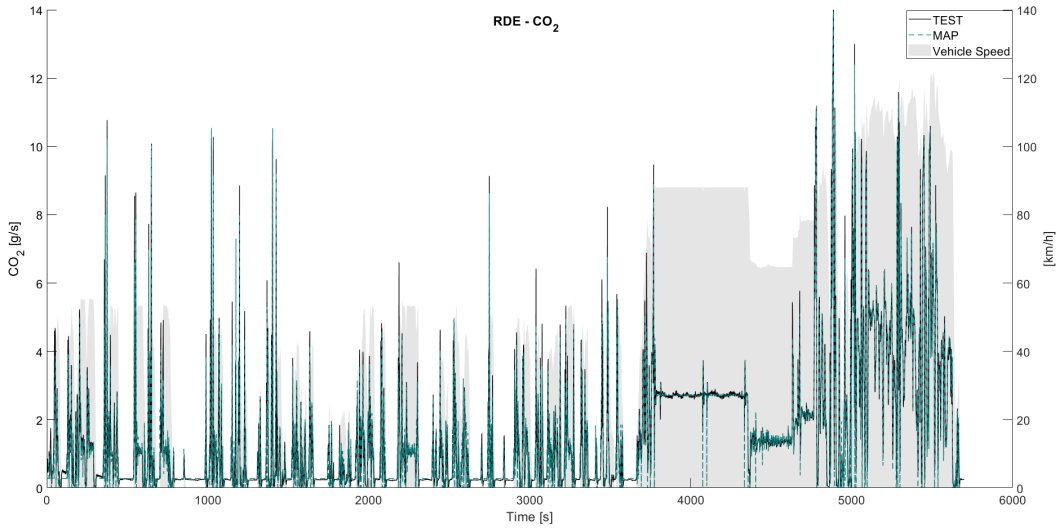

Figure 4.15: Engine A RDE CO_2 [g/s] emissions test versus engine map.

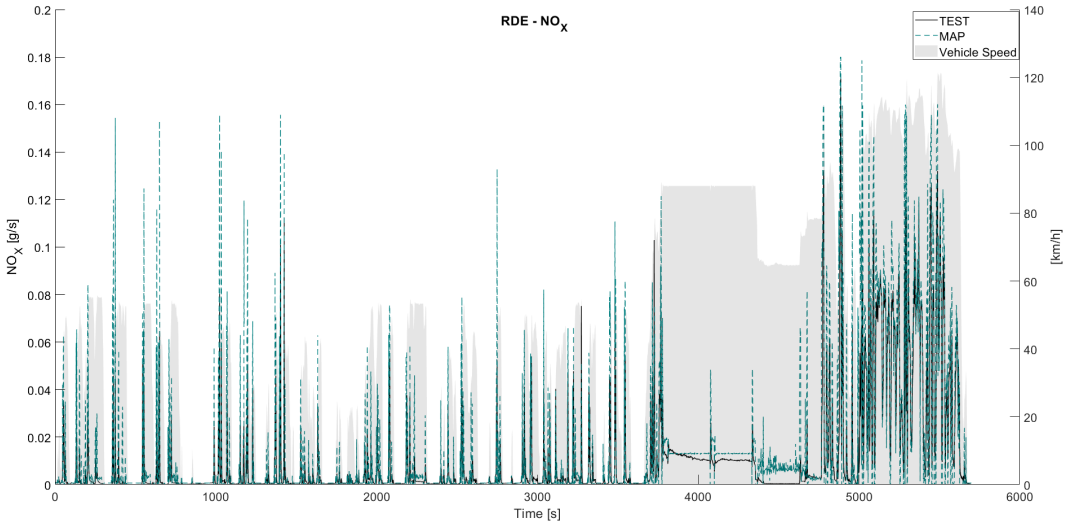

Figure 4.16: Engine A RDE NO_X [g/s] emissions test versus engine map.

Figures 4.17 and 4.18 show the instantaneous CO_2 and NO_X emissions of RDE 1 versus the emissions obtained by interpolation in the engine maps.

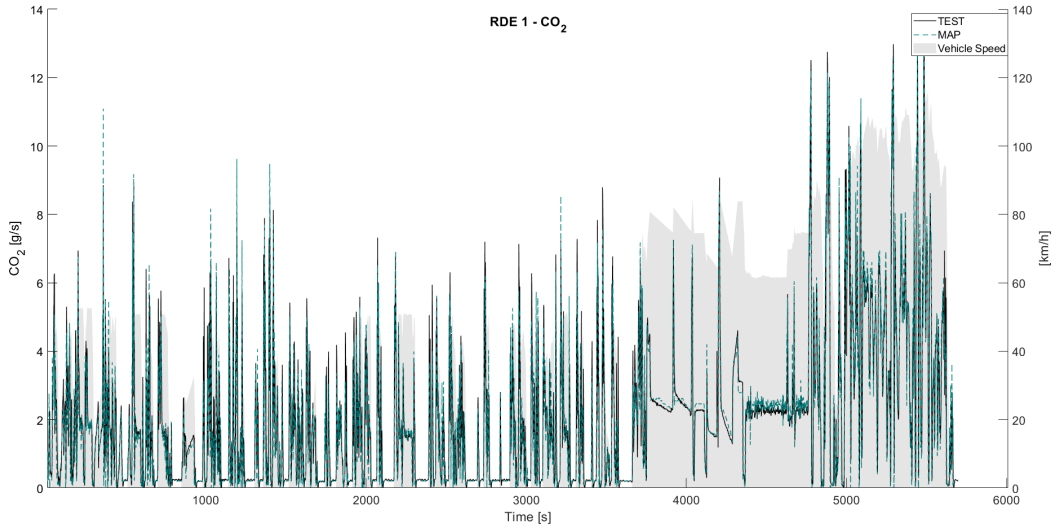

Figure 4.17: Engine B RDE 1 CO_2 [g/s] emissions test versus engine map.

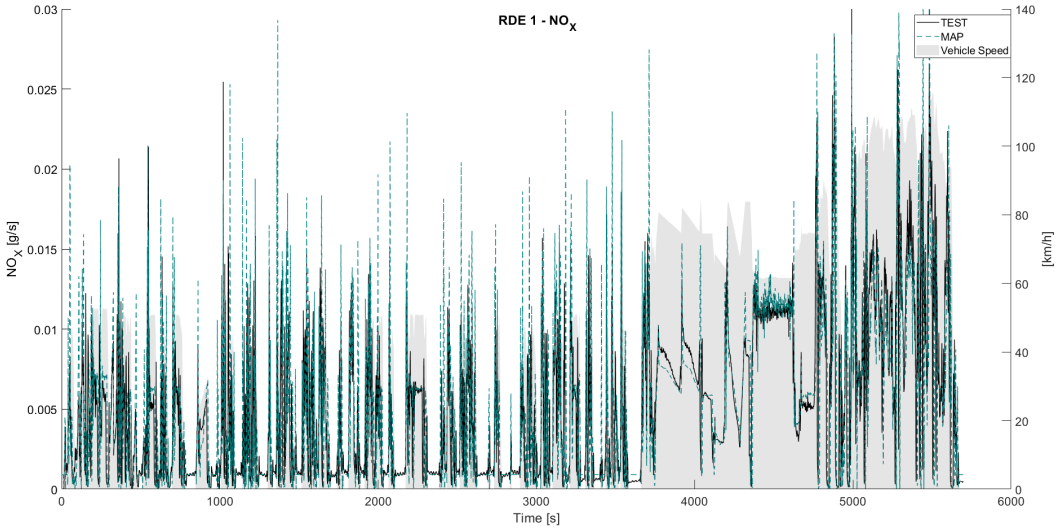

Figure 4.18: Engine B RDE 1 NO_X [g/s] emissions test versus engine map.

As can be observed, especially in the case of engine B, there is a good correlation between emissions obtained in the test and the emissions from the

steady-state map study, however, in the case of engine A and specifically in NO_X, this correlation is not as exact. The divergencies are produced due to different reasons, the first and the main are produced due to interpolations errors, especially in the case of NO_X since, these do not have a total linear behaviour. Other discrepancies are explained due to the dynamics of the cycle since, the combustion processes change compared to the steady-state test, the more transient the RDE cycle is.

Table 4.5 list the final emissions obtained in the test plotted in the figures 4.15, 4.16, 4.17 and 4.18.

	CO2 [kg]			**NOX [g]**		
	Test	**Map**	ϵ_{CO2}	**Test**	**Map**	ϵ_{NOx}
ENGINE A	9.125	8.791	-3.65%	58.732	80.031	36.26%
ENGINE B	11.56	11.38	-1.61%	28.88	29.32	1.50%

Table 4.5: CO_2 and NO_X pollutants from RDE cycles versus map emissions in the engines A and B

As can be observed, the correlation improves considerably in the study performed in engine B, especially in the case of NO_X emissions. It happens as a consequence of the number of points performed in each one of the steady-state studies, concretely 301 points in engine B instead of 56 in engine B since, fewer points in the interpolation cause more significant errors. However, it would be necessary to find a balance between the number of points and an acceptable error since, performing a too extensive map would require high time and cost.

During the steady-state tests, multiple variables were recorded and additionally, AMF, FMF, outlet compressor pressure (P2), and inlet turbine pressure (P3) were compared with the RDE 1 results in engine B. Figures 4.19, 4.20, 4.21, 4.22 shows the AMF, FMF, P2, and P3 comparison respectively.

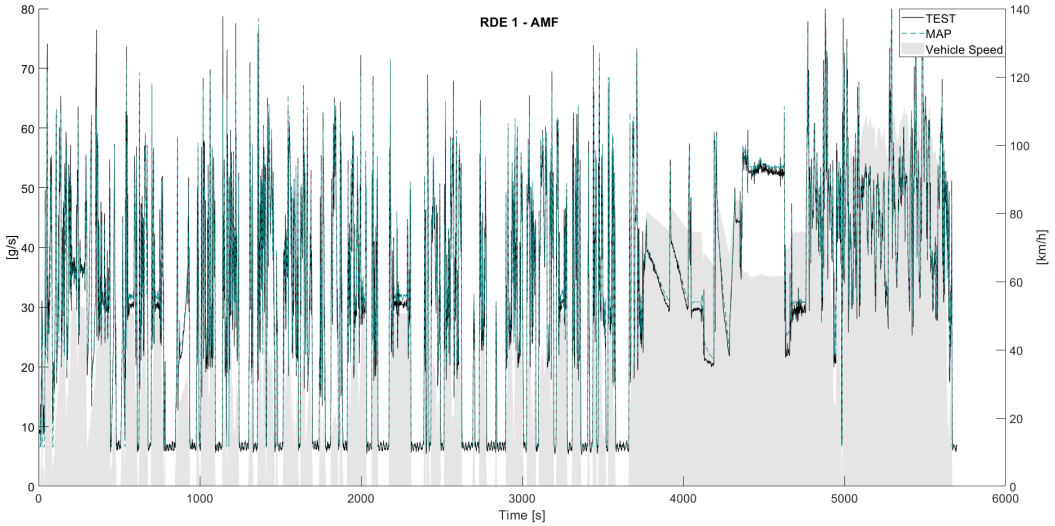

Figure 4.19: Engine B RDE 1 AMF [g/s] test versus engine map.

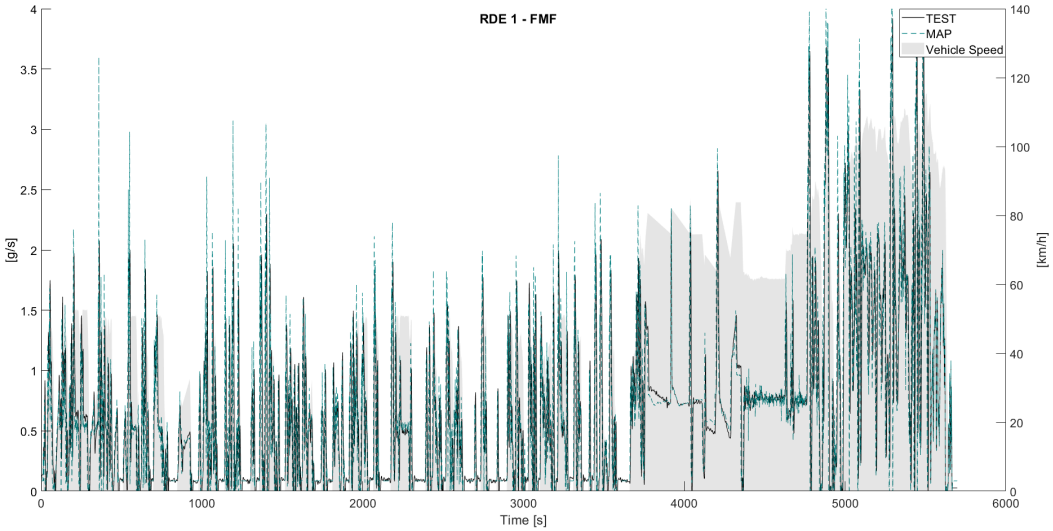

Figure 4.20: Engine B RDE 1 FMF [g/s] test versus engine map.

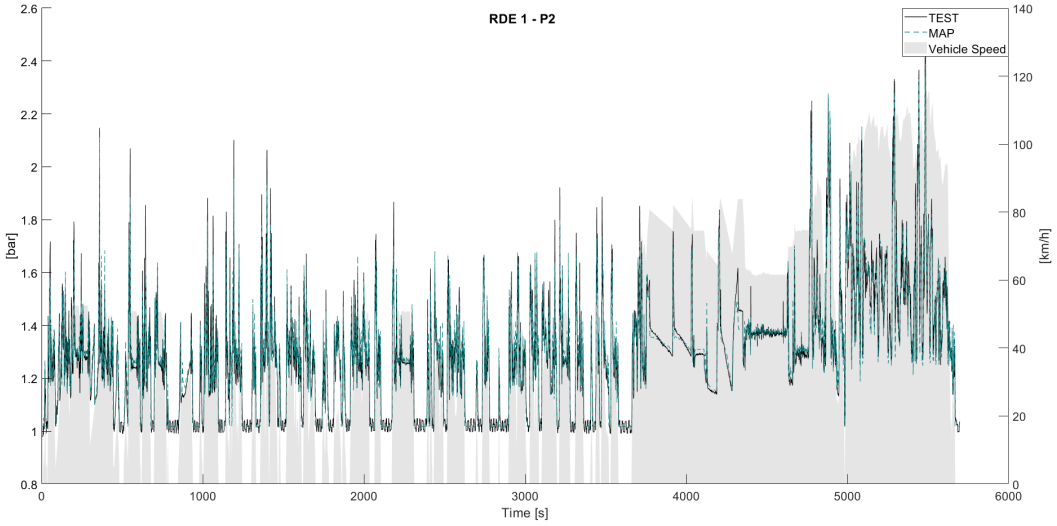

Figure 4.21: Engine B RDE 1 P2 [bar] test versus engine map.

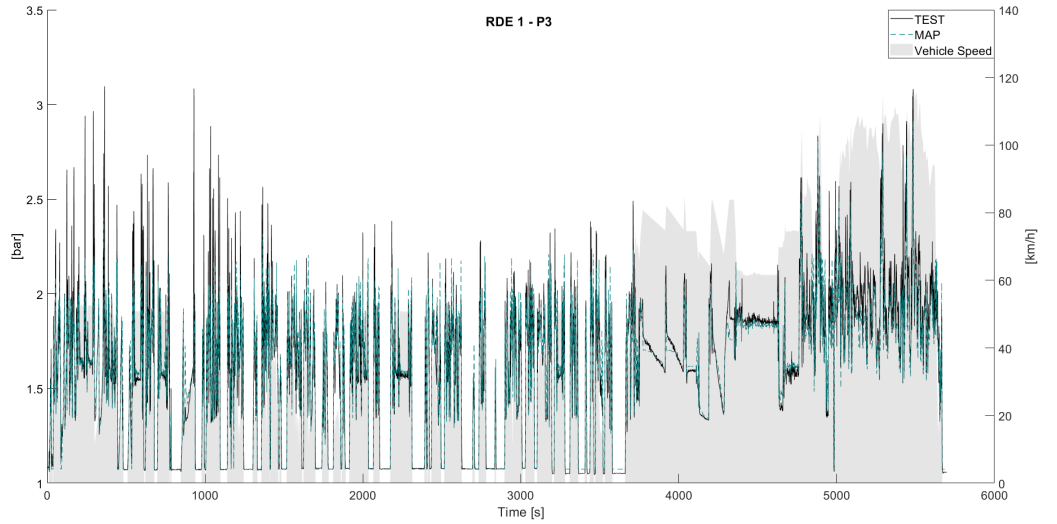

Figure 4.22: Engine B RDE 1 P3 [bar] test versus engine map.

In this case, applying the same methodology to calculate errors of the Chapter 3, with the equation 3.11, which is a modification of the original

definition of the Symmetric Mean Average Percentage Error (SMAPE) defined by Flores [74], the error of each variable is presented in the table 4.6.

	AMF	**FMF**	**P2**	**P3**
Error [%]	2.47%	5.81%	1.52%	2.04%

Table 4.6: AMF, FMF, P2, and P3 RDE 1 cycle versus map emissions in the engine B

As can be observed, very low errors were obtained, the highest error belongs to the FMF, like in the Chapter 3, and as it was explained, it is due to fast variations and the acquisition frequency. Analysing the cumulated values of the fuel mass consumption, the discrepancies are lower, being around 2.1%. Similar value to those found in CO_2.

This assessment would confirm even more the feasibility of this method to analyse RDE cycles through steady-state points.

Making a deeper analysis in the engine B, figures 4.23 (a to c) and 4.24 (a to c) show three fractions of 150 seconds of CO_2 and NO_X emissions in RDE 1 corresponding to urban, rural, and motorway driving phases respectively. Absolutes differences between emission concentrations in dynamic and steady operation are presented in Figures 4.23 (d to f) and 4.24(d to f). Finally, Figures 4.23 (g to i) and 4.24(g to i) represent the distribution of the emissions absolute error for these species.

It is also possible to affirm that, urban zones show the worst correlation due to their more dynamic feature. However, rural and motorway zones were characterised by quasi-steady operation, so better correspondence was obtained between RDE and steady-state maps, especially for fuel consumption.

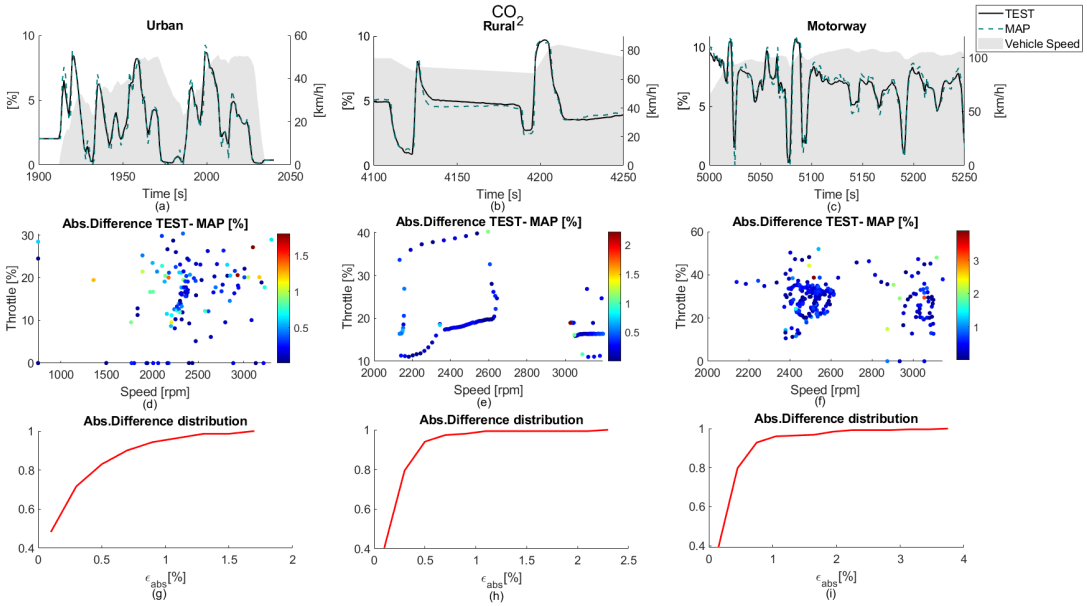

Figure 4.23: CO_2 emissions comparison between RDE 1 and engine map in (a) urban, rural, and motorway driving phases.

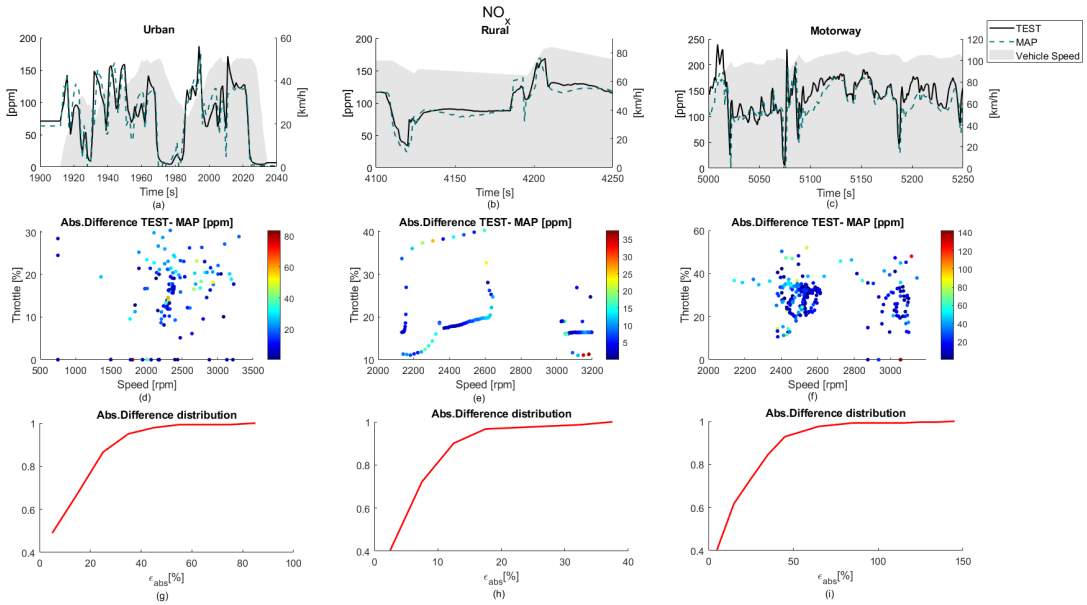

Figure 4.24: NO_X emissions comparison between RDE 1 and engine map in (a) urban, rural, and motorway driving phases.

Table 4.7 shows the comparison of the CO_2 and NO_X emissions data for all tested RDEs. The corresponding errors are also presented. This summary of the results points out minimal differences between pollutants measured during the tests and pollutants extracted from a steady-state engine map. In the case of CO_2 emissions, the correlation is better, having errors around 1%, which fell into the measurement error margin of the measuring device. In the case of NO_X emissions, the deviation from the engine map estimate increases. However, it was still low enough to understand the effects of the driving cycles as a function of their definition, especially considering the use of state-of-the-art NO_X aftertreatment systems of high conversion efficiency.

	CO_2 [kg]			NO_X [g]		
	Test	**Map**	ϵ_{CO2}	**Test**	**Map**	ϵ_{NOx}
RDE 1	11.56	11.38	-1.61%	28.89	29.32	1.50%
RDE 2	11.36	11.21	-1.34%	31.16	30.04	-3.62%
RDE 3	11.68	11.82	1.19%	32.08	33.28	3.74%
RDE 4	12.21	12.38	1.34%	31.55	31.96	1.31%
RDE 5	10.66	10.57	-0.77%	27.85	28.87	3.65%
RDE 6	9.68	9.61	0.79%	18.38	17.57	4.39%

Table 4.7: CO_2 and NO_X pollutants from RDE cycles versus map emissions.

Looking at CO_2 errors in table 4.7, the most significant errors were found in RDEs 1, 2, 3, and 4 cycles, where the specific emissions were also maximum. On the contrary, RDEs 5 and 6 presented the lowest errors. These results agree with the dynamic solicitations of the cycles since, RDEs 5 and 6 were generated to be less aggressive than RDEs 1 to 4. A clear tendency was not found in the case of NO_X errors. In any case, differences were kept below 5% in all cases.

For a more comprehensive analysis, to discern the importance of the number of points in obtaining emissions from the steady-state tests, an additional study was performed on engine B. Firstly, the points with 15% of throttle were removed, and in the second step, alternative engine speeds were also removed to reduce the number of points, in other words, now the regime increments are 200rpm instead of 100rpm. Figures 4.25 and 4.26 show the errors obtained in absolute amounts, in the RDEs 1-6 with three different maps with 301, 275 and 144 points. The study with engine A with 56 points has been plotted, and also the trendlines that best fit in each case with dashed lines along with their respective equations and coefficients of determination or R-squared (R^2).

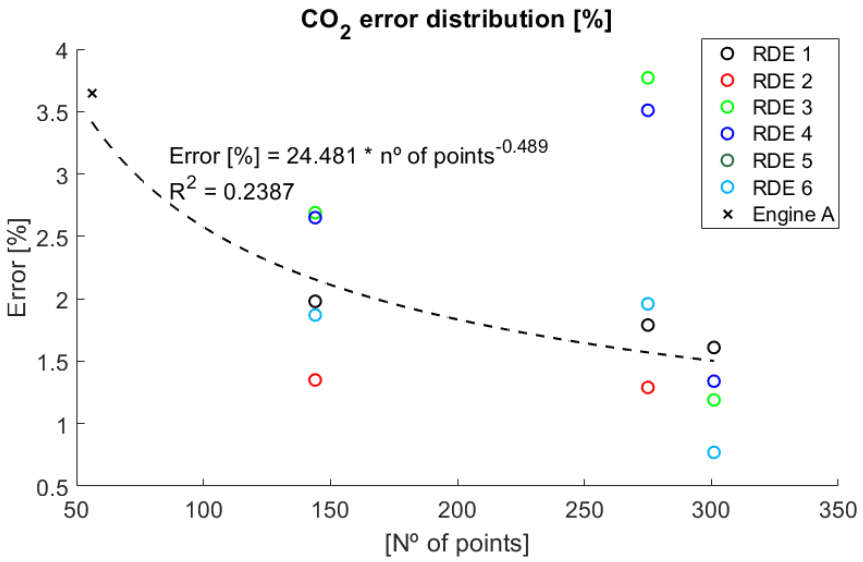

Figure 4.25: CO_2 emission RDE cycles versus three different engine map emissions.

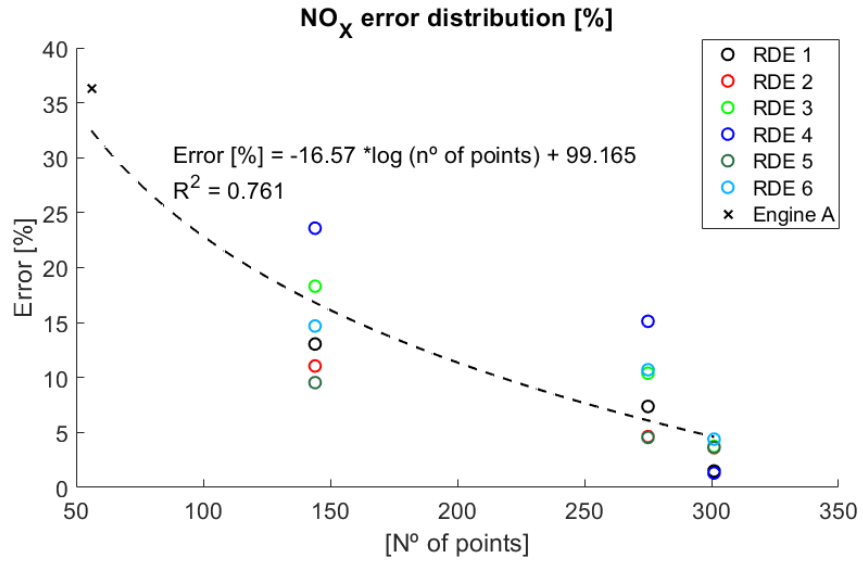

Figure 4.26: NO_X emission RDE cycles versus three different engine map emissions.

Figure 4.25 show that the CO_2 improves with a higher number of points

measured, but the errors with a low quantity of points are not extremely tragic, and the trendline has a low R^2, so in the case of CO_2 the number of points is not so crucial, and the found discrepancies are due to the fact that combustions in RDE conditions are more dynamic and would move away from combustions in a steady-state test.

The NO_X dependency associated with the number of points is much higher, as can be observed in figure 4.26, so the error increases considerably as the number of points on the map decreases. In this case, the NO_X discrepancies are more linked with the interpolation errors, and besides, the R^2 of the trendline, which is high enough, reaffirms it.

Furthermore, analysing both figures 4.25 4.26, removing the points with 15% involves a high discrepancy increment. It is due to different reasons, first, it is a point where the engine works in many phases of the cycle, and second, these points were also performed during the steady-state tests because the engine changes a lot its behaviour in this zone, and therefore the CO_2 and NO_X emissions.

As previously commented, measuring the PM along the entire driving cycle was not possible during the tests. However, three periods of 500 seconds corresponding to three zones (Urban, rural, and motorway) in RDE 1 were considered. Figure 4.27 shows RDE PM mass emissions compared to those obtained from the steady-state map.

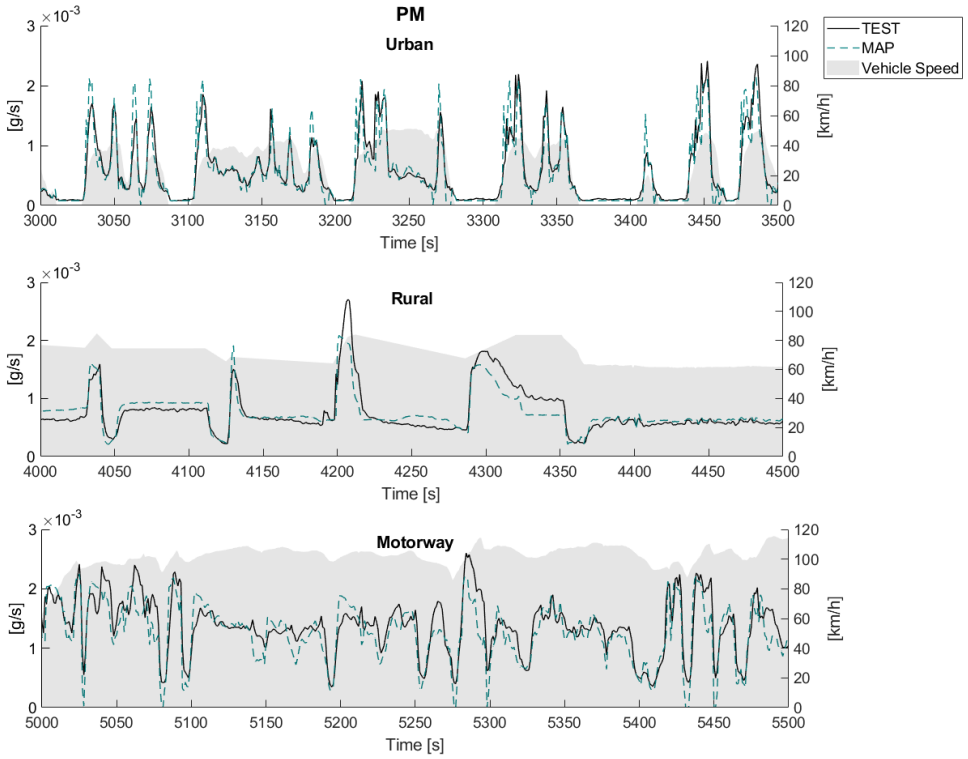

Figure 4.27: RDE 1 periods PM mass emissions [g/s] test versus engine map.

As can be seen in figure 4.27, emissions show a significant correlation between measured emissions and those obtained from the steady-state map. Table 4.8 shows the accumulated values of these three phases and the total values representing their summation.

	PM mass [g]		
	Test	**Map**	ϵ_{PM}
Urban period	0.285	0.276	3.4%
Rural period	0.383	0.385	-0.5%
Motorway period	0.672	0.643	4.4%
TOTAL	1.340	1.303	2.8%

Table 4.8: PM mass emissions from RDE 1 versus map emissions.

Looking at PM differences, the higher discrepancies appear during the urban and motorway periods, which are characterised by more dynamic conditions due to steeper accelerations. In any case, interpolation can also be a beneficial tool to estimate the PM in an RDE cycle since, the obtained errors are relatively low, considering the complexity of this species.

4.5 Conclusions

This study has performed several RDE cycles with different dynamic characteristics on an engine test bench. First, an on-road cycle was performed in a vehicle as a baseline; then, a second cycle was defined using transient manoeuvres extracted from a WLTP cycle; finally, four additional cycles were determined using a computational tool to generate RDE-compliant conditions from a sub-set of acceleration and deceleration ramps, replicating different driver behaviour. This methodology aims at reducing cost, time, and uncertainties involved in performing a cycle on road, such as climatological conditions, PEMS accuracy, traffic status, and driver behaviour. This is particularly relevant for future powertrain systems development since, different technologies or calibration strategies can be assessed more reliably and robustly while ensuring RDE representative conditions.

The results showed how RDE cycles performed with the same driver behaviour produced significant emissions dispersion. For instance, variations of 12.74% in the case of NO_X and 7.42% in CO_2 were found between different cycles. Moreover, a significant improvement was seen from an emissions perspective when the gear shift was adjusted to achieve lower engine speed. Particularly, drawdowns in NO_X and CO_2 emissions of 34% and 9.2%, respectively, were noted. Instead, CO and THC emissions were mainly linked to the engine and after-treatment temperature, so the best results are achieved when the engine load increases.

Finally, an attempt was made to estimate the cycle emissions from steady-state tests. The comparison between such estimation and the actual RDE test emissions showed a good correlation, within 1.6% accuracy for CO_2 and 4.6% in the case of NO_X. The deviations observed were due to two phenomena: on one hand, all emissions during the engine warm-up period differ from the estimations since, the engine map was performed after a warming-up period. On the other hand, concerning the particular case of NO_X emissions, the re-

sults show a non-linear behaviour as a function of speed and load, inducing an uncertainty linked to the interpolation inside the steady-state map. This uncertainty could be reduced by performing a complete engine map, which lowers variations of speed and load between adjacent points but at the cost of higher test bench time. In any case, the analysis performed in this study confirms that steady-state maps can be used to provide a meaningful approximation of these emissions during a realistic certification cycle.

Chapter 4 Bibliography

[1] J. M. Luján, V. Bermudez, B. Pla, and F. Redondo. "Engine test bench feasibility for the study and research of real driving cycles: Pollutant emissions uncertainty characterization". *International Journal of Engine Research* 0(0) (2021), p. 0. DOI: 10.1177/14680874211007999 (cit. on pp. xi, 56, 112).

[51] T. Bodisco and A. Zare. "Practicalities and driving dynamics of a real driving emissions (RDE) Euro 6 regulation homologation test". *Energies* 12(12) (2019), p. 2306 (cit. on pp. 8, 53, 56).

[54] R. Varella, B. Giechaskiel, L. Sousa, and G. Duarte. "Comparison of portable emissions measurement systems (PEMS) with laboratory grade equipment". *Applied Sciences* 8(9) (2018), p. 1633 (cit. on pp. 8, 56).

[64] *COMMISSION REGULATION (EU) 2018/1832 of 5 November 2018 amending Directive 2007/46/EC of the European Parliament and of the Council, Commission Regulation (EC) No 692/2008 and Commission Regulation (EU) 2017/1151 for the purpose of improving the emission type approval tests and procedures for light passenger and commercial vehicles, including those for in-service conformity and real-driving emissions and introducing devices for monitoring the consumption of fuel and electric energy.* 2018. URL: https://eur-lex.europa.eu/legal-content/EN/TXT/HTML/?uri=CELEX:32018R1832\&from=EN (cit. on pp. 20, 24, 40, 56, 99).

[66] J. M. Luján, V. Bermúdez, V. Dolz, and J. Monsalve-Serrano. "An assessment of the real-world driving gaseous emissions from a Euro 6 light-duty diesel vehicle using a portable emissions measurement system

(PEMS)". *Atmospheric Environment* 174 (2018), pp. 112–121 (cit. on pp. 20, 35, 58).

[74] B. E. Flores. "A pragmatic view of accuracy measurement in forecasting". *Omega* 14(2) (1986), pp. 93–98. URL: https://ideas.repec.org/a/eee/jomega/v14y1986i2p93-98.html (cit. on pp. 47, 83).

[75] J Merkisz and J Pielecha. "Comparison of Real Driving Emissions tests". *IOP Conference Series: Materials Science and Engineering* 421 (2018), p. 042055. DOI: 10.1088/1757-899x/421/4/042055. URL: https://doi.org/10.1088/1757-899x/421/4/042055 (cit. on p. 56).

[76] M. Andrych-Zalewska, Z. Chlopek, J. Merkisz, and J. Pielecha. "Investigations of Exhaust Emissions from a Combustion Engine under Simulated Actual Operating Conditions in Real Driving Emissions Test". *Energies* 14(4) (2021). ISSN: 1996-1073. DOI: 10.3390/en14040935. URL: https://www.mdpi.com/1996-1073/14/4/935 (cit. on p. 56).

[77] K. Kurtyka and J. Pielecha. "The evaluation of exhaust emission in RDE tests including dynamic driving conditions". *Transportation Research Procedia* 40 (2019). TRANSCOM 2019 13th International Scientific Conference on Sustainable, Modern and Safe Transport, pp. 338–345. ISSN: 2352-1465. DOI: https://doi.org/10.1016/j.trpro.2019.07.050. URL: https://www.sciencedirect.com/science/article/pii/S2352146519302121 (cit. on p. 56).

[78] J. M. Luján, C. Guardiola, B. Pla, and V. Pandey. "Impact of driving dynamics in RDE test on NOx emissions dispersion". *Proceedings of the Institution of Mechanical Engineers, Part D: Journal of Automobile Engineering* 234(6) (2020), pp. 1770–1778. DOI: 10.1177/0954407019881581. eprint: https://doi.org/10.1177/0954407019881581. URL: https://doi.org/10.1177/0954407019881581 (cit. on p. 56).

[79] T. Donateo, M. Giovinazzi, and A. Tamborrino. "Reproducing Real World Emission Tests with a Traffic Simulator" (2018). ISSN: 0148-7191. DOI: https://doi.org/10.4271/2018-37-0001. URL: https://doi.org/10.4271/2018-37-0001 (cit. on p. 56).

[80] M. Lyu, X. Bao, Y. Wang, and R. Matthews. "Analysis of emissions from various driving cycles based on real driving measurements obtained in a high-altitude city". *Proceedings of the Institution of Mechanical Engineers, Part D: Journal of Automobile Engineering* 234(6) (2020), pp. 1563–1571. DOI: 10.1177/0954407019898959. eprint:

https://doi.org/10.1177/0954407019898959. URL: https://doi.org/10.1177/0954407019898959 (cit. on p. 56).

[81] J. Czerwinski, Y. Zimmerli, A. Hüssy, D. Engelmann, P. Bonsack, E. Remmele, and G. Huber. "Testing and evaluating real driving emissions with PEMS". *Combustion Engines* 174(3) (2018), pp. 17–25. ISSN: 2300-9896. DOI: 10.19206/CE-2018-302. URL: https://doi.org/10.19206/CE-2018-302 (cit. on p. 56).

[82] J. Gallus, U. Kirchner, R. Vogt, and T. Benter. "Impact of driving style and road grade on gaseous exhaust emissions of passenger vehicles measured by a Portable Emission Measurement System (PEMS)". *Transportation Research Part D: Transport and Environment* 52 (2017), pp. 215–226. ISSN: 1361-9209. DOI: https://doi.org/10.1016/j.trd.2017.03.011. URL: https://www.sciencedirect.com/science/article/pii/S1361920916306769 (cit. on p. 56).

[83] L. Zhang, X. Hu, R. Qiu, and J. Lin. "Comparison of real-world emissions of LDGVs of different vehicle emission standards on both mountainous and level roads in China". *Transportation Research Part D: Transport and Environment* 69 (Apr. 2019), pp. 24–39. DOI: 10.1016/j.trd.2019.01.020 (cit. on p. 56).

[84] M. Faria, G. Duarte, R. Aliandro Varella, T. Farias, and P. Baptista. "How do road grade, road type and driving aggressiveness impact vehicle fuel consumption? Assessing potential fuel savings in Lisbon, Portugal". *Transportation Research Part D Transport and Environment* 72 (July 2019), pp. 148–161. DOI: 10.1016/j.trd.2019.04.016 (cit. on p. 56).

[85] G. Triantafyllopoulos, D. Katsaounis, D. Karamitros, L. Ntziachristos, and Z. Samaras. "Experimental assessment of the potential to decrease diesel NOx emissions beyond minimum requirements for Euro 6 Real Drive Emissions (RDE) compliance". *The Science of the total environment* 618 (Oct. 2017). DOI: 10.1016/j.scitotenv.2017.09.274 (cit. on p. 56).

[86] M. Andrych-Zalewska, Z. Chlopek, J. Merkisz, and J. Pielecha. "Research on Exhaust Emissions in Dynamic Operating States of a Combustion Engine in a Real Driving Emissions Test". *Energies* 14(18) (2021). ISSN: 1996-1073. DOI: 10.3390/en14185684. URL: https://www.mdpi.com/1996-1073/14/18/5684 (cit. on p. 56).

[87] A. T. Zachiotis and E. G. Giakoumis. "Non-regulatory parameters effect on consumption and emissions from a diesel-powered van over the WLTC". *Transportation Research Part D: Transport and Environment* 74 (2019), pp. 104–123. ISSN: 1361-9209. DOI: https://doi.org/10.1016/j.trd.2019.07.019. URL: https://www.sciencedirect.com/science/article/pii/S1361920919302731 (cit. on p. 56).

[88] Y. Zhiwen, Y. Liu, L. Wu, S. Martinet, Y. Zhang, M. Andre, and H. Mao. "Real-world gaseous emission characteristics of Euro 6b light-duty gasoline- and diesel-fueled vehicles". *Transportation Research Part D: Transport and Environment* 78 (Jan. 2020), p. 102215. DOI: 10.1016/j.trd.2019.102215 (cit. on p. 56).

[89] A. Taborda, R. Varella, T. Farias, and G. Duarte. "Evaluation of technological solutions for compliance of environmental legislation in light-duty passenger: A numerical and experimental approach". *Transportation Research Part D: Transport and Environment* 70 (2019), pp. 135–146. ISSN: 1361-9209. DOI: https://doi.org/10.1016/j.trd.2019.04.004. URL: https://www.sciencedirect.com/science/article/pii/S136192091830720X (cit. on p. 56).

[90] A. Broatch, X. Margot, A. Gil, E. Galindo, and R. Soler. "Definition of wind blowers for vehicles testing at chassis-dyno facilities using a CFD approach". *Transportation Research Part D: Transport and Environment* 55 (2017), pp. 99–112. ISSN: 1361-9209. DOI: https://doi.org/10.1016/j.trd.2017.06.029. URL: https://www.sciencedirect.com/science/article/pii/S1361920917300068 (cit. on p. 56).

[91] J. Rodríguez-Fernández, J. J. Hernández, Ángel Ramos, and A. Calle-Asensio. "Fuel economy, NOx emissions and lean NOx trap efficiency: Lessons from current driving cycles". *International Journal of Engine Research* (2021). DOI: https://doi.org/10.1177/14680874211005080 (cit. on pp. 56, 99).

[92] J. Claßen, S. Krysmon, F. Dorscheidt, S. Sterlepper, and S. Pischinger. "Real Driving Emission Calibration—Review of Current Validation Methods against the Background of Future Emission Legislation". *Applied Sciences* 11(12) (2021). ISSN: 2076-3417. DOI: 10.3390/app11125429. URL: https://www.mdpi.com/2076-3417/11/12/5429 (cit. on p. 56).

[93] B. Giechaskiel et al. "Inter-Laboratory Correlation Exercise with Portable Emissions Measurement Systems (PEMS) on Chassis Dynamometers".

Applied Sciences 8(11) (2018). ISSN: 2076-3417. DOI: 10.3390/app8112275. URL: https://www.mdpi.com/2076-3417/8/11/2275 (cit. on p. 56).

[94] R. Suarez-Bertoa, M. Pechout, M. Vojtíšek, and C. Astorga. "Regulated and Non-Regulated Emissions from Euro 6 Diesel, Gasoline and CNG Vehicles under Real-World Driving Conditions". *Atmosphere* 11(2) (2020). ISSN: 2073-4433. DOI: 10.3390/atmos11020204. URL: https://www.mdpi.com/2073-4433/11/2/204 (cit. on p. 56).

[95] J. Czerwiński, P. Comte, Y. Zimmerli, and F. Reutimann. "Testing emissions of passenger cars in laboratory and on-road (PEMS, RDE)". *Combustion Engines* 166(3) (2016), pp. 17–23. ISSN: 2300-9896. DOI: 10.19206/CE-2016-326. URL: https://doi.org/10.19206/CE-2016-326 (cit. on p. 56).

[96] K. Tucki. "A Computer Tool for Modelling CO2 Emissions in Driving Tests for Vehicles with Diesel Engines". *Energies* 14(2) (2021). ISSN: 1996-1073. DOI: 10.3390/en14020266. URL: https://www.mdpi.com/1996-1073/14/2/266 (cit. on p. 57).

[97] L. Thibault, P. Degeilh, O. Lepreux, L. Voise, G. Alix, and G. Corde. "A new GPS-based method to estimate real driving emissions" (2016), pp. 1628–1633. DOI: 10.1109/ITSC.2016.7795776 (cit. on p. 57).

[98] P. Fernandes, E. Macedo, B. Bahmankhah, R. Tomas, J. Bandeira, and M. Coelho. "Are internally observable vehicle data good predictors of vehicle emissions?" *Transportation Research Part D: Transport and Environment* 77 (2019), pp. 252–270. ISSN: 1361-9209. DOI: https://doi.org/10.1016/j.trd.2019.11.004. URL: https://www.sciencedirect.com/science/article/pii/S1361920919308557 (cit. on p. 57).

[99] C. Guardiola, B. Pla, P. Bares, E. Chappell, and R. Burke. "Improving CO2 emission assessment of diesel-based powertrains in dynamic driving cycles by data fusion techniques". *Proceedings of the Institution of Mechanical Engineers, Part D: Journal of Automobile Engineering* 235(2-3) (2021), pp. 362–372. DOI: 10.1177/0954407020949477. eprint: https://doi.org/10.1177/0954407020949477. URL: https://doi.org/10.1177/0954407020949477 (cit. on p. 57).

[100] T. Donateo and M. Giovinazzi. "Building a cycle for Real Driving Emissions". *Energy Procedia* 126 (2017). ATI 2017 - 72nd Conference of the Italian Thermal Machines Engineering Association, pp. 891–898.

ISSN: 1876-6102. DOI: https://doi.org/10.1016/j.egypro.2017.08.307. URL: https://www.sciencedirect.com/science/article/pii/S1876610217338213 (cit. on p. 58).

[101] H. S. Chong, Y. Park, S. Kwon, and Y. Hong. "Analysis of real driving gaseous emissions from light-duty diesel vehicles". *Transportation Research Part D: Transport and Environment* 65 (2018), pp. 485–499. ISSN: 1361-9209. DOI: https://doi.org/10.1016/j.trd.2018.09.015. URL: https://www.sciencedirect.com/science/article/pii/S1361920918304395 (cit. on p. 65).

[102] K. T., H. Y., N. K., and T. Toda. ""High Efficiency Diesel Engine with Low Heat Loss Combustion Concept - Toyota's Inline 4-Cylinder 2.8-Liter ESTEC 1GD-FTV Engine". *SAE Technical Paper 2016-01-0658* (2016). DOI: https://doi.org/10.4271/2016-01-0658 (cit. on p. 66).

Chapter 5

RDE assessment under different temperatures scenarios

Contents

5.1 Introduction

In 1946, the Russian physicist Yákov Borísovich Zeldóvich [103] postulated the thermal mechanism of NO_X generation. It has a strong temperature dependence [104]. The following chemical formulas 5.1 describe the extended Zeldovich mechanism.

$$\begin{aligned} N_2 + O &\rightarrow NO + N \\ N + O_2 &\rightarrow NO + O \\ N + OH &\rightarrow NO + H \end{aligned} \tag{5.1}$$

The reactions mentioned above are highly affected by the combustion temperature, so nitrogen oxide (NO) production increases as this temperature increases. There are other less important mechanisms. These are the prompt mechanism by Fenimore[105], the N_2O intermediate mechanism, and the fuel contribution mechanism, which is mainly governed by fuel richness [106, 107].

According to the EEA [108], most atmospheric NO_2 is emitted in the form of NO and later on, it is rapidly oxidised, becoming nitrogen dioxide when it reacts with the atmospheric oxygen. NO_2 in the presence of hydrocarbons and ultraviolet light is the primary tropospheric ozone and nitrates aerosol source. Furthermore, both substances represent a significant fraction of mass particles with a diameter less than 2.5 micrometres, known as PM2,5, found in the ambient air. People exposed to tropospheric ozone can suffer respiratory symptoms, airway inflammation, and lung cancer [109].

In addition, NO_X interacts with water, oxygen and other chemicals in the atmosphere that can form acid rain [110], which can harm sensitive ecosystems such as lakes and forests. Another possible effect is produced by the nitrate particles resulting from NO_X, making hazy air challenging to see through.

For a given technology, pollutant emissions are also influenced by ambient conditions. As mentioned above, combustion temperature directly influences the production of NO_2 and NO [111]. Among other parameters, the combustion temperature is influenced by the intake temperature. Consequently, it is expected that the emissions of the engines will also be different when operating under different temperature conditions. Given that the regulation allows the type-approval tests to be carried out in a wide ambient temperature range,

as will be indicated later, the final emission values collected from the same engine and route may differ considerably if the ambient temperatures where the tests are carried out are different.

Along with the direct effect of temperature on emissions, engines can automatically modify calibration conditions, which can also affect pollutant emissions.

Current RDE regulation [64] establishes that the test shall be conducted within a specified ambient temperature range. Moderate temperature conditions were set when the ambient temperature is greater than or equal to 0°C and lower than or equal to 30 °C. Extended temperature conditions are considered for temperatures between -7°C and 0°C and from 30°C to 35°C. There are essential variations in RDE tests under different ambient temperatures [112] [113]. Suppose this temperature range is wider, arriving at extreme temperatures. In that case, it can lead to large differences in fuel consumption and emissions, as studies already carried out in NEDC and WLTC cycles show [91]. Differences are produced due to the behaviour change of the engine, and the aftertreatment system [114].

Extended conditions can also be reached through altitudes above 700 meters and lower or equal to 1300 meters above sea level. If some part of the RDE cycle or the entire test is performed outside of normal or extended conditions, the test is not considered valid. During a particular phase of the cycle, if temperature, altitude or both enter in extended conditions, pollutant emissions must be divided by 1.6 during this determined interval, except for CO_2 emissions.

Several experimental and modelling studies point out great differences when altitude is modified. On the one hand, the PEMS reduces its efficiency [115] and on the other hand, in the engine behaviour and after treatments systems which implies large variations in emissions and fuel consumption [116] [117] [118], especially during the warm-up period [119] [120].

There are RDE cycles simulation works [121] [122] and previous studies in NEDC and WLTC show great differences when the temperature is modified [123] [124] [91] [125]. In short, RDE procedures involve many boundary conditions that greatly affect emissions [126].

5.2 RDE cycles under different intake temperatures

This section aims to study the influence of intake manifold temperature on pollutant emissions in a diesel engine under RDE conditions. It may be due to an improvement in the efficiency of the WCAC, or the same WCAC with a different ambient temperature, which would change the intake temperature.

Two different RDE tests were carried out having two different WCAC outlet temperatures, so the effect of changing the exhaust WCAC air mass flow temperature (T2') can be studied under the standard control strategies in all tests that were performed. The RDE cycle was previously studied in Chapter 2.

The tests were analysed, focusing on pollutant emissions. The polluting substances evaluated are the THC, NO_X, CO, and the CO_2 emissions strongly linked to fuel consumption.

5.2.1 Material and Methods

The simulated vehicle in the test cell is the vehicle A, described in Chapter 3, which is a C-segment passenger car. This type of vehicle is the second segment sold in 2020, with a market share of 16.97% [127], representing a considerable part of the European fleet. It also used engine A to perform the RDE cycle.

It was developed under Euro 5 regulation when pollutant limits were verified using the NEDC cycle. It has two EGR systems, HP and LP. During the engine warming up, the HP EGR strategy is used. Engine electronic control unit switches towards LP EGR as a function of coolant and ambient temperatures.

The engine has two aftertreatment systems: DPF and DOC . Thanks to EGR, DPF and DOC, this engine fulfils the EURO 5 requirements.

5.2.2 Results

A significant amount of data was collected during the test in continuous mode. The acquisition time was 1 Hz, as RDE regulation requires. Together with other data, temperatures, pressures, mass fuel flows, pollutant concentrations,

torque, and engine speed were measured.

Even though T2' is regulated in each test by a PID controller, considering the significant transient conditions of RDE tests, which produce different intake temperature conditions (variation of EGR rates, AMF and outlet compressor temperature), it was not possible to accurately match the temperature setpoint as figure 2 shows. The coolant tank's high thermal inertia and physic WCAC characteristics hinder having a T2' precise regulation. In any case, the change of intake temperature for the different tests is significant (20°C or 35°C), reducing the effect of small variations on the global conclusions, and T2' data represent realistic conditions. Figure 5.1 presents T2' and exhaust manifold temperature (T3).

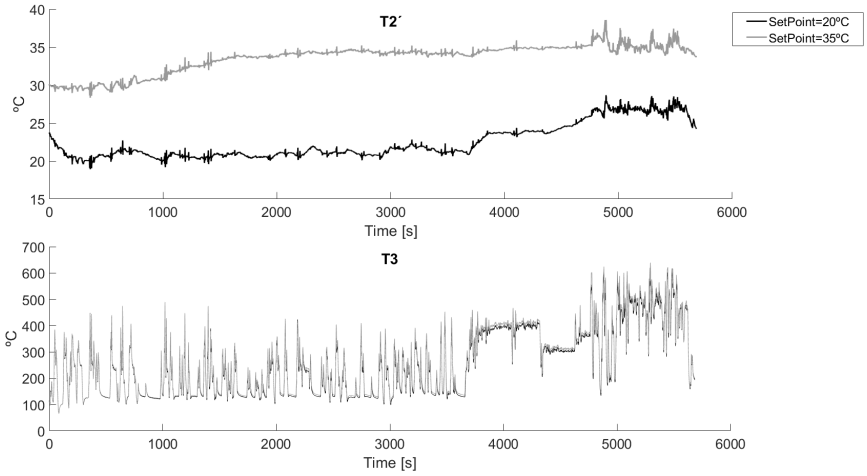

Figure 5.1: T2' and T3.

The first consequence of lowing the intake temperature is an air density increase. It entails a better breathing capacity of the engine, which, once the desired AMF stipulated by the engine control unit (ECU) is reached, the air density increase allows to increase the EGR mass flow quantity, and more EGR means fewer NO_X emissions.

A lower combustion temperature also helps to prevent NO_X emissions. The T3 (that is related to the combustion temperature) is also shown in figure 5.1.

Although in the case of T3, significant variations are not noticed in figure 5.1, table 5.1 presents the average temperatures for the four tests by zones, where these differences can be easily noticed.

	T2'_35°C	**T2'_20°C**	**Abs.Diff**	**T3_35°C**	**T3_20°C**	**Abs.Diff**
Urban	30.84°C	20.99°C	-9.85°C	195.15°C	189.05°C	-6.10°C
Rural	34.94°C	24.29°C	-10.65°C	363.27°C	351.18°C	-12.10°C
Motorway	35.06°C	26.68°C	-8.38°C	456.54°C	443.06°C	-13.49°C
Total	32.32°C	22.47°C	-9.85°C	266.95°C	258.52°C	-8.42°C

Table 5.1: T2' and T3.

Figure 5.2 represents the instantaneous and accumulated emissions using solid and dashed lines on the left and right axis, respectively.

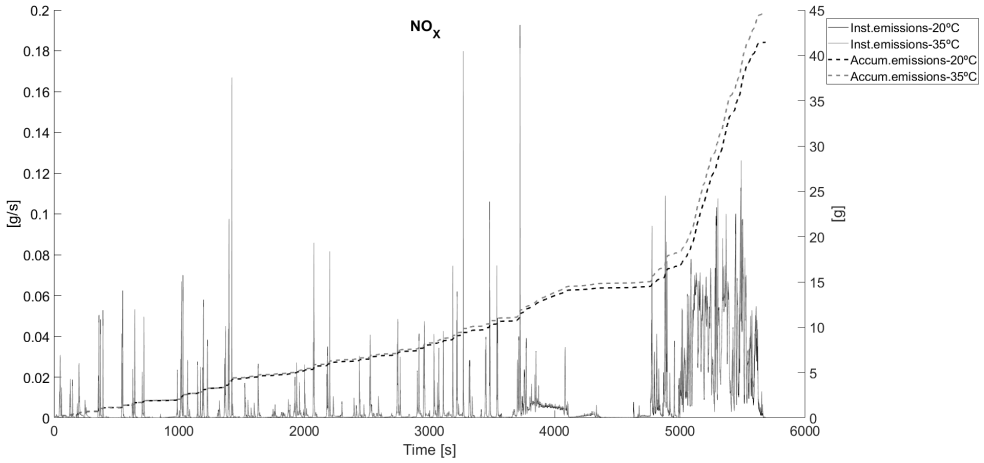

Figure 5.2: Instantaneous and accumulated NO_X emissions.

In figure 5.2, the differences between instantaneous NO_X emissions are not easy to notice; however, focusing on accumulated emissions, differences are evident.

Table 5.2 shows the NO_X emissions obtained from each one of the RDE phases: urban, rural and motorway.

	NO_X__**35°C [g]**	NO_X__**20°C [g]**	**20°C Vs 35°C**
Urban	11.795	11.366	-3.63%
Rural	4.577	4.205	-8.12%
Motorway	28.228	25.858	-8.40%
Total	44.60	41.43	-7.11%

Table 5.2: NO_X emissions by zones.

Table 5.2 presents more considerable reductions registered for higher load zones (Rural and motorway), and according to what was described in Chapter 3, it is possible to confirm these improvements with a confidence interval of 95% since, the difference is higher than the uncertainty which is 3.13%.

The highest NO_X emissions are produced during these zones, as shown in figure 5.2. Two main reasons justify this effect: a lower mixture temperature and an EGR rate increase.

Knowing the EGR rate values can be helpful to deeply understand the effect of intake temperature and the EGR rate on NO_X emissions. In this way, the EGR rate can be easily estimated using CO_2 volumetric concentration in the intake manifold [128], as equation 5.2 shows. However, this methodology is inaccurate for RDE cycles due to the high transient dynamics, which produce fast variations in the $CO_{2intake}$, and $CO_{2tailpipe}$ concentrations, and it leads to errors in the calculation of the EGR rate.

$$EGR_{rate}[\%] = \frac{CO_{2_{intake}}[\%] - CO_{2_{ambient}}[\%]}{CO_{2_{tailpipe}}[\%] - CO_{2_{ambient}}[\%]} * 100 \tag{5.2}$$

Nevertheless, the EGR rate can also be calculated through volumetric engine efficiency. To do that, engine volumetric efficiency was characterised for several engine speeds (between 1000 and 2500rpm) using specific engine tests without EGR. Later, using a linear regression study, the volumetric efficiency (Vol. eff) can be experimentally characterised (for this particular engine) as a function of the engine speed as equation 5.3 shows.

$$Vol.eff[\%] = (0.585 + 0.000193 * n - 0.0000000314 * n^2) \tag{5.3}$$

Where:

- n=engine speed[rpm].

Once the volumetric efficiency was obtained, the theoretical AMF can be calculated using the intake temperature and pressure, as the equation 5.4 shows. The difference between theoretical and measured AMFs represents the EGR mass flow, calculated as shown in equation 5.5, which allows calculating the EGR rate with equation 5.6.

$$AMF_{theo}[g/s] = Vol.eff[\%] * \frac{P2'[Pa]}{R * T2'[K]} * D[m^3] * i * z * n[rpm] * \frac{1000}{60} \quad (5.4)$$

$$EGR_{massflow}[g/s] = AMF_{theo.}[g/s] - AMF_{measured}[g/s] \quad (5.5)$$

$$EGR_{rate}[\%] = \frac{EGR_{massflow}[g/s]}{AMF_{massflow}[g/s] + EGR_{massflow}[g/s]} * 100 \quad (5.6)$$

Where:

- R = Universal gas constant [kg/mol*K]
- D = Engine displacement $[m^3]$
- n = Engine speed [rpm].
- P2' = water charge air cooler outlet pressure [Pa].
- i = 0.5 (Due to it is a four-stroke engine).
- z = Number of cylinders.

Figure 5.3 shows the EGR rates during the RDE tests in each one of their zones, calculated through the volumetric efficiency approach since, it is more reliable in transient tests.

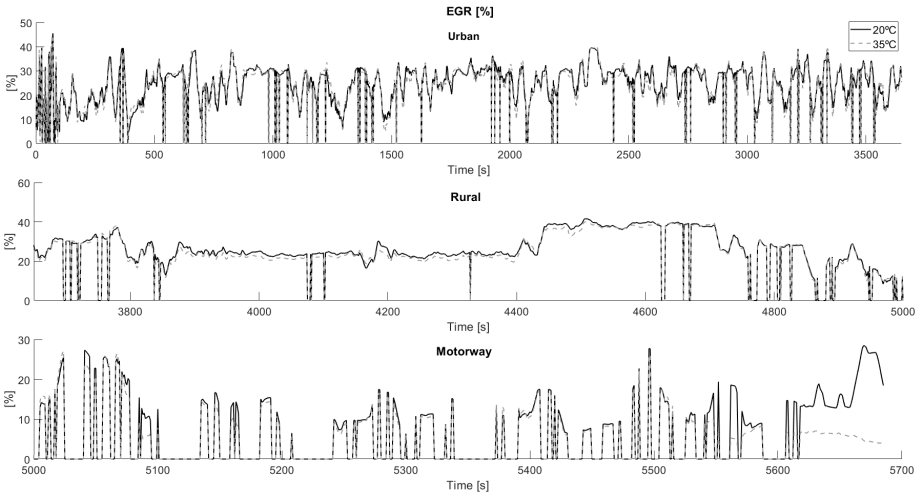

Figure 5.3: EGR rates calculated through volumetric efficiency.

Figure 5.3 shows that EGR rates are similar for the tests performed with different T2', nevertheless in the case of T2'=35°C, slightly lower EGR rates are noticed, as was expected due to the higher intake density in tests at 20°C. Considering that the ECU assign the AMF setpoint (which only depends on the engine operative conditions) using EGRvalves actuation, in case of higher air intake density, the EGR mass flow must increase due to the higher total gases that the engine aspirates. This reaffirms the drop in NO_X emissions obtained in tests with T2'=20°C.

Four different fractions of the tests in different phases of the cycles were analysed to make a deeper analysis. In particular, a situation where the EGR is enabled and another where the EGR valves are completely closed (high load conditions).

As shown in figure 5.4, the vehicle speed is high enough and practically does not vary during each one of these phases. The fact that the vehicle speed does not change helps to analyse the engine behaviour since, it could be similar to a steady test.

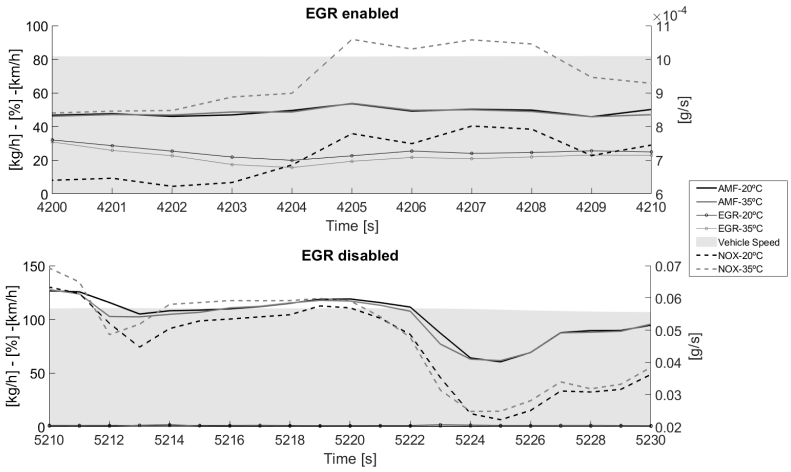

Figure 5.4: Air mass flow [kg/h], EGR rate [%], Vehicle speed [km/h] and NO_X emissions [g/s] with and without EGR.

The other three variables are represented in the four graphics: AMF in kilograms per hour, and EGR rate (%) calculated through volumetric efficiency, which are referenced on the left axis and NO_X emissions in grams per second on the right axis.

The graphic at the top side of figure 5.4 shows fractions of the test where the EGR valve is open. EGR rates vary between 40%-20%. In this case, AMF is controlled by look-up tables in the ECU.

The graphic at the bottom side of the figure 5.4 presents a phase without EGR. They can be seen as the two lines representing the EGR rate overlapping in zero. In these cases, the AMFs are similar, even if it is slightly higher in the case of the test at 20°C.

Focusing on NO_X, both tests performed with lower temperature show lower emissions, which would confirm the dependence of emissions on temperature, so lower intake temperatures results in less NO_X emissions.

Figure 5.5 shows the lambda values of the same phases shown in figure 5.4. The graphic at the top shows a phase when the EGR is activated. The graphic at the bottom shows a phase when the EGR is disactivated due to high dynamic solicitations.

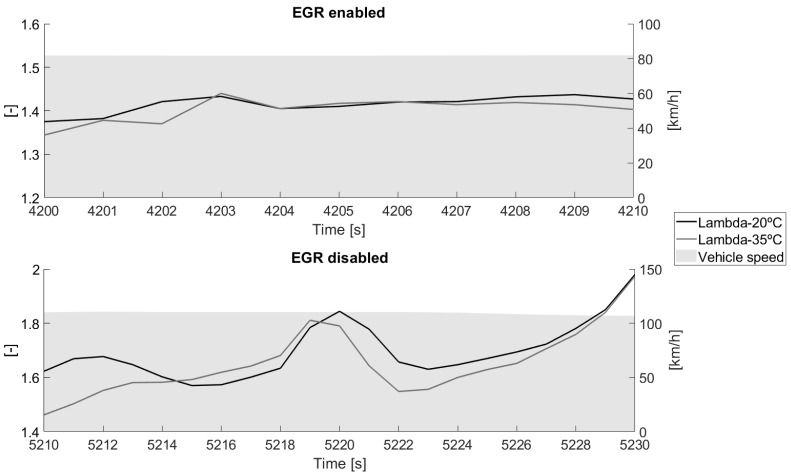

Figure 5.5: Lambda values measured.

Higher values of lambda can be observed in the case where the intake temperature is lower, which represents lean conditions. The increase of lambda when EGR is activated is produced for two reasons. The first reason is the increase of oxygen in the combustion chamber. In this case, two situations must be analysed. Effectively, at part load, the AMF is regulated by the ECU, but as the intake density grows up, the EGR flow must increase (the engine aspirates more mixture). In this case, the lambda increase is due to the oxygen supply from the EGR flow to the combustion chamber. The second situation appears at high loads (EGR disabled); the ECU does not control the air but the intake pressure, which is why the lower temperature (higher density) causes the airflow (O_2) to increase.

The second reason is the fuel consumption reduction, produced by the small increase in engine efficiency. Figure 5.6 and table 5.3 show a small CO_2 reduction which justifies the fuel consumption reduction. This effect appears as a consequence of the higher oxygen quantity in the combustion chamber, which produces a faster combustion [129].

Figure 5.6 shows the tailpipe CO_2 measurements. On the left axis, instantaneous values with solid lines are represented. On the right axis, dashed lines represent the accumulated values.

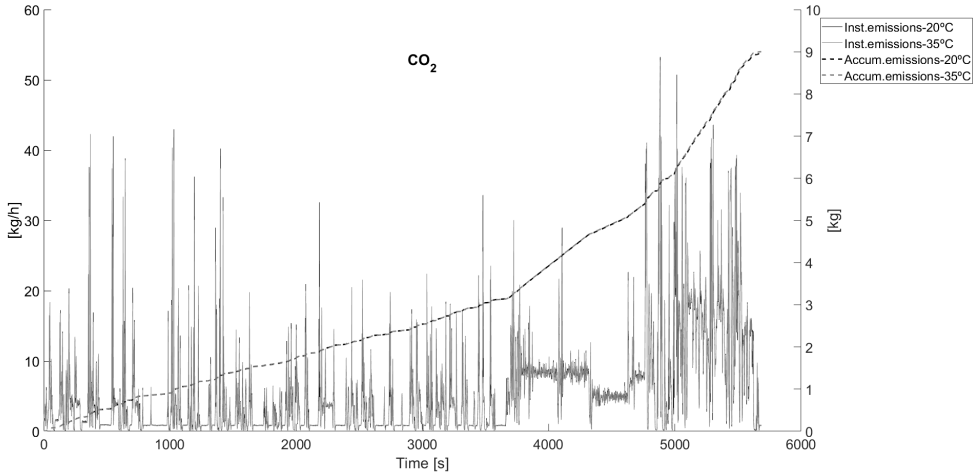

Figure 5.6: Instantaneous and accumulated CO_2 emissions.

Lines in figure 5.6 do not show divergences between the tests, and all the lines are practically overlapped. However, the final values shown in table 5.3 presents non-negligible differences.

	CO2_35°C [kg]	**CO2_20°C [kg]**	**20°C Vs 35°C**
Urban	3.135	3.138	0.11%
Rural	2.935	2.931	-0.11%
Motorway	2.932	2.886	-1.55%
Total	9.002	8.957	-0.50%

Table 5.3: CO_2 emissions by zones.

The results show a better performance in terms of CO_2 emissions in case the test is at 20°C. A reduction of 0,50% was obtained. It confirms the premise of improving engine performance by lowering the engine inlet temperature due to a higher air-fuel ratio (AFR) which causes a more complete and earlier start of the combustion processes since, the mixing time is reduced [129]. The O_2 concentration at the exhaust (tailpipe) can be checked to corroborate this condition.

Figure 5.7 shows the oxygen concentration measured during a specific part

of the RDE urban zone, where the vehicle is stopped at the beginning, performs an acceleration, then maintains a certain vehicle speed, and finally, brakes come to control. On the left axis, the O_2 concentration values with solid lines are represented. On the right axis, the vehicle speed is expressed in grey.

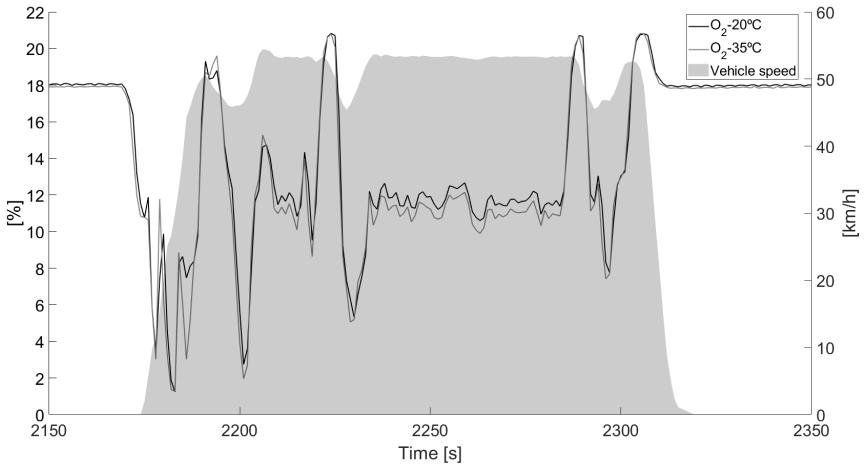

Figure 5.7: O_2 concentrations and vehicle speed during a specific part of RDE urban zone.

As shown in figure 5.7, higher O_2 concentrations are measured when the test is carried out with a 20°C intake temperature setpoint. The O_2 increments, as in the case of lambda, can be analysed in two different situations. First, when the EGR is controlled, the AMF is set constant independently of T2' for a given engine condition. An EGR flow increase is produced in this case due to a higher intake density. This new EGR quantity contains a O_2 concentration determined by the AFR. Due to the AMF is constant, but the fuel consumption was reduced, the AFR increases, forcing a gain of O_2 concentration in the exhaust gases.

The other case appears when EGR saturation conditions are reached (EGR valve fully opened and back pressure valve fully closed) or the EGR is disabled. In these conditions, the higher air density involves an AMF increase with the subsequent O_2 gain. On the one hand, it indicates more efficient combustion, which explains the improvements in CO_2. On the other hand, although a priori, a significant quantity of oxygen would produce a greater NO_X emission,

it was proved previously that they were reduced, mainly due to a high EGR rate and, consequently, lower combustion temperature.

Concerning the CO and THC emissions, figure 5.8 shows the accumulative emissions. The vehicle speed profile is also represented in grey shadows, having the data at the right axis.

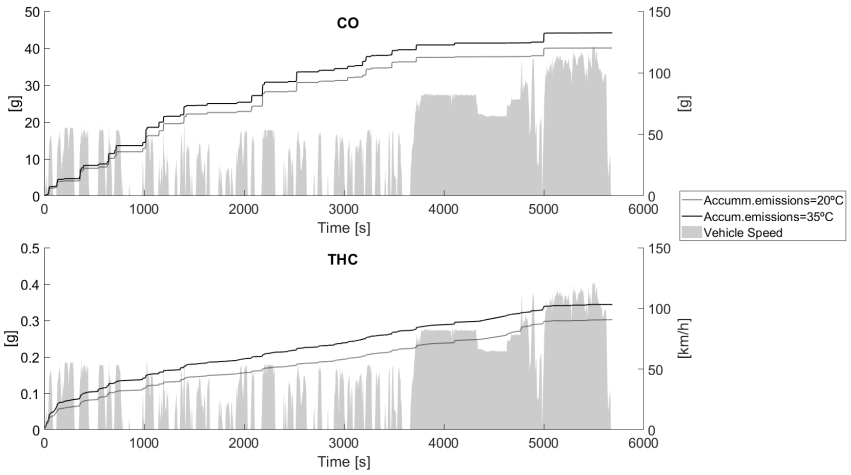

Figure 5.8: Vehicle speed profile and accumulated THC and CO emissions.

In figure 5.8, it can be observed that a large part of THC emissions is produced during the warming-up of the engine and aftertreatment systems. After that, THC emissions present an almost constant value since, no great slope changes in the accumulated emissions are observed. However, CO emissions show constant fluctuations. The large steps are produced during strong accelerations, as observed in the vehicle speed profile. Table 5.4 and table 5.5 shows CO and THC emissions by zones of the cycle and total values.

	CO_35°C [g]	**CO_20°C [g]**	**20°C Vs 35°C**
Urban	36.290	39.574	-8.30%
Rural	1.666	2.054	-18.88%
Motorway	2.087	2.506	-16.72%
Total	40.043	44.134	-9.27%

Table 5.4: CO emissions by zones.

	THC_35°C [g]	**THC_20°C [g]**	**20°C Vs 35°C**
Urban	0.273	0.223	-18.25%
Rural	0.056	0.068	21.07%
Motorway	0.015	0.012	-24.33%
Total	0.344	0.302	-12.15%

Table 5.5: THC emissions by zones.

The results denote a decrease of CO and THC when running with a colder intake temperature. Lower CO emissions obtained at lower temperatures are due to the AFR increase, involving more oxygen proportion that helps to oxide the CO. Although THC emissions are usually higher at low temperatures, in the case of T2'=20°C, the higher AFR compensates for this effect, and the THC emissions are lower.

5.3 RDE cycles under different ambient temperatures

RDE guidelines are vast and complex, and these must all be within specific values to get a valid cycle. On the one hand, these regulate the trip characteristics by distances, average vehicle speeds, dynamic solicitations etc. And on the other hand, external conditions such as altitude and ambient temperature are regulated. However, temperature and altitude acceptable ranges are pretty broad. When the temperature is greater than or equal to 0°C and lower than or equal to 30 °C, and the altitude is from 0 to 700 meters above sea level, the RDE cycle is carried out under normal conditions. But the tests can also be carried out in extended conditions, which can be obtained by temperature between -7°C and 0°C, from 30°C to 35°C or by altitude higher than 700 meters and lower or equal to 1300 meters above sea level.

The current European regulation establishes that if during a particular phase or the entire cycle, it enters in extended conditions, pollutant emissions excepting CO_2 will be divided by 1.6.

The objective of this study is to analyse the influence of ambient temperature on pollutant emissions in the same route. In order to do that, six different

cycles were carried out in engine B described in Chapter 3 under four different ambient temperatures, two temperatures where the cycle is within the range of normal conditions, concretely 3°C and 20°C, and two temperatures where the cycle is performed in extended conditions, with temperatures of -5°C and 32°C, thanks to it is installed in a climatic engine test cell.

Therefore a total of 24 tests were analysed. All the tests were performed in an engine test bench since, the feasibility of performing them was widely proved [1], reducing as much as possible the uncertainties that occur when the tests are performed on-road [130].

5.3.1 RDE cycles

The six different cycles are the same as in Chapter 4.

5.3.2 Material and methods

In this case, the engine is installed on a climatic test bench where the ambient temperature can be modified thanks to a cooling machine, as figure 5.9 shows.

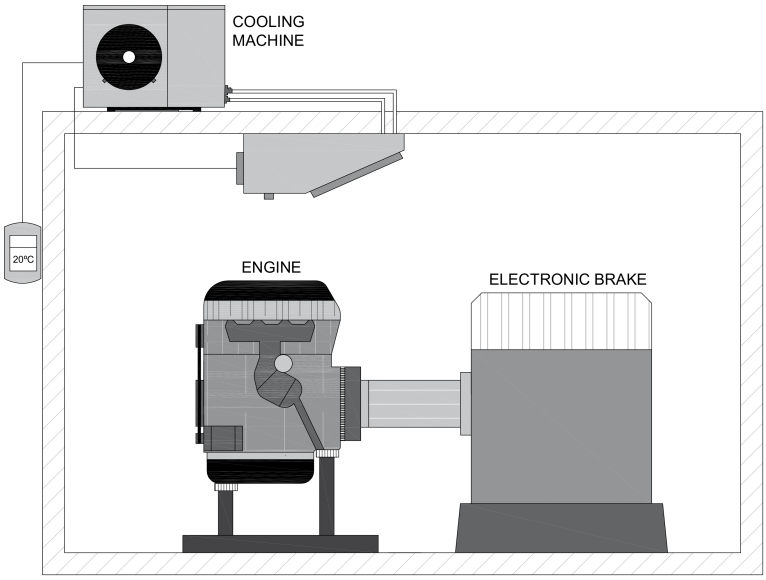

Figure 5.9: Engine test cell.

To perform this analysis, it was used the engine and vehicle B.

In this study, besides the previous pollutant emissions measured (NO_X,CO, THC) and CO_2, the particulate mass was obtained throughout an opacimeter and the methodology described in Chapter 3.

5.3.3 Results

Data were recorded at 1Hz acquisition frequency as RDE regulation requieres.

In the first place, CO_2 accumulated emissions linked with the fuel consumption are analysed, figure 5.10 shows them, and the vehicle speed profile referenced in the right axis profile is represented.

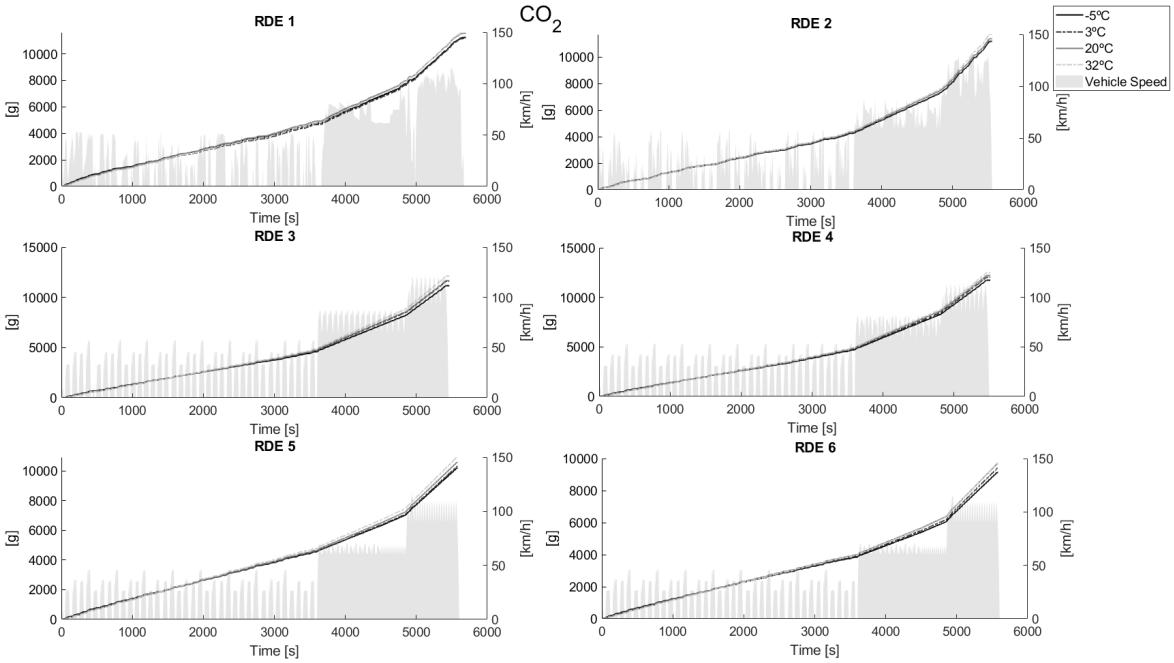

Figure 5.10: Accumulated CO_2 emissions (left axis) and vehicle speed (right axis).

Looking at figure 5.10, no significant differences are detected between cycles at different temperatures. However, it is possible to say that cycles at 32°C and 20°C generally have larger emissions values, involving higher fuel consumption. Concretely, the tests at the highest and lowest temperature (32°C vs -5°C) have increased from 3.6% to 8.6% depending on the cycle.

Figure 5.11 helps to understand the engine behaviour at two extreme temperatures, -5°C and 32°C.

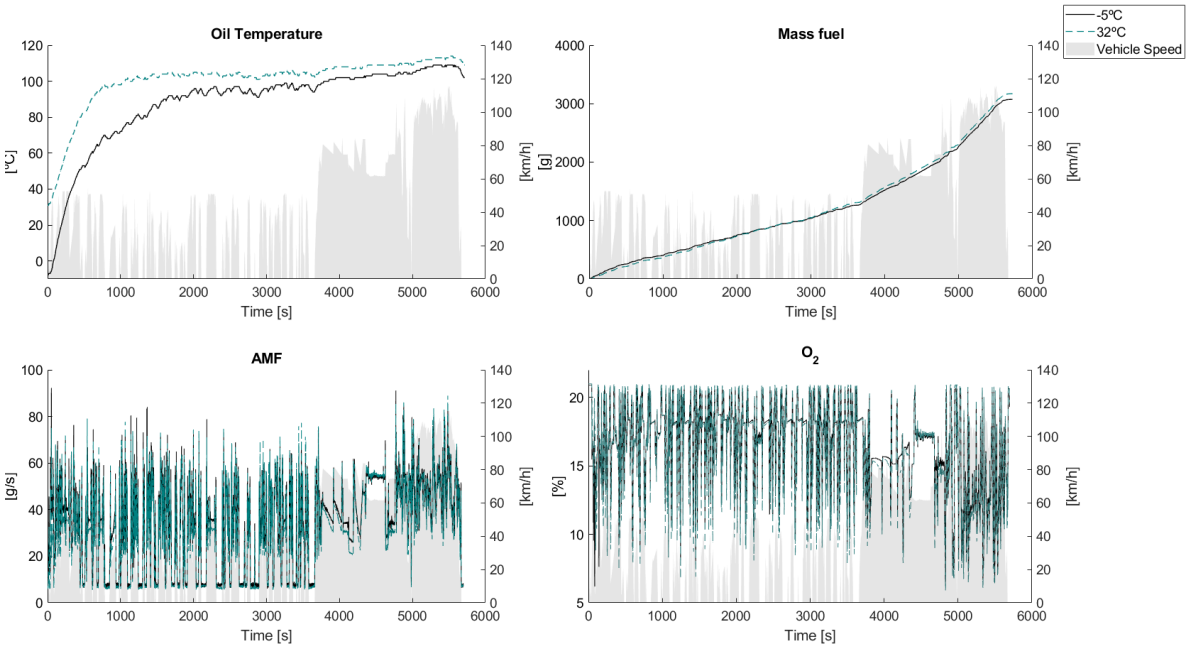

Figure 5.11: Oil temperature, accumulated fuel mass consumption, air mass flow (AMF) and exhaust O_2 concentration.

On the top left of figure 5.10 the oil temperature is plotted, which is strongly linked with the coolant temperature and affects fuel mass consumption and, therefore, CO_2 emissions. It is possible to see how at the beginning of the cycle, where the oil is at a shallow temperature in the test at -5°C, the efficiency is lower due to many reasons, in the first place, its low viscosity produces an engine efficiency worsening. Secondly, there are higher heat losses due to the low ambient temperature, and thirdly the combustion shape is also affected, and its efficiency is deteriorated.

As the oil warms up, this situation reverses, and the test at -5°C has a lower final consumption. To explain the fuel improvement in the test at -5°C serves the bottom graphics where this test shows a higher AMF and O_2 concentration, which means that at this temperature EGR rate is lower, which produces a more excellent engine performance.

NO_X emissions probably are the primary concern of manufacturers when approving new vehicles, and above all, vehicles with diesel engines. Currently,

all the vehicles have to incorporate different engine strategies and aftertreatment systems to get below the type approval limits. Figure 5.12 shows the accumulative NO_X emissions of each of the 24 tests and the vehicle speed profiles.

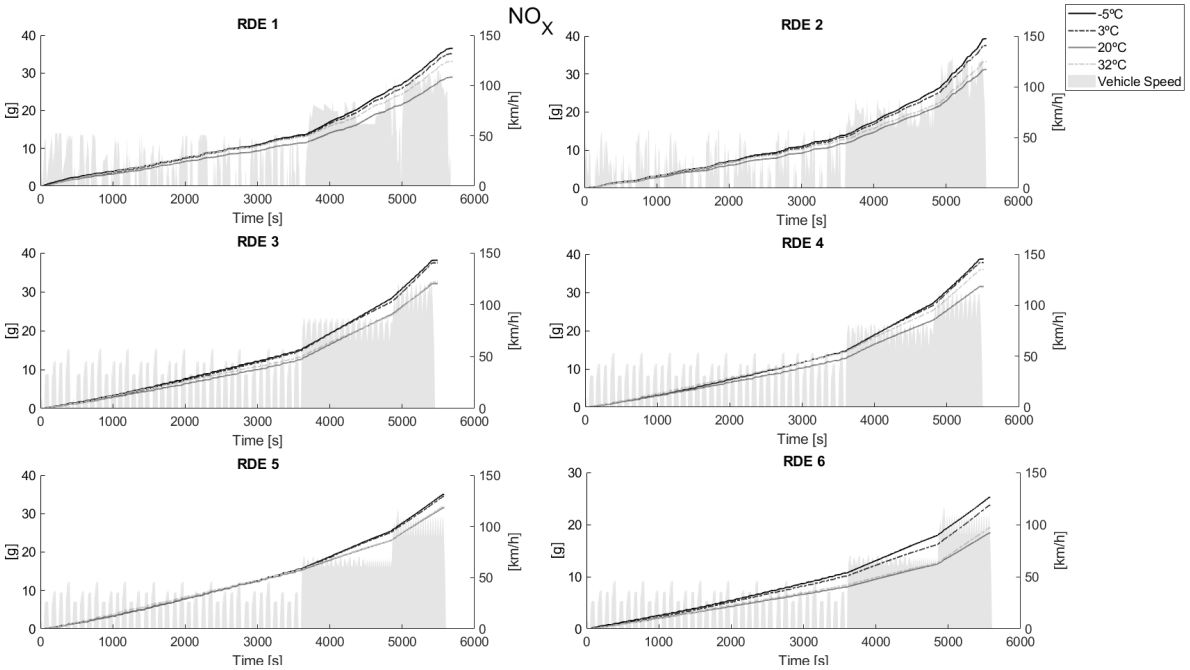

Figure 5.12: Accumulated NOX emissions (left axis) and vehicle speed (right axis).

Regarding figure 5.12, it can be easily verified significant differences between the tests, concretely unlike CO_2, tests at higher ambient temperature show lower emissions since, tests with higher temperatures, as was shown in figure 5.11 have higher EGR rates.

Figure 5.13 shows an analysis of a part of the RDE 1 cycle, concretely from 3800 to 4600 seconds, this part belongs to the urban zone where there are different phases with constant speed, accelerations and decelerations, so different dynamic solicitations can be under study. EGR rate, AMF, EGR valve position, NO_X emissions, intake manifold temperature named T2' and exhaust manifold temperature called T3 are represented.

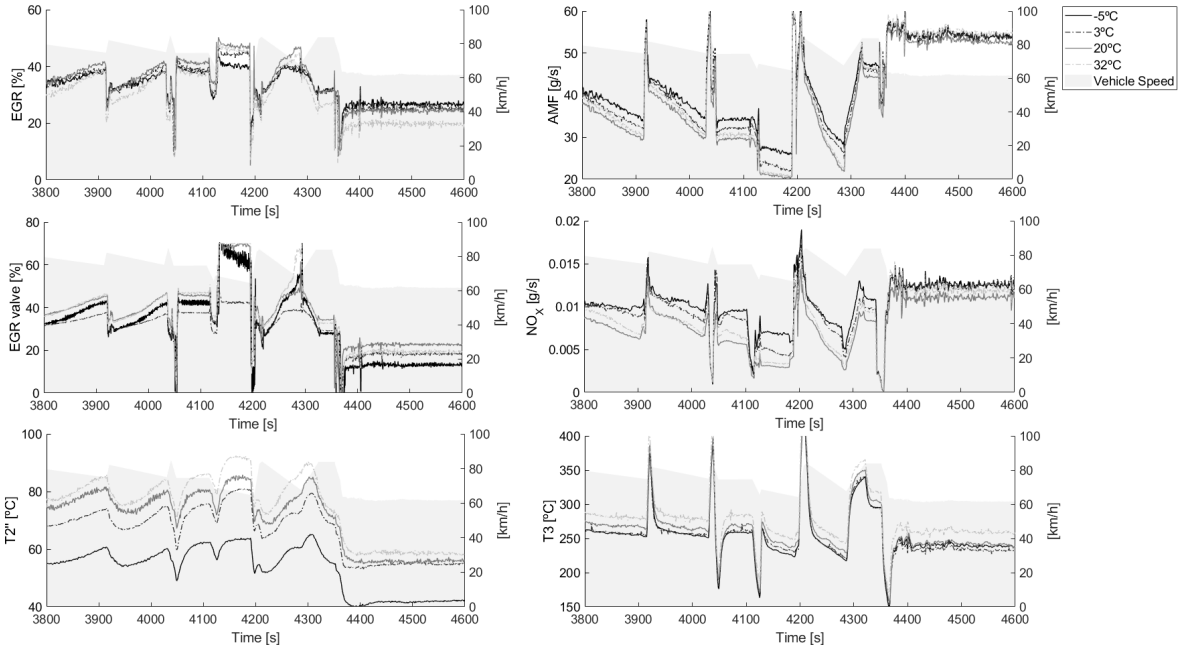

Figure 5.13: EGR rate [%], air mass flow (AMF) [g/s], EGR valve position [%] , instantaneous NO_X emissions [g/s], intake manifold temperature (T2') [°C] and exhaust manifold temperature(T3) [°C] of RDE 1.

Figure 5.13 makes easy to understand the engine behaviour regarding NO_X emissions when it is tested under different temperatures. EGR rate varies depending on engine operation conditions for all cycles, but the test at 20°C shows the highest values except 4350s to 4600, while the maximum values are obtained in case of the test at -5°C. However, NO_X emissions are more significant than at 20°C and looking at AMF can be observed how the AMF is more critical due to a lower air density. As a consequence of the AMF increase, combustion improves and is reflected in T3 similarly in these two tests despite a great T2' gap.

AMF points out a clear trend from more to less: -5°C, 3°C, 32°C and 20°C. This is usually produced because ECU guidelines adjust the AMF to a specific setpoint to provide normal engine behaviour. NO_X emissions also show a clear tendency, it is lower temperatures that make higher emissions, except for the test at 32°C where the tendency changes, obtaining more NO_X emissions than 20°C. On the one hand, the increase of NO_X emissions is

due to a decrease in EGR rates, and on the other hand, lower air intake temperature leads to a lower generation of them. Consequently, the test at 20°C perfectly compromises ambient temperature and EGR rate to obtain the lowest emissions.

THC emissions are represented in figure 5.14; these emissions are produced due to failing combustion processes.

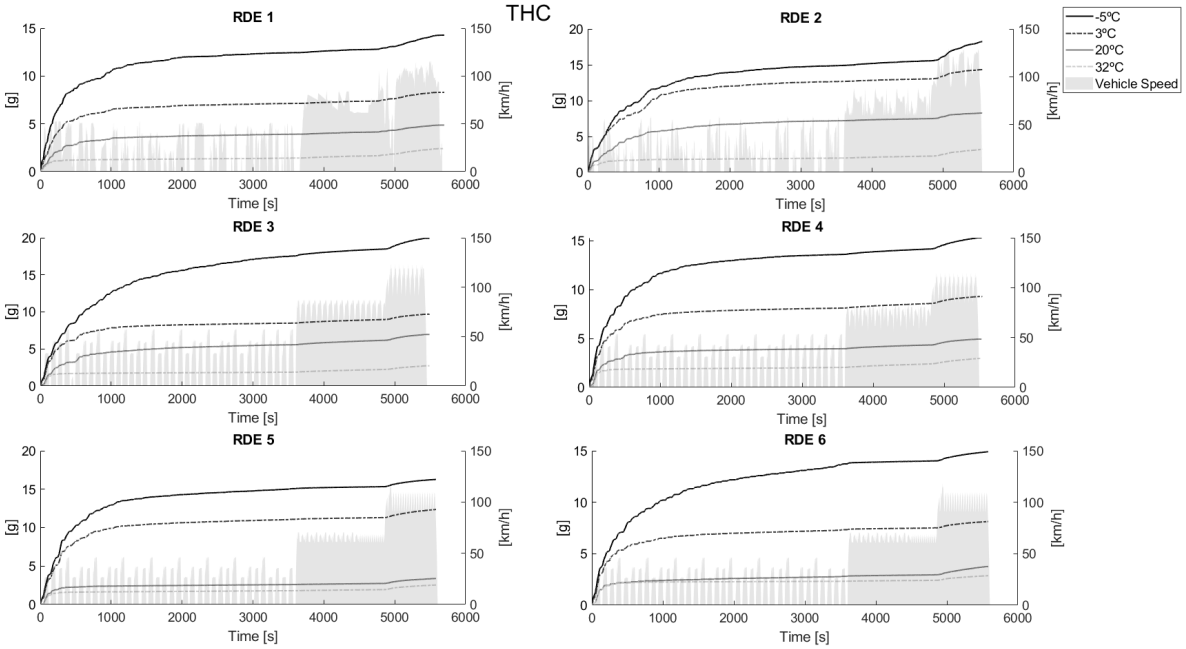

Figure 5.14: Accumulated THC emissions (left axis) and vehicle speed (right axis).

Predictably, minor temperatures imply higher THC emissions, on one hand, this is because DOC has a lower efficiency at low temperatures, which is the reason why car manufacturers try to reduce the warming-up period by employing different strategies [131]. Besides, it was easily noticed that the more significant gap was produced during the warming-up aftertreatment period. On the other hand, low air temperatures can produce incomplete combustions or, in a worst-case scenario, misfiring in the combustion chamber, leading to THC emissions.

Figure 5.15 shows CO emissions. These emissions are produced due to

incomplete reactions, leading to CO production.

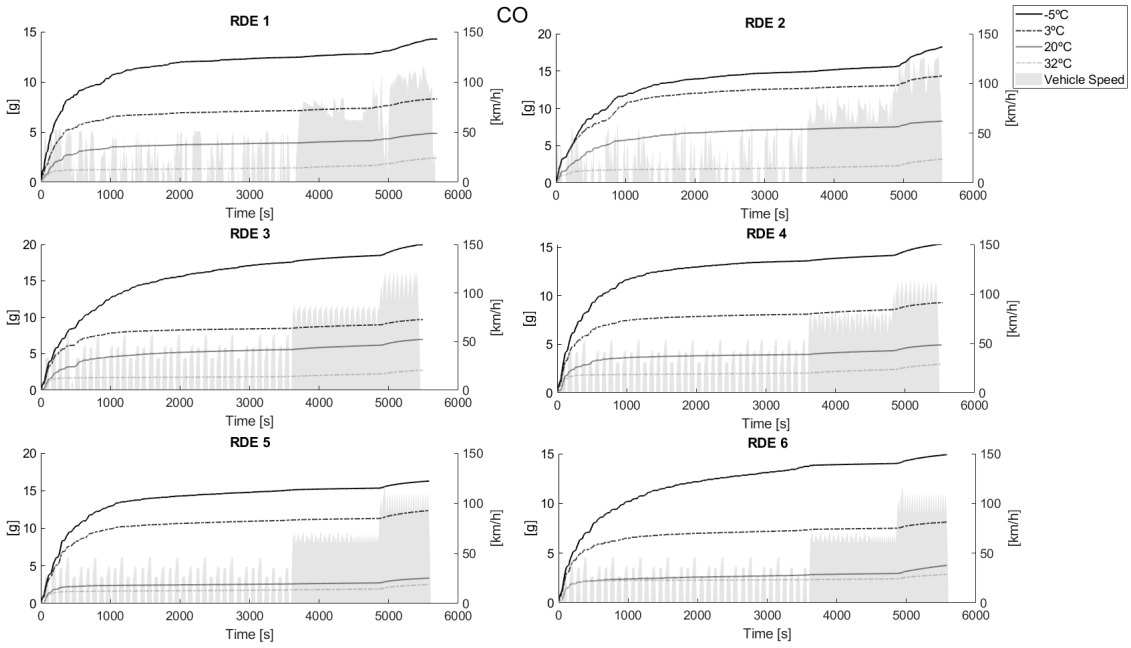

Figure 5.15: Accumulated CO emissions (left axis) and vehicle speed (right axis).

As figure 5.15 shows, lower intake air temperature produces more CO emissions since, it can worsen the combustion, besides the aftertreatment warming-up issue previously commented in THC emissions.

THC and CO emission results can be justified in the figure 5.16. It illustrates the first ten minutes of cycle 1, where most of the THC and CO emissions are produced. Fuel mass flow, relative fuel-air ratio (Fr), AMF and intake manifold temperature (T2") are represented.

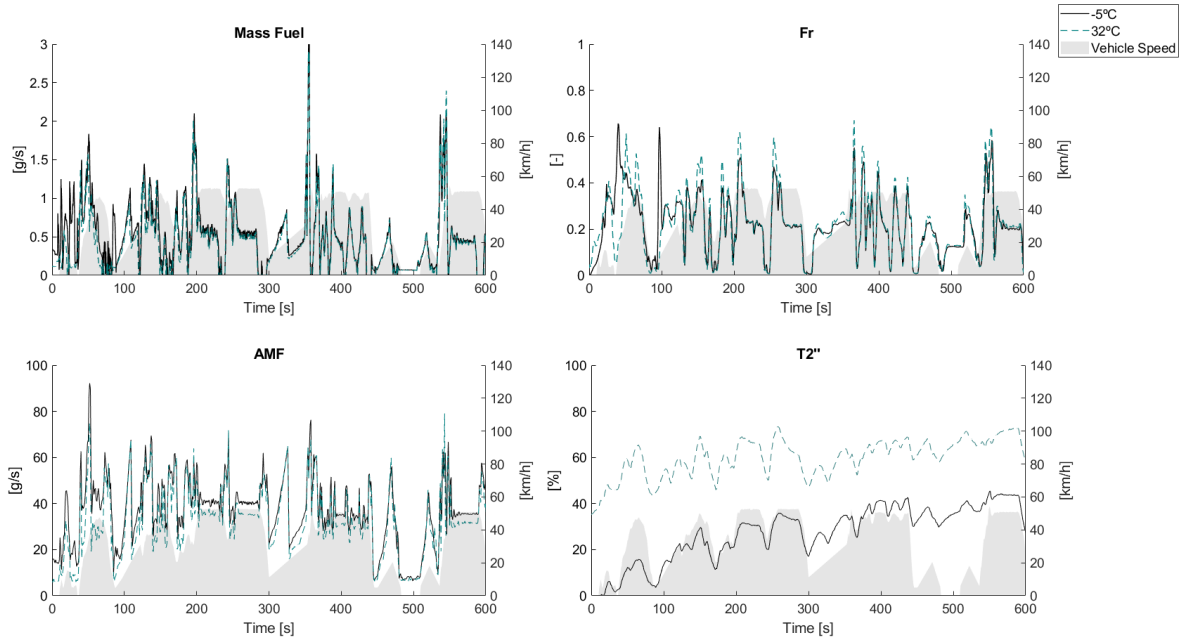

Figure 5.16: Fuel mass flow [g/s], relative fuel-air ratio (Fr), Air mass flow (AMF) [g/s], and intake manifold temperature (T2") [°C].

During the warm-up period, it can be observed that the fuel mass flow increases to obtain the desired torque, especially during the first 100 seconds. To get a suitable Fr similar to the test at 32°C is necessary an AMF increase, which leads to lower EGR rates which entail more NO_X emissions, as was commented previously. It implies that the ambient temperature mainly causes more significant CO and THC emissions, as T2" shows. Moreover, the DOC efficiency is enormously worsened at low temperatures. The Fr shows similar values in both tests since, the fuel mass flow increased at low temperatures, and the AMF is higher due to the EGR flow reduction.

Finally, figure 5.17 represents PM emissions. Although the engine has installed a DPF, the opacity measurement was made upstream to eliminate the uncertainty that could produce the DPF. Furthermore, the estimation from opacity to particulate mass was designed for raw measurements.

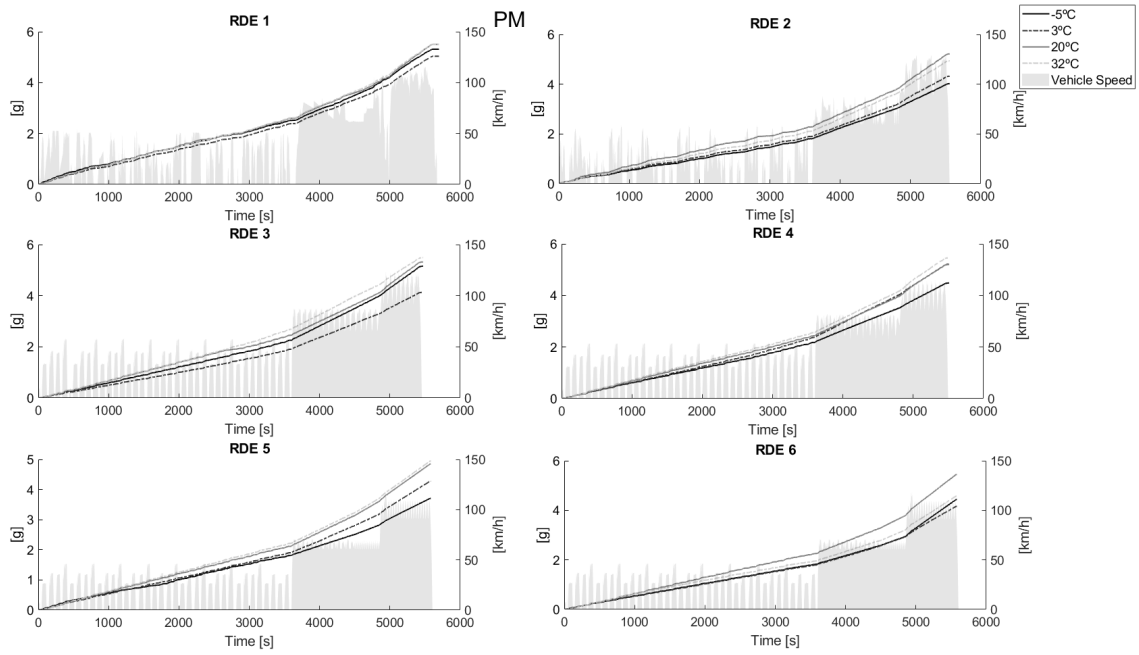

Figure 5.17: Accumulated PM emissions (left axis) and vehicle speed (right axis).

PM emissions do not show a clear tendency, although, for all cycles, tests with higher temperatures (32°C and 20°C) produced fewer emissions than the other two (-5°C and 3°C). Going back to NO_X emissions, it is proved the well-known trade-off between them and the PM emissions since, tests with low NO_X emission lead to more PM and vice versa.

Additionally, in this section, a dispersion study of cycles 3, 4, 5 and 6 was carried out. These cycles repeat different speed sequences throughout the cycle. In this case, it was analysed the pollutant emissions among the first three sequences in cycle 3, where the engine is working in a warm-up period. Each of these sequences has an approximate duration of 6 minutes, and figure 5.18 shows the accumulated emissions of these three sequences. Moreover, vehicle speed and oil temperatures have been presented at the bottom right.

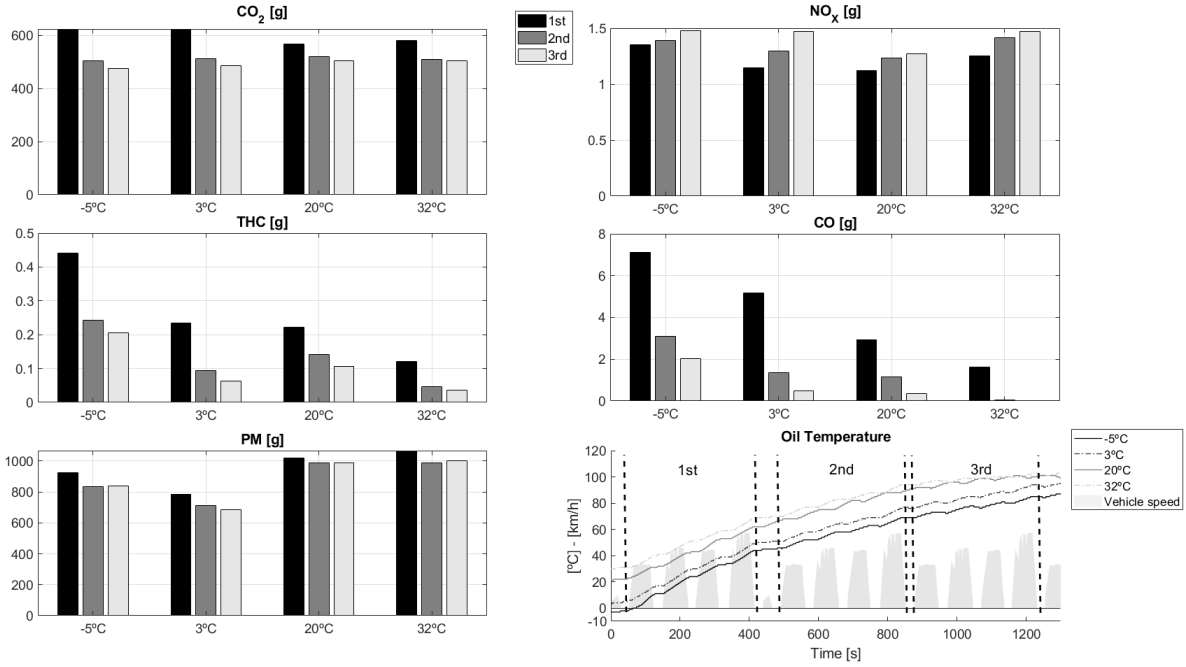

Figure 5.18: Accumulated emissions of the first three sequences in cycle 3, vehicle speed profile and oil temperatures..

As can be observed in figure 5.18, CO_2 and NO_X follow opposite trends when the engine is hotter, CO_2 emissions decrease and NO_X emissions increase. THC, CO and PM follow the same trend as CO_2, although PM does not have such a notable reduction as the other two. In this case, it must be considered that the opacimeter is located upstream of the FAP, so its efficiency does not affect it.

PM emissions are lower in tests at -5°C and 3°C tests due to smaller EGR rates imposed by ECU. The reductions produced in the second and third sequences result from improved combustion in the chamber.

CO_2 emissions in the first sequence are higher in low-temperature tests. However, in the second and third sequences, the opposite trend was observed. This is because, in the first sequence, the engine has lower efficiency in the tests at -5°C and 3°C. After all, the combustion is worse than in the case of the engine works at higher temperatures and, together with an increase in mechanical losses when the oil is at such a low temperature.

5.3.4 Emission regulation results

The newest RDE regulations, as described in Chapter 2, established a new concept known as RF that affects pollutant emissions weighting.

In this study, all the RDE cycles have lower CO_2 emissions than those obtained in the case of the WLTC, so RF is equal to 1. The cycles that enter into extended conditions in compliance with the European regulation would affect final and urban emissions. All the cycles were carried out in this study at -5°C and 32°C. So, excepting CO_2 emissions, the rest should be divided by 1.6. It makes that cycles at 32°C would have the lowest values of NO_X, THC and CO emissions and cycles at -5°C of PM.

Figure 5.19 and 5.20 show raw (tail pipe) and final emissions (after applying the RF factor) results for all tests in the urban part and the entire cycle since, the European regulation controls that the emissions are under the limit in both cases.

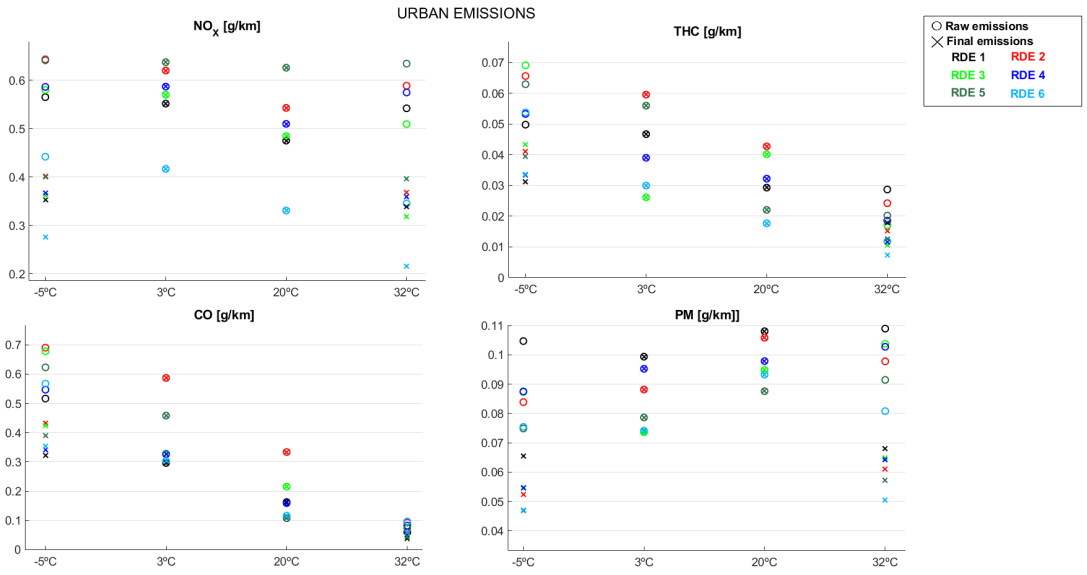

Figure 5.19: Urban raw and final emissions.

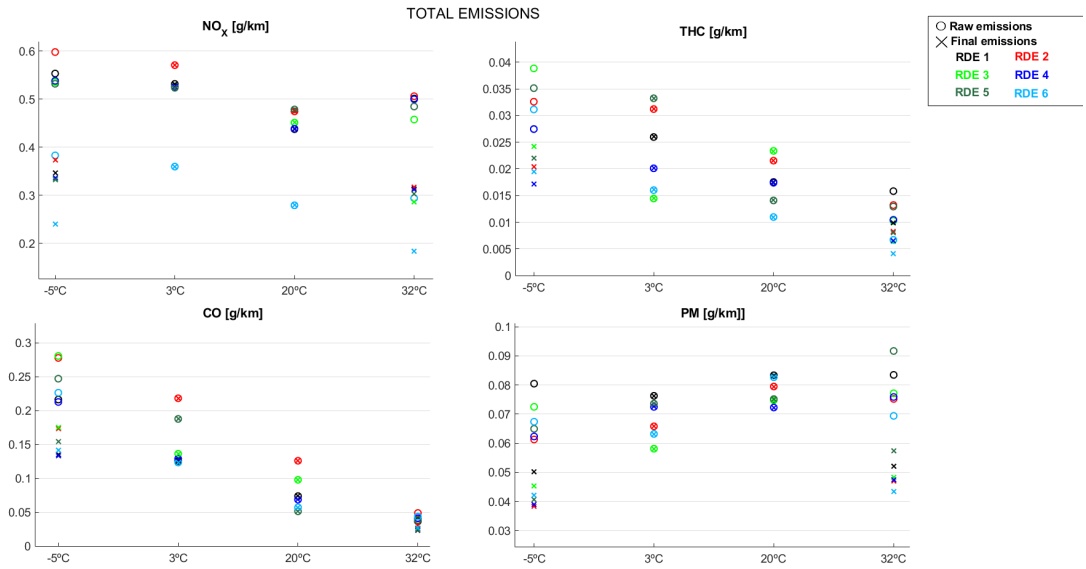

Figure 5.20: Total raw and final emissions.

As can be observed, there are different pollutant tendencies. Focusing on raw values, NO_X emissions are reduced when the temperature increases except when it arrives until 32°C, where this tendency changes and NO_X emissions rise again. CO and THC emissions present the same tendency, and more temperature leads to fewer emissions. In the case of PM, its tendency indicates an improvement at a lower temperature, except for the test at -5°C. On the other hand, the final emissions that only change from raw emission in tests at -5°C and 32°C as regulation dictates, would cause a significant reduction in these tests at the time of carrying out a homologation of the vehicle.

5.4 Conclussions

RDE tests were performed on a light-duty Euro 6 diesel engine and a van euro 6 diesel engine. In the case of the light-duty vehicle, the tests were carried out by setting different intake air temperatures: 20°C and 35°C. A significant drop in NO_X, 7.1% in the RDE cycles, was measured in case the test was performed at 20°C, which can be confirmed thanks to the statistical analysis

of the Chapter 3.

A not negligible increase in EGR mass flow was noted when the test was performed at low temperatures (20°C) due to the higher intake density. As the Electronic Control Unit has controlled fresh air mass flow through the EGR valves actuation, higher intake density produces more EGR mass flow (additional EGR). Consequently, a reduction of NO_X emissions was obtained from tests performed at 20°C. This reduction is also produced due to the lower intake temperature.

Slight differences in CO_2 emissions were registered when comparing tests at different intake temperatures. A reduction of 0.5% was obtained for tests at 20°C.

During both the engine and the aftertreatment devices warming up, a significant amount of THC and CO are registered in any case. These emissions were permanently lowered in the case of the test with T2'=20°C due to the air density increase, which produces an O_2 gain in the combustion chamber.

In the other study case, a van was simulated in RDE tests with four different ambient temperatures. In terms of engine efficiency, represented in CO_2 emissions, tests at -5°C and 3°C present the highest values of efficiency, mainly due to lower EGR rates. In spite of during the warm-up period, tests with these two temperatures have lower efficiency, it is compensated later until reaching lower emission values.

The lowest NO_X emissions are produced in the test at 20°C, and this situation is explained because the WLTC are performed around this temperature, and hence, vehicle manufacturers concentrate their efforts on achieving a proper calibration in this situation.

As expected, CO and THC emissions present lower values at high ambient temperatures, mainly for better combustion and a faster warming-up of the aftertreatment device, providing greater efficiency.

In the case of PM, they fulfilled the well-known trade-off between NO_X and them and seemed to have a linear ascent relationship with temperature due to the EGR rate increases.

Finally, after applying the current regulation, final emissions show that tests at 32°C have the lowest emissions values, except PM. Still, it has to be

considered that were measured upstream of the DPF. It possibly also would be lesser if they were measured downstream of the aftertreatment due to a faster warming-up and better efficiency at higher temperatures.

Chapter 5 Bibliography

[1] J. M. Luján, V. Bermudez, B. Pla, and F. Redondo. "Engine test bench feasibility for the study and research of real driving cycles: Pollutant emissions uncertainty characterization". *International Journal of Engine Research* 0(0) (2021), p. 0. DOI: 10.1177/14680874211007999 (cit. on pp. xi, 56, 112).

[64] *COMMISSION REGULATION (EU) 2018/1832 of 5 November 2018 amending Directive 2007/46/EC of the European Parliament and of the Council, Commission Regulation (EC) No 692/2008 and Commission Regulation (EU) 2017/1151 for the purpose of improving the emission type approval tests and procedures for light passenger and commercial vehicles, including those for in-service conformity and real-driving emissions and introducing devices for monitoring the consumption of fuel and electric energy.* 2018. URL: https://eur-lex.europa.eu/legal-content/EN/TXT/HTML/?uri=CELEX:32018R1832\&from=EN (cit. on pp. 20, 24, 40, 56, 99).

[91] J. Rodríguez-Fernández, J. J. Hernández, Ángel Ramos, and A. Calle-Asensio. "Fuel economy, NOx emissions and lean NOx trap efficiency: Lessons from current driving cycles". *International Journal of Engine Research* (2021). DOI: https://doi.org/10.1177/14680874211005080 (cit. on pp. 56, 99).

[103] Y. B. Zeldóvich. *The oxidation of nitrogen in combustión and explosion.* Ed. by A. Physicochim. 1946 (cit. on p. 98).

[104] G. P. Merker, B. Hohlbaum, and M. Rauscher. *Two-Zone Model for Calculation of Nitrogen-Oxide Formation in Direct-Injection Diesel Engines.* SAE International, 1993. DOI: https://doi.org/10.4271/932454 (cit. on p. 98).

[105] C. P. Fenimore. *Formation of nitric oxide in premixed hydrocarbon flames.* 1971 (cit. on p. 98).

[106] S. R. Turns et al. *Introduction to combustion.* Vol. 287. McGraw-Hill Companies, 1996 (cit. on p. 98).

[107] J. B. Heywood. *Internal combustion engine fundamentals*. McGraw-Hill Education, 2018 (cit. on p. 98).

[108] E. E. Agency., ed. *Air quality guidelines. Global update 2005. Particulate matter, ozone, nitrogen dioxide and sulfuric dioxide*. 2005. ISBN: 92 890 2192 6 (cit. on p. 98).

[109] M. Lippmann. "Health Effects of Ozone a Critical Review". *JAPCA* 39 (June 1989), pp. 672–95. DOI: 10.1080/08940630.1989.10466554 (cit. on p. 98).

[110] L. Cox. *Nitrogen oxides (NOx) why and how they are controlled*. U.S. Environmental Protection Agency, Office of Air Quality Planning, Standards, Information Transfer, and Program Integration Division, Clean Air Technology Center, 1999. ISBN: 9781428902800. URL: https://books.google.es/books?id=kSJY-EVi1KEC (cit. on p. 98).

[111] J. M. Desantes, J. J. López, P. Redón, and J. Arrégle. "Evaluation of the Thermal NO formation mechanism under low-temperature diesel combustion conditions". *International Journal of Engine Research* 13(6) (2012), pp. 531–539. DOI: 10.1177/1468087411429638. eprint: https://doi.org/10.1177/1468087411429638. URL: https://doi.org/10.1177/1468087411429638 (cit. on p. 98).

[112] R. A. Varella, G. Duarte, P. Baptista, P. Mendoza Villafuerte, and L. Sousa. "Analysis of the Influence of Outdoor Temperature in Vehicle Cold-Start Operation Following EU Real Driving Emission Test Procedure". *SAE International Journal of Commercial Vehicles* 10(2) (2017), pp. 596–697. ISSN: 1946-391X. DOI: https://doi.org/10.4271/2017-24-0140. URL: https://doi.org/10.4271/2017-24-0140 (cit. on p. 99).

[113] D. Engelmann, Y. Zimmerli, J. Czerwinski, and P. Bonsack. "Real Driving Emissions in Extended Driving Conditions". *Energies* 14(21) (2021). ISSN: 1996-1073. DOI: 10.3390/en14217310. URL: https://www.mdpi.com/1996-1073/14/21/7310 (cit. on p. 99).

[114] V. Bermúdez, J. R. Serrano, P. Piqueras, and B. Diesel. "Fuel consumption and aftertreatment thermal management synergy in compression ignition engines at variable altitude and ambient temperature". *International Journal of Engine Research* 0(0) (0), p. 14680874211035015. DOI: 10.1177/14680874211035015. eprint: https://doi.org/10.1177/14680874211035015. URL: https://doi.org/10.1177/14680874211035015 (cit. on p. 99).

[115] S. Funk. "Real World NOx Sensor Accuracy Assessment and Implications for REAL NOx Tracking". In: *SAE WCX Digital Summit*. SAE International, 2021. DOI: https://doi.org/10.4271/2021-01-0593. URL: https://doi.org/10.4271/2021-01-0593 (cit. on p. 99).

[116] Y. Wang, Y. Ge, J. Wang, X. Wang, H. Yin, L. Hao, and J. Tan. "Impact of altitude on the real driving emission (RDE) results calculated in accordance to moving averaging window (MAW) method". *Fuel* 277 (2020), p. 117929. ISSN: 0016-2361. DOI: https://doi.org/10.1016/j.fuel.2020.117929. URL: https://www.sciencedirect.com/science/article/pii/S001623612030925X (cit. on p. 99).

[117] H. Wang et al. "The real driving emission characteristics of light-duty diesel vehicle at various altitudes". *Atmospheric Environment* 191 (2018), pp. 126–131. ISSN: 1352-2310. DOI: https://doi.org/10.1016/j.atmosenv.2018.07.060. URL: https://www.sciencedirect.com/science/article/pii/S1352231018305132 (cit. on p. 99).

[118] J. Serrano, P. Piqueras, E. Sanchis, and B. Diesel. "A modelling tool for engine and exhaust aftertreatment performance analysis in altitude operation". *Results in Engineering* 4 (2019), p. 100054. ISSN: 2590-1230. DOI: https://doi.org/10.1016/j.rineng.2019.100054. URL: https://www.sciencedirect.com/science/article/pii/S2590123019300544 (cit. on p. 99).

[119] P. Bielaczyc, J. Woodburn, J. Merkisz, and J. Pielecha. "RDE Testing of Passenger Cars: The Effect of the Cold Start on the Emissions Results" (2019). ISSN: 0148-7191. DOI: https://doi.org/10.4271/2019-01-0747. URL: https://doi.org/10.4271/2019-01-0747 (cit. on p. 99).

[120] B. Du, L. Zhang, Y. Geng, Y. Zhang, H. Xu, and G. Xiang. "Testing and evaluation of cold-start emissions in a real driving emissions test". *Transportation Research Part D: Transport and Environment* 86 (2020), p. 102447. ISSN: 1361-9209. DOI: https://doi.org/10.1016/j.trd.2020.102447. URL: https://www.sciencedirect.com/science/article/pii/S1361920920306349 (cit. on p. 99).

[121] D. Engelmann, Y. Zimmerli, J. Czerwinski, and P. Bonsack. "Real Driving Emissions in Extended Driving Conditions". *Energies* 14(21) (2021). ISSN: 1996-1073. DOI: 10.3390/en14217310. URL: https://www.mdpi.com/1996-1073/14/21/7310 (cit. on p. 99).

[122] B. Giechaskiel, D. Komnos, and G. Fontaras. "Impacts of Extreme Ambient Temperatures and Road Gradient on Energy Consumption and CO2 Emissions of a Euro 6d-Temp Gasoline Vehicle". *Energies* 14(19) (2021). ISSN: 1996-1073. DOI: 10.3390/en14196195. URL: https://www.mdpi.com/1996-1073/14/19/6195 (cit. on p. 99).

[123] R. García-Contreras, A. Gómez, P. Fernández-Yáñez, and O. Armas. "Estimation of thermal loads in a climatic chamber for vehicle testing". *Transportation Research Part D: Transport and Environment* 65 (2018), pp. 761–771. ISSN: 1361-9209. DOI: https://doi.org/10.1016/j.trd.2017.11.010. URL: https://www.sciencedirect.com/science/article/pii/S136192091730771X (cit. on p. 99).

[124] J. Ko, D. Jin, W. Jang, C.-L. Myung, S. Kwon, and S. Park. "Comparative investigation of NOx emission characteristics from a Euro 6-compliant diesel passenger car over the NEDC and WLTC at various ambient temperatures". *Applied Energy* 187 (2017), pp. 652–662. ISSN: 0306-2619. DOI: https://doi.org/10.1016/j.apenergy.2016.11.105. URL: https://www.sciencedirect.com/science/article/pii/S0306261916317366 (cit. on p. 99).

[125] A Calle-Asensio, J. Hernández, J Rodríguez-Fernández, M Lapuerta, A Ramos, and J Barba. "Effect of advanced biofuels on WLTC emissions of a Euro 6 diesel vehicle with SCR under different climatic conditions". *International Journal of Engine Research* 22(12) (2021), pp. 3433–3446. DOI: 10.1177/14680874211001256. eprint: https://doi.org/10.1177/14680874211001256. URL: https://doi.org/10.1177/14680874211001256 (cit. on p. 99).

[126] X. Wang et al. "Proceedings of Real Driving Emission (RDE) Measurement in China" (2018). ISSN: 0148-7191. DOI: https://doi.org/10.4271/2018-01-0653. URL: https://doi.org/10.4271/2018-01-0653 (cit. on p. 99).

[127] L. Ciferri. "SUVs, crossovers continue to grow market share in Europe, ANE's segment-by-segment analysis shows." *Automotive News Europe.* (2020). DOI: https://europe.autonews.com/sales-segment/suvs-crossovers-continue-grow-market-share-europe-anes-segment-segment-analysis-shows (cit. on p. 100).

[128] J. M. Luján, H. Climent, L. M. García-Cuevas, and A. Moratal. "Volumetric efficiency modelling of internal combustion engines based on a novel adaptive learning algorithm of artificial neural networks". *Ap-*

plied Thermal Engineering 123 (2017), pp. 625–634. ISSN: 1359-4311. DOI: https://doi.org/10.1016/j.applthermaleng.2017.05.087. URL: https://www.sciencedirect.com/science/article/pii/S1359431116319573 (cit. on p. 103).

[129] C. A. Idicheria and L. M. Pickett. "Ignition, soot formation, and end-of-combustion transients in diesel combustion under high-EGR conditions". *International Journal of Engine Research* 12(4) (2011), pp. 376–392. DOI: 10.1177/1468087411399505 (cit. on pp. 107, 108).

[130] T. Donateo and M. Giovinazzi. "Some Repeatability and Reproducibility Issues in Real Driving Emission Tests" (2018). ISSN: 0148-7191. DOI: https://doi.org/10.4271/2018-01-5020. URL: https://doi.org/10.4271/2018-01-5020 (cit. on p. 112).

[131] K. R. Vos, G. M. Shaver, M. C. Joshi, and J. James McCarthy. "Implementing variable valve actuation on a diesel engine at high-speed idle operation for improved aftertreatment warm-up". *International Journal of Engine Research* 21(7) (2020), pp. 1134–1146. DOI: 10.1177/1468087419880639. eprint: https://doi.org/10.1177/1468087419880639. URL: https://doi.org/10.1177/1468087419880639 (cit. on p. 118).

Chapter 6

Global Conclusions

Contents

6.1 Introduction

In this last chapter, the achievements and milestones obtained from the entire document are listed. The most important findings and contributions of the studies are listed in Section 6.2. In section 6.3, the main limitations found during the study are enumerated. Finally, section 6.4 exposes possible future prospects and research to continue and complete the RDE cycle study.

6.2 Summary of findings and contributions

6.2.1 Main original contributions

Carrying out the study of RDE cycles in this thesis involves different tasks to help to understand and analyse them. In order to do that, several experimental tests, data analysis, and computing were performed. The highlighted contributions of this thesis are listed below.

- The feasibility of performing different RDE cycles in an engine test bench has been proved.
- The errors dispersion in parametric measures such as speed, torque, pressure temperatures, etc. that were obtained after replicating the same RDE cycle in an engine test bench are extremely low, which eliminates uncertainties produced on-road and makes the engine test bench as an extraordinary tool for research on combustion engines.
- Regarding pollutant emissions and fuel consumption, especially NO_X and CO_2, errors are also considerably lower, much lower than if these cycles were performed on-road. In the first place, the PEMS have lower accuracy than a stationary system, which leads to more uncertainties. Secondly, there are a significant number of factors like driver behaviour, temperature, and traffic conditions that have a strong influence on the results. THC and CO dispersions between repetitions of the same cycle are more extensive due to the complexity of these substances, which are mainly produced during the warming-up and are significantly affected by the aftertreatment state.

- After performing six RDE cycles with different dynamic solicitations and also different driver behaviour, it can be stated that very different cycles can fulfil perfectly the current regulation, and significant differences between pollutant emissions and fuel consumption can be obtained.
- The RDE cycle, based on the speed sections of the WLTC, involves both cycles presenting very similar dynamic conditions, where high load conditions are achieved, and the engine is tested in a wide area of operation.
- Different driver behaviours can fulfil RDE regulations and produce very differentiated polluting emissions under the same vehicle, same route and the same instantaneous vehicle speed, which leaves a large margin to manufacturers when passing the regulation.
- Comparing emissions obtained from the RDE tests versus steady-state tests proved a good correlation, especially in the case of CO_2 emissions. The errors found in NO_X emissions are due to two different reasons: first, all emissions during the engine warm-up period vary since, the engine stay-state tests were carried out with the engine previously warmed up, and secondly, NO_X emissions have a non-linear behaviour as a function of speed and torque, leading uncertainty during the interpolation. In any case, this tool can significantly help provide a realistic approximation of a previous cycle performed on the engine test bench.
- Improving the WCAC efficiency to reduce the intake air mass flow temperature can lead to an apparent reduction in polluting emissions in RDE cycles, and therefore improving the air quality and reducing the greenhouse effect in real driving conditions.
- RDE regulation leaves a large margin in terms of temperatures for carrying out the tests, and the results under extreme conditions leave clear conclusions. Moderate temperatures around 20°C have the best NO_X emissions values which is explained due to the temperature ranges of the tests used in previous regulations, where manufacturers have worked harder to improve the calibration of their engines.
  CO_2 emissions show the best result in tests at the lowest temperature, around -5°C, because at very low temperatures, the engine modifies its strategy and reduces the EGR rates, improving the engine performance.
  THC and CO emissions show similar behaviours, the lowest emissions are produced in tests at higher temperatures due to better and more complete combustions and higher aftertreatment efficiency.

6.2.2 Other findings

In addition to the main contributions, after the studies performed in this thesis, other conclusions have been obtained and are listed below.

- After analysing the WLTC, a RDE cycle was created throughout different phases of this cycle, which means that the dynamic solicitations of the WLTC are in the same order as the RDE cycles, which speaks well of this cycle and how representative could it be of real driving conditions.
- The RDE regulation has tried to unify and clarify the RDE cycles through several modifications during the last years.
  The parameter known as NTE tried to facilitate the adaptation of manufacturers to the new RDE cycles, which differed significantly from the previous NEDC. Another important action was removing the power binning intervals methodology, which appeared in the regulation 2016/427 [36] that later was removed in the following regulations to establish the MAW as the only validation method of RDE cycles. Later parameters like RF and the value of 1.6 in case of performing the RDE in extended conditions try to unify the polluting emissions of different routes typologies, driver behaviours or ambient conditions.

6.3 Limitations

The listed objectives in Chapter 1 have been wholly accomplished. However, some limitations were faced during the realisation of the different experimental studies found in this document.

- One of the greatest limitations was due to the complete and complex experimental validation that was carried out. This validation, despite the fact that the RDE cycles have their essence on road, was carried out in a test bench for the automotive industry. But it would have been very positive to have a full-time vehicle and to have able to carry out specific routes with different instructions for vehicle speed, temperature, driver behaviour, etc. But even if a real vehicle had been available, it would have been very complex or even impossible to obtain different real ambient and adequate traffic conditions to be able to confirm what was

previously calculated with the steady-state maps, or what was obtained from the tests. In any case, this limitation reinforces the theme of the thesis and justifies it, insofar as doing this is impossible, making it the ideal choice reproducing it in an engine test bench.

- Another limitation was found during the design of RDE cycles, it would be interesting the provision data of other different RDE cycles performed on road, and avoinding carrying out cycles that were generated by software, imitating these conditions.
- Finally, the European regulation has also presented impediments since, during the development of the study, this has changed, modifying what is considered a valid RDE cycle, and therefore the tests had to be adapted.

6.4 Suggestions for future studies

The different studies carried out in this thesis open different avenues of research since, a methodology for the RDE cycle assessment was stipulated. Below a short list of suggestions for future studies is listed.

- One of the most significant studies that can be carried out in the future is the application of the interpolation tool in the other way. After generating a RDE cycle with the MATLAB tool, using the interpolation tool and through the torque and engine speed can be possible to obtain the fuel consumption and pollutant emissions without performing the RDE cycle in the engine test bench.
- Following with the study of the previous item, it should be needed to validate it. In order to do that, it is necessary to perform the cycle in the test bench to make later a comparison between the results obtained from the steady state map and the measured ones and analyse the divergence.
- Another interesting study consists of performing these RDE cycles in a chassis dynamometer with the same vehicles simulated in the engine test bench.
- Finally, continuing with the previous study, to complete the analysis would be interesting to perform the RDE cycles designed on road, as far as possible, taking into account different extern factors such as traffic,

ambient temperatures and pressure, etc. so perhaps, it should be done in a closed circuit, in order to try to replicate the cycle with greater similarity.

- Besides the changes in ambient temperature, another future study would involve changing the ambient pressure and/or air humidity since, it can significantly affect the engine behaviour and, therefore, the fuel consumption and pollutant emissions. So characterising real driving cycles under different ambient pressure, which mean different altitudes above the sea level, would provide wide data about how the vehicles behave under these conditions.

- Following the previous study, it would be of great interest to analyse how affects the results the accumulated altitude as well as the number of passengers or weight carried by the vehicle.

- Finally, the developed methodology for studying and analysing RDE cycles can be used in diverse powertrain typologies as well as hybrid and electric vehicles, or new solutions such as hydrogen engines, fuel cell vehicles, synthetics fuels and biofuels, etc.

Chapter 6 Bibliography

[36] *COMMISSION REGULATION (EU) 2016/427 of 10 March 2016 amending Regulation (EC) No 692/2008 as regards emissions from light passenger and commercial vehicles (Euro 6)*. 2016. URL: https://eur-lex.europa.eu/legal-content/EN/TXT/PDF/?uri=CELEX:32016R0427 (cit. on pp. 7, 20, 50, 134).

Global bibliography

[1] J. M. Luján, V. Bermudez, B. Pla, and F. Redondo. "Engine test bench feasibility for the study and research of real driving cycles: Pollutant emissions uncertainty characterization". *International Journal of Engine Research* 0(0) (2021), p. 0. DOI: 10.1177/14680874211007999 (cit. on pp. xi, 56, 112).

[2] J. M. Luján, H. Climent, S. Ruiz, and F. Redondo. "Analysis of pollutant emissions and fuel consumption, during real driving cycles in different intake temperature scenarios". *Proceedings of the Institution of Mechanical Engineers, Part D: Journal of Automobile Engineering* 0(0) (2022), p. 0. DOI: 10.1177/09544070221078402 (cit. on p. xi).

[3] J. M. Luján, P. Piqueras, J. de la Morena, and F. Redondo. "Experimental Characterization of Real Driving Cycles in a Light-Duty Diesel Engine under Different Dynamic Conditions". *Applied Sciences* 12(5) (2022). DOI: 10.3390/app12052472 (cit. on p. xi).

[4] *World population prospects*. Vol. volume II. demographic profiles, 2019 (cit. on p. 2).

[5] *World Bank Group*. 2020 (cit. on p. 2).

[6] *Global EV Outlook 2019*. 2019 (cit. on p. 2).

[7] R. D. Reitz et al. "IJER editorial: The future of the internal combustion engine". *International Journal of Engine Research* 21(1) (2020), pp. 3–10. DOI: 10.1177/1468087419877990 (cit. on p. 2).

[8] EEA. *Air quality in Europe—2019 report*. 2019 (cit. on pp. 2, 6).

[9] A. Ortiz and C. Guerreiro. *Air Quality in Europe - 2020 report*. Nov. 2020. DOI: 10.2800/786656 (cit. on p. 2).

[10] *National emissions reported to the Convention on Long-range Transboundary Air Pollution (LRTAP Convention)*. 2020 (cit. on p. 3).

[11] N. Hooftman, M. Messagie, J. Van Mierlo, and T. Coosemans. "A review of the European passenger car regulations – Real driving emissions vs local air quality". *Renewable and Sustainable Energy Reviews* 86 (2018), pp. 1–21. ISSN: 1364-0321. DOI: https://doi.org/10.1016/j.rser.2018.01.012. URL: https://www.sciencedirect.com/science/article/pii/S1364032118300182 (cit. on p. 4).

[12] G. P. Chossière, R. Malina, F. Allroggen, S. D. Eastham, R. L. Speth, and S. R. Barrett. "Country- and manufacturer-level attribution of air quality impacts due to excess NOx emissions from diesel passenger vehicles in Europe". *Atmospheric Environment* 189 (2018), pp. 89–97. ISSN: 1352-2310. DOI: https://doi.org/10.1016/j.atmosenv.2018.06.047. URL: https://www.sciencedirect.com/science/article/pii/S1352231018304382 (cit. on p. 4).

[13] L. Hao, Z. Zhao, H. Yin, J. Wang, L. Li, W. Lu, Y. Ge, and Åke Sjödin. "Study of durability of diesel vehicle emissions performance based on real driving emission measurement". *Chemosphere* 297 (2022), p. 134171. ISSN: 0045-6535. DOI: https://doi.org/10.1016/j.chemosphere.2022.134171. URL: https://www.sciencedirect.com/science/article/pii/S0045653522006646 (cit. on p. 4).

[14] M. Lapuerta, Ángel Ramos, D. Fernández-Rodríguez, and I. González-García. "High-pressure versus low-pressure exhaust gas recirculation in a Euro 6 diesel engine with lean-NOx trap: Effectiveness to reduce NOx emissions". *International Journal of Engine Research* 20(1) (2019), pp. 155–163. DOI: 10.1177/1468087418817447. eprint: https://doi.org/10.1177/1468087418817447. URL: https://doi.org/10.1177/1468087418817447 (cit. on p. 4).

[15] A. van Niekerk, B. Drew, N. Larsen, and P. Kay. "Impact of low NOx strategies on holistic emission reduction from a CI engine over transient conditions". *International Journal of Engine Research* 22(11) (2021), pp. 3286–3299. DOI: 10.1177/1468087420973887. eprint: https://doi.org/10.1177/1468087420973887. URL: https://doi.org/10.1177/1468087420973887 (cit. on p. 4).

[16] *Provisional Report. World Meteorological Organization (WMO)*. 2020 (cit. on p. 4).

[17] *Center for Climate and Energy Solutions. Outcomes of the UN climate change conference in Paris. In: 21st session of the conference of the parties to the United Nations framework convention on climate change (COP 21).* 2015 (cit. on p. 4).

[18] P. D. A. M. and P. J.S. "The Development of Motor Vehicle Exhaust Emission Standards in California.Carbon footprint: current methods of estimation." *Environ Monit Assess* 178 (2011), pp. 135–160. DOI: https://doi.org/10.1007/s10661-010-1678-y (cit. on p. 4).

[19] *Energy Technology Perspectives 2014.* 2014. URL: https://www.iea.org/reports/energy-technology-perspectives-2014 (cit. on p. 4).

[20] *Global EV Outlook 2019.* Paris, 2019. URL: https://www.iea.org/reports/global-ev-outlook-2019 (cit. on p. 4).

[21] *Regulation (EC) No 443/2009 of the European Parliament and of the Council of 23 April 2009 setting emission performance standards for new passenger cars as part of the Community's integrated approach to reduce CO 2 emissions from light-duty vehicles.* 2009. URL: http://data.europa.eu/eli/reg/2009/443/oj (cit. on p. 4).

[22] *Regulation (EU) 2019/631 of the European Parliament and of the Council of 17 April 2019 setting CO2 emission performance standards for new passenger cars and for new light commercial vehicles, and repealing Regulations (EC) No 443/2009 and (EU) No 510/2011.* 2019. URL: http://data.europa.eu/eli/reg/2019/631/oj (cit. on p. 4).

[23] *Health effects of particulate matter.* 2013 (cit. on p. 5).

[24] J. A. Maga and G. C. Hass. "The Development of Motor Vehicle Exhaust Emission Standards in California". *Journal of the Air Pollution Control Association* 10(5) (1960), pp. 393–414. DOI: 10.1080/00022470.1960.10467949 (cit. on p. 5).

[25] *Council Directive 91/441/EEC of 26 June 1991 amending Directive 70/220/EEC on the approximation of the laws of the Member States relating to measures to be taken against air pollution by emissions from motor vehicles.* 1991 (cit. on p. 5).

[26] *Directive 98/69/EC of the European Parliament and of the Council of 13 October 1998 relating to measures to be taken against air pollution by emissions from motor vehicles and amending Council Directive 70/220/EEC.* 1998 (cit. on p. 5).

[27] G. Fontaras and P. Dilara. "The evolution of European passenger car characteristics 2000–2010 and its effects on real-world CO2 emissions and CO2 reduction policy". *Energy Policy* 49 (2012). Special Section: Fuel Poverty Comes of Age: Commemorating 21 Years of Research and Policy, pp. 719–730. ISSN: 0301-4215. DOI: https://doi.org/10.1016/j.enpol.2012.07.021 (cit. on p. 5).

[28] M. Weiss, P. Bonnel, R. Hummel, U. Manfredi, R. Colombo, G. Lanappe, P. Lelijour, and M. Sculati. "Analyzing on-road emissions of light-duty vehicles with Portable Emissions Measurement Systems (PEMS)". *JRC Scientific and Technical Reports* (2011) (cit. on p. 6).

[29] L. Pelkmans and P. Debal. "Comparison of on-road emissions with emissions measured on chassis dynamometer test cycles". *Transportation Research Part D: Transport and Environment* 11(4) (2006), pp. 233–241. ISSN: 1361-9209. DOI: https://doi.org/10.1016/j.trd.2006.04.001 (cit. on p. 6).

[30] R. Suarez Bertoa, M. Astorga-Llorens, V. Franco, Z. Kregar, V. Valverde Morales, M. Clairotte, J. Pavlovic, and B. Giechaskiel. "On-road vehicle emissions beyond RDE conditions, EUR 29905 EN". *Publications Office of the European Union* (2011). DOI: 10.2760/214318 (cit. on p. 6).

[31] V. Franco, F. P. Sánchez, J. German, and P. Mock. "Real-world exhaust emissions from modern diesel cars". *communications* 49(30) (2014), pp. 847129–102 (cit. on p. 6).

[32] U. Tietge, P. Mock, N. Zacharof, and V. Franco. "Real-world fuel consumption of popular European passenger car models". *The international council of clean transportation (ICCT)* (2015) (cit. on p. 6).

[33] *Diesel gate: Who? What? How?* September, 2016. URL: //www.transportenvironment.org/sites/te/files/2016_09_Dieselgate_report_who_what_how_FINAL_0.pdf (cit. on p. 6).

[34] F. Baumgärtner and P. Letmathe. "External costs of the Dieselgate – Peccadillo or substantial consequences?" *Transportation Research Part D: Transport and Environment* 87 (2020), p. 102501. ISSN: 1361-9209. DOI: https://doi.org/10.1016/j.trd.2020.102501. URL: https://www.sciencedirect.com/science/article/pii/S136192092030688X (cit. on p. 6).

[35] *REPORT on the inquiry into emission measurements in the automotive sector(2016/2215(INI)) Committee of Inquiry into Emission Measurements in the Automotive Sector*. A8-0049/2017, 2017 (cit. on p. 7).

[36] *COMMISSION REGULATION (EU) 2016/427 of 10 March 2016 amending Regulation (EC) No 692/2008 as regards emissions from light passenger and commercial vehicles (Euro 6)*. 2016. URL: https://eur-lex.europa.eu/legal-content/EN/TXT/PDF/?uri=CELEX:32016R0427 (cit. on pp. 7, 20, 50, 134).

[37] N. Ligterink, P. van Mensch, and R. Cuelenaere. "NEDC - WLTP comparative testing" (Oct. 2016). DOI: 10.13140/RG.2.2.19039.66723 (cit. on p. 7).

[38] P Bielaczyc, A Szczotka, and J Woodburn. "Carbon dioxide emissions and fuel consumption from passenger cars tested over the NEDC and WLTC – an overview and experimental results from market-representative vehicles". *IOP Conference Series: Earth and Environmental Science* 214 (2019), p. 012136. DOI: 10.1088/1755-1315/214/1/012136. URL: https://doi.org/10.1088/1755-1315/214/1/012136 (cit. on p. 7).

[39] M. Tutuianu, P. Bonnel, B. Ciuffo, T. Haniu, N. Ichikawa, A. Marotta, J. Pavlovic, and H. Steven. "Development of the World-wide harmonized Light duty Test Cycle (WLTC) and a possible pathway for its introduction in the European legislation". *Transportation Research Part D: Transport and Environment* 40 (2015), pp. 61–75. ISSN: 1361-9209. DOI: https://doi.org/10.1016/j.trd.2015.07.011. URL: https://www.sciencedirect.com/science/article/pii/S1361920915001030 (cit. on p. 7).

[40] H. Lee and K. Lee. "Comparative Evaluation of the Effect of Vehicle Parameters on Fuel Consumption under NEDC and WLTP". *Energies* 13(16) (2020). ISSN: 1996-1073. DOI: 10.3390/en13164245. URL: https://www.mdpi.com/1996-1073/13/16/4245 (cit. on p. 7).

[41] A. Ramos, J. Muñoz, F. Andrés, and O. Armas. "NOx emissions from diesel light duty vehicle tested under NEDC and real-word driving conditions". *Transportation Research Part D: Transport and Environment* 63 (2018), pp. 37–48. ISSN: 1361-9209. DOI: https://doi.org/10.1016/j.trd.2018.04.018. URL: https://www.sciencedirect.com/science/article/pii/S1361920918301767 (cit. on p. 7).

[42] J. Pielecha, A. Merkisz-Guranowska, and I. Jacyna-Gołda. "A New Ecological Research – Real Driving Emissions". *Journal of Kones* 21 (May 2014), pp. 259–265. DOI: 10.5604/12314005.1133902 (cit. on p. 7).

[43] P. Bielaczyc, J. Woodburn, J. Merkisz, and J. Pielecha. "Analysis of Emission Factors in RDE Tests As Well as in NEDC and WLTC Chassis Dynamometer Tests" (2016). ISSN: 0148-7191. DOI: https://doi.org/10.4271/2016-01-0980. URL: https://doi.org/10.4271/2016-01-0980 (cit. on p. 7).

[44] (Cit. on p. 7).

[45] A Clenci, V Sălan, R Niculescu, V Iorga-Simăn, and C Zaharia. "Assessment of real driving emissions via portable emission measurement system". *IOP Conference Series: Materials Science and Engineering* 252 (2017), p. 012084. DOI: 10.1088/1757-899x/252/1/012084. URL: https://doi.org/10.1088/1757-899x/252/1/012084 (cit. on p. 7).

[46] G. Vagnoni, M. Eisenbarth, J. Andert, G. Sammito, J. Schaub, M. Reke, and M. Kiausch. "Smart rule-based diesel engine control strategies by means of predictive driving information". *International Journal of Engine Research* 20(10) (2019), pp. 1047–1058. DOI: 10.1177/1468087419835696 (cit. on p. 8).

[47] J. Manuel Lujan, B. Pla, P. Bares, and V. Pandey. "Adaptive calibration of Diesel engine injection for minimising fuel consumption with constrained NO x emissions in actual driving missions". *International Journal of Engine Research* (2020), p. 1468087420918800 (cit. on p. 8).

[48] J. Krammer and A. Nahtigal. "Model Based Assessment of Real-Driving Emissions - A Variation Study on Design and Operation Parameter" (2019). ISSN: 0148-7191. DOI: https://doi.org/10.4271/2019-26-0241. URL: https://doi.org/10.4271/2019-26-0241 (cit. on p. 8).

[49] J. Andert, F. Xia, S. Klein, D. Guse, R. Savelsberg, R. Tharmakulasingam, M. Thewes, and J. Scharf. "Road-to-rig-to-desktop: Virtual development using real-time engine modelling and powertrain co-simulation". *International Journal of Engine Research* 20(7) (2019), pp. 686–695. DOI: 10.1177/1468087418767221 (cit. on p. 8).

[50] F. Payri, J. Martín, F. J. Arnau, and S. Artham. "Analysis of temperature and altitude effects on the Global Energy Balance during WLTC". *International Journal of Engine Research* 0(0) (2021), p. 14680874211034292. DOI: 10.1177/14680874211034292. eprint: https://doi.org/10.1177/14680874211034292. URL: https://doi.org/10.1177/14680874211034292 (cit. on p. 8).

[51] T. Bodisco and A. Zare. "Practicalities and driving dynamics of a real driving emissions (RDE) Euro 6 regulation homologation test". *Energies* 12(12) (2019), p. 2306 (cit. on pp. 8, 53, 56).

[52] J. Czerwinski, P. Comte, Y. Zimmerli, and F. Reutimann. "Testing emissions of passenger cars in laboratory and on-road (PEMS, RDE)". *Combustion Engines* 55 (2016) (cit. on pp. 8, 53).

[53] G. Triantafyllopoulos, D. Katsaounis, D. Karamitros, L. Ntziachristos, and Z. Samaras. "Experimental assessment of the potential to decrease diesel NOx emissions beyond minimum requirements for Euro 6 Real Drive Emissions (RDE) compliance". *Science of the Total Environment* 618 (2018), pp. 1400–1407 (cit. on pp. 8, 53).

[54] R. Varella, B. Giechaskiel, L. Sousa, and G. Duarte. "Comparison of portable emissions measurement systems (PEMS) with laboratory grade equipment". *Applied Sciences* 8(9) (2018), p. 1633 (cit. on pp. 8, 56).

[55] J. Claßen et al. "Statistically supported real driving emission calibration: Using cycle generation to provide vehicle-specific and statistically representative test scenarios for Euro 7". *International Journal of Engine Research* 21(10) (2020), pp. 1783–1799. DOI: 10.1177/1468087420935221. URL: https://doi.org/10.1177/1468087420935221 (cit. on p. 8).

[56] J. Claßen, S. Pischinger, S. Krysmon, S. Sterlepper, F. Dorscheidt, M. Doucet, C. Reuber, M. Görgen, J. Scharf, M. Nijs, et al. "Statistically supported real driving emission calibration: Using cycle generation to provide vehicle-specific and statistically representative test scenarios for Euro 7". *International Journal of Engine Research* 21(10) (2020), pp. 1783–1799 (cit. on p. 8).

[57] P. Roberts, A. Mason, A. Headley, L. Bates, S. Whelan, and K. Tabata. "RDE Plus - A Road to Rig Development Methodology for Whole Vehicle RDE Compliance: Road to Engine Perspective" (2021). ISSN:

0148-7191. DOI: https://doi.org/10.4271/2021-01-1223. URL: https://doi.org/10.4271/2021-01-1223 (cit. on p. 8).

[58] J. M. Luján, H. Climent, S. Ruiz, and A. Moratal. "Influence of ambient temperature on diesel engine raw pollutants and fuel consumption in different driving cycles". *International Journal of Engine Research* 20(8-9) (2019), pp. 877–888 (cit. on p. 9).

[59] R. Suarez-Bertoa, V. Valverde, M. Clairotte, J. Pavlovic, B. Giechaskiel, V. Franco, Z. Kregar, and C. Astorga. "On-road emissions of passenger cars beyond the boundary conditions of the real-driving emissions test". *Environmental Research* 176 (2019), p. 108572. ISSN: 0013-9351. DOI: https://doi.org/10.1016/j.envres.2019.108572. URL: https://www.sciencedirect.com/science/article/pii/S001393511930369X (cit. on p. 20).

[60] Z. A and B. P. "Real Driving Emissions Regulation". (KJ-NA-30123-EN-N (online),KJ-NA-30123-EN-E) (2020). ISSN: 1831-9424 (online),1831-9424. DOI: 10.2760/176284(online),10.2760/531926 (cit. on p. 20).

[61] E. Commission, J. R. Centre, V Franco, J Pavlovic, R Suarez-Bertoa, C Astorga, M Clairotte, B Giechaskiel, V Valverde, and Z Kregar. *On-road vehicle emissions beyond RDE conditions : experimental assessment addressing EU Real-Driving Emission (RDE)*. Publications Office, 2019. DOI: doi/10.2760/683267 (cit. on p. 20).

[62] M. Weiss, P. Bonnel, J. Kühlwein, A. Provenza, U. Lambrecht, S. Alessandrini, M. Carriero, R. Colombo, F. Forni, G. Lanappe, et al. "Will Euro 6 reduce the NOx emissions of new diesel cars?–Insights from on-road tests with Portable Emissions Measurement Systems (PEMS)". *Atmospheric Environment* 62 (2012), pp. 657–665 (cit. on p. 20).

[63] *COMMISSION REGULATION (EU) 2017/1151 of 1 June 2017 supplementing Regulation (EC) No 715/2007 of the European Parliament and of the Council on type-approval of motor vehicles with respect to emissions from light passenger and commercial vehicles (Euro 5 and Euro 6) and on access to vehicle repair and maintenance information, amending Directive 2007/46/EC of the European Parliament and of the Council, Commission Regulation (EC) No 692/2008 and Commission Regulation (EU) No 1230/2012 and repealing Commission Regulation (EC) No 692/2008*. 2017. URL: https://eur-lex.europa.eu/legal-content/EN/TXT/?uri=celex\%3A32017R1151 (cit. on p. 20).

[64] *COMMISSION REGULATION (EU) 2018/1832 of 5 November 2018 amending Directive 2007/46/EC of the European Parliament and of the Council, Commission Regulation (EC) No 692/2008 and Commission Regulation (EU) 2017/1151 for the purpose of improving the emission type approval tests and procedures for light passenger and commercial vehicles, including those for in-service conformity and real-driving emissions and introducing devices for monitoring the consumption of fuel and electric energy.* 2018. URL: https://eur-lex.europa.eu/legal-content/EN/TXT/HTML/?uri=CELEX:32018R1832\&from=EN (cit. on pp. 20, 24, 40, 56, 99).

[65] M. V. Prati, G. Meccariello, L. Della Ragione, and M. A. Costagliola. *Real driving emissions of a light-duty vehicle in Naples. Influence of road grade.* Tech. rep. SAE Technical Paper, 2015 (cit. on p. 20).

[66] J. M. Luján, V. Bermúdez, V. Dolz, and J. Monsalve-Serrano. "An assessment of the real-world driving gaseous emissions from a Euro 6 light-duty diesel vehicle using a portable emissions measurement system (PEMS)". *Atmospheric Environment* 174 (2018), pp. 112–121 (cit. on pp. 20, 35, 58).

[67] R. A. Varella, J. P. Ribau, P. C. Baptista, L. Sousa, and G. O. Duarte. "Novel approach for connecting real driving emissions to the European vehicle laboratorial certification test procedure". *Environmental Science and Pollution Research* 26(34) (2019), pp. 35163–35182 (cit. on p. 20).

[68] B. Du, L. Zhang, Y. Geng, Y. Zhang, H. Xu, and G. Xiang. "Testing and evaluation of cold-start emissions in a real driving emissions test". *Transportation Research Part D: Transport and Environment* 86 (2020), p. 102447. ISSN: 1361-9209. DOI: https://doi.org/10.1016/j.trd.2020.102447. URL: https://www.sciencedirect.com/science/article/pii/S1361920920306349 (cit. on p. 20).

[69] L. Chen, B. Du, L. Zhang, J. Han, B. Chen, X. Zhang, Y. Li, and J. Zhang. "Analysis of real-driving emissions from light-duty gasoline vehicles: A comparison of different evaluation methods with considering cold-start emissions". *Atmospheric Pollution Research* 12(5) (2021), p. 101065. ISSN: 1309-1042. DOI: https://doi.org/10.1016/j.apr.2021.101065. URL: https://www.sciencedirect.com/science/article/pii/S1309104221001318 (cit. on p. 20).

[70] J. Claßen et al. "Statistically supported real driving emission calibration: Using cycle generation to provide vehicle-specific and statistically representative test scenarios for Euro 7". *International Journal of Engine Research* 21(10) (2020), pp. 1783–1799. DOI: 10.1177/1468087420935221 (cit. on p. 32).

[71] J. M. Luján, H. Climent, S. Ruiz, and A. Moratal. "Influence of ambient temperature on diesel engine raw pollutants and fuel consumption in different driving cycles". *International Journal of Engine Research* 20(8-9) (2019), pp. 877–888. DOI: 10.1177/1468087418792353 (cit. on p. 32).

[72] D. Campos Navarro. *Estudio de las emisiones de escape en motores de combustión interna alternativos utilizando diferentes sistemas de control de contaminantes*. Universidad Politecnica de Valencia. Departamento de Máquinas y Mo-tores Térmicos, 2016 (cit. on p. 38).

[73] B. N. Taylor and C. E. Kuyatt. "Guidelines for evaluating and expressing the uncertainty of NIST measurement results" (1994) (cit. on p. 46).

[74] B. E. Flores. "A pragmatic view of accuracy measurement in forecasting". *Omega* 14(2) (1986), pp. 93–98. URL: https://ideas.repec.org/a/eee/jomega/v14y1986i2p93-98.html (cit. on pp. 47, 83).

[75] J Merkisz and J Pielecha. "Comparison of Real Driving Emissions tests". *IOP Conference Series: Materials Science and Engineering* 421 (2018), p. 042055. DOI: 10.1088/1757-899x/421/4/042055. URL: https://doi.org/10.1088/1757-899x/421/4/042055 (cit. on p. 56).

[76] M. Andrych-Zalewska, Z. Chlopek, J. Merkisz, and J. Pielecha. "Investigations of Exhaust Emissions from a Combustion Engine under Simulated Actual Operating Conditions in Real Driving Emissions Test". *Energies* 14(4) (2021). ISSN: 1996-1073. DOI: 10.3390/en14040935. URL: https://www.mdpi.com/1996-1073/14/4/935 (cit. on p. 56).

[77] K. Kurtyka and J. Pielecha. "The evaluation of exhaust emission in RDE tests including dynamic driving conditions". *Transportation Research Procedia* 40 (2019). TRANSCOM 2019 13th International Scientific Conference on Sustainable, Modern and Safe Transport, pp. 338–345. ISSN: 2352-1465. DOI: https://doi.org/10.1016/j.trpro.2019.07.050. URL: https://www.sciencedirect.com/science/article/pii/S2352146519302121 (cit. on p. 56).

[78] J. M. Luján, C. Guardiola, B. Pla, and V. Pandey. "Impact of driving dynamics in RDE test on NOx emissions dispersion". *Proceedings of the Institution of Mechanical Engineers, Part D: Journal of Automobile Engineering* 234(6) (2020), pp. 1770–1778. DOI: 10.1177/0954407019881581. eprint: https://doi.org/10.1177/0954407019881581. URL: https://doi.org/10.1177/0954407019881581 (cit. on p. 56).

[79] T. Donateo, M. Giovinazzi, and A. Tamborrino. "Reproducing Real World Emission Tests with a Traffic Simulator" (2018). ISSN: 0148-7191. DOI: https://doi.org/10.4271/2018-37-0001. URL: https://doi.org/10.4271/2018-37-0001 (cit. on p. 56).

[80] M. Lyu, X. Bao, Y. Wang, and R. Matthews. "Analysis of emissions from various driving cycles based on real driving measurements obtained in a high-altitude city". *Proceedings of the Institution of Mechanical Engineers, Part D: Journal of Automobile Engineering* 234(6) (2020), pp. 1563–1571. DOI: 10.1177/0954407019898959. eprint: https://doi.org/10.1177/0954407019898959. URL: https://doi.org/10.1177/0954407019898959 (cit. on p. 56).

[81] J. Czerwinski, Y. Zimmerli, A. Hüssy, D. Engelmann, P. Bonsack, E. Remmele, and G. Huber. "Testing and evaluating real driving emissions with PEMS". *Combustion Engines* 174(3) (2018), pp. 17–25. ISSN: 2300-9896. DOI: 10.19206/CE-2018-302. URL: https://doi.org/10.19206/CE-2018-302 (cit. on p. 56).

[82] J. Gallus, U. Kirchner, R. Vogt, and T. Benter. "Impact of driving style and road grade on gaseous exhaust emissions of passenger vehicles measured by a Portable Emission Measurement System (PEMS)". *Transportation Research Part D: Transport and Environment* 52 (2017), pp. 215–226. ISSN: 1361-9209. DOI: https://doi.org/10.1016/j.trd.2017.03.011. URL: https://www.sciencedirect.com/science/article/pii/S1361920916306769 (cit. on p. 56).

[83] L. Zhang, X. Hu, R. Qiu, and J. Lin. "Comparison of real-world emissions of LDGVs of different vehicle emission standards on both mountainous and level roads in China". *Transportation Research Part D: Transport and Environment* 69 (Apr. 2019), pp. 24–39. DOI: 10.1016/j.trd.2019.01.020 (cit. on p. 56).

[84] M. Faria, G. Duarte, R. Aliandro Varella, T. Farias, and P. Baptista. "How do road grade, road type and driving aggressiveness impact vehicle fuel consumption? Assessing potential fuel savings in Lisbon, Portu-

gal". *Transportation Research Part D Transport and Environment* 72 (July 2019), pp. 148–161. DOI: 10.1016/j.trd.2019.04.016 (cit. on p. 56).

[85] G. Triantafyllopoulos, D. Katsaounis, D. Karamitros, L. Ntziachristos, and Z. Samaras. "Experimental assessment of the potential to decrease diesel NOx emissions beyond minimum requirements for Euro 6 Real Drive Emissions (RDE) compliance". *The Science of the total environment* 618 (Oct. 2017). DOI: 10.1016/j.scitotenv.2017.09.274 (cit. on p. 56).

[86] M. Andrych-Zalewska, Z. Chlopek, J. Merkisz, and J. Pielecha. "Research on Exhaust Emissions in Dynamic Operating States of a Combustion Engine in a Real Driving Emissions Test". *Energies* 14(18) (2021). ISSN: 1996-1073. DOI: 10.3390/en14185684. URL: https://www.mdpi.com/1996-1073/14/18/5684 (cit. on p. 56).

[87] A. T. Zachiotis and E. G. Giakoumis. "Non-regulatory parameters effect on consumption and emissions from a diesel-powered van over the WLTC". *Transportation Research Part D: Transport and Environment* 74 (2019), pp. 104–123. ISSN: 1361-9209. DOI: https://doi.org/10.1016/j.trd.2019.07.019. URL: https://www.sciencedirect.com/science/article/pii/S1361920919302731 (cit. on p. 56).

[88] Y. Zhiwen, Y. Liu, L. Wu, S. Martinet, Y. Zhang, M. Andre, and H. Mao. "Real-world gaseous emission characteristics of Euro 6b light-duty gasoline- and diesel-fueled vehicles". *Transportation Research Part D: Transport and Environment* 78 (Jan. 2020), p. 102215. DOI: 10.1016/j.trd.2019.102215 (cit. on p. 56).

[89] A. Taborda, R. Varella, T. Farias, and G. Duarte. "Evaluation of technological solutions for compliance of environmental legislation in light-duty passenger: A numerical and experimental approach". *Transportation Research Part D: Transport and Environment* 70 (2019), pp. 135–146. ISSN: 1361-9209. DOI: https://doi.org/10.1016/j.trd.2019.04.004. URL: https://www.sciencedirect.com/science/article/pii/S136192091830720X (cit. on p. 56).

[90] A. Broatch, X. Margot, A. Gil, E. Galindo, and R. Soler. "Definition of wind blowers for vehicles testing at chassis-dyno facilities using a CFD approach". *Transportation Research Part D: Transport and Environment* 55 (2017), pp. 99–112. ISSN: 1361-9209. DOI: https://doi.org/

10.1016/j.trd.2017.06.029. URL: https://www.sciencedirect.com/science/article/pii/S1361920917300068 (cit. on p. 56).

[91] J. Rodríguez-Fernández, J. J. Hernández, Ángel Ramos, and A. Calle-Asensio. "Fuel economy, NOx emissions and lean NOx trap efficiency: Lessons from current driving cycles". *International Journal of Engine Research* (2021). DOI: https://doi.org/10.1177/14680874211005080 (cit. on pp. 56, 99).

[92] J. Claßen, S. Krysmon, F. Dorscheidt, S. Sterlepper, and S. Pischinger. "Real Driving Emission Calibration—Review of Current Validation Methods against the Background of Future Emission Legislation". *Applied Sciences* 11(12) (2021). ISSN: 2076-3417. DOI: 10.3390/app11125429. URL: https://www.mdpi.com/2076-3417/11/12/5429 (cit. on p. 56).

[93] B. Giechaskiel et al. "Inter-Laboratory Correlation Exercise with Portable Emissions Measurement Systems (PEMS) on Chassis Dynamometers". *Applied Sciences* 8(11) (2018). ISSN: 2076-3417. DOI: 10.3390/app8112275. URL: https://www.mdpi.com/2076-3417/8/11/2275 (cit. on p. 56).

[94] R. Suarez-Bertoa, M. Pechout, M. Vojtíšek, and C. Astorga. "Regulated and Non-Regulated Emissions from Euro 6 Diesel, Gasoline and CNG Vehicles under Real-World Driving Conditions". *Atmosphere* 11(2) (2020). ISSN: 2073-4433. DOI: 10.3390/atmos11020204. URL: https://www.mdpi.com/2073-4433/11/2/204 (cit. on p. 56).

[95] J. Czerwiński, P. Comte, Y. Zimmerli, and F. Reutimann. "Testing emissions of passenger cars in laboratory and on-road (PEMS, RDE)". *Combustion Engines* 166(3) (2016), pp. 17–23. ISSN: 2300-9896. DOI: 10.19206/CE-2016-326. URL: https://doi.org/10.19206/CE-2016-326 (cit. on p. 56).

[96] K. Tucki. "A Computer Tool for Modelling CO2 Emissions in Driving Tests for Vehicles with Diesel Engines". *Energies* 14(2) (2021). ISSN: 1996-1073. DOI: 10.3390/en14020266. URL: https://www.mdpi.com/1996-1073/14/2/266 (cit. on p. 57).

[97] L. Thibault, P. Degeilh, O. Lepreux, L. Voise, G. Alix, and G. Corde. "A new GPS-based method to estimate real driving emissions" (2016), pp. 1628–1633. DOI: 10.1109/ITSC.2016.7795776 (cit. on p. 57).

[98] P. Fernandes, E. Macedo, B. Bahmankhah, R. Tomas, J. Bandeira, and M. Coelho. "Are internally observable vehicle data good predictors of vehicle emissions?" *Transportation Research Part D: Transport and Environment* 77 (2019), pp. 252–270. ISSN: 1361-9209. DOI: https://doi.org/10.1016/j.trd.2019.11.004. URL: https://www.sciencedirect.com/science/article/pii/S1361920919308557 (cit. on p. 57).

[99] C. Guardiola, B. Pla, P. Bares, E. Chappell, and R. Burke. "Improving CO2 emission assessment of diesel-based powertrains in dynamic driving cycles by data fusion techniques". *Proceedings of the Institution of Mechanical Engineers, Part D: Journal of Automobile Engineering* 235(2-3) (2021), pp. 362–372. DOI: 10.1177/0954407020949477. eprint: https://doi.org/10.1177/0954407020949477. URL: https://doi.org/10.1177/0954407020949477 (cit. on p. 57).

[100] T. Donateo and M. Giovinazzi. "Building a cycle for Real Driving Emissions". *Energy Procedia* 126 (2017). ATI 2017 - 72nd Conference of the Italian Thermal Machines Engineering Association, pp. 891–898. ISSN: 1876-6102. DOI: https://doi.org/10.1016/j.egypro.2017.08.307. URL: https://www.sciencedirect.com/science/article/pii/S1876610217338213 (cit. on p. 58).

[101] H. S. Chong, Y. Park, S. Kwon, and Y. Hong. "Analysis of real driving gaseous emissions from light-duty diesel vehicles". *Transportation Research Part D: Transport and Environment* 65 (2018), pp. 485–499. ISSN: 1361-9209. DOI: https://doi.org/10.1016/j.trd.2018.09.015. URL: https://www.sciencedirect.com/science/article/pii/S1361920918304395 (cit. on p. 65).

[102] K. T., H. Y., N. K., and T. Toda. ""High Efficiency Diesel Engine with Low Heat Loss Combustion Concept - Toyota's Inline 4-Cylinder 2.8-Liter ESTEC 1GD-FTV Engine". *SAE Technical Paper 2016-01-0658* (2016). DOI: https://doi.org/10.4271/2016-01-0658 (cit. on p. 66).

[103] Y. B. Zeldóvich. *The oxidation of nitrogen in combustión and explosion.* Ed. by A. Physicochim. 1946 (cit. on p. 98).

[104] G. P. Merker, B. Hohlbaum, and M. Rauscher. *Two-Zone Model for Calculation of Nitrogen-Oxide Formation in Direct-Injection Diesel Engines.* SAE International, 1993. DOI: https://doi.org/10.4271/932454 (cit. on p. 98).

[105] C. P. Fenimore. *Formation of nitric oxide in premixed hydrocarbon flames*. 1971 (cit. on p. 98).

[106] S. R. Turns et al. *Introduction to combustion*. Vol. 287. McGraw-Hill Companies, 1996 (cit. on p. 98).

[107] J. B. Heywood. *Internal combustion engine fundamentals*. McGraw-Hill Education, 2018 (cit. on p. 98).

[108] E. E. Agency., ed. *Air quality guidelines. Global update 2005. Particulate matter, ozone, nitrogen dioxide and sulfuric dioxide*. 2005. ISBN: 92 890 2192 6 (cit. on p. 98).

[109] M. Lippmann. "Health Effects of Ozone a Critical Review". *JAPCA* 39 (June 1989), pp. 672–95. DOI: 10.1080/08940630.1989.10466554 (cit. on p. 98).

[110] L. Cox. *Nitrogen oxides (NOx) why and how they are controlled*. U.S. Environmental Protection Agency, Office of Air Quality Planning, Standards, Information Transfer, and Program Integration Division, Clean Air Technology Center, 1999. ISBN: 9781428902800. URL: https://books.google.es/books?id=kSJY-EVi1KEC (cit. on p. 98).

[111] J. M. Desantes, J. J. López, P. Redón, and J. Arrégle. "Evaluation of the Thermal NO formation mechanism under low-temperature diesel combustion conditions". *International Journal of Engine Research* 13(6) (2012), pp. 531–539. DOI: 10.1177/1468087411429638. eprint: https://doi.org/10.1177/1468087411429638. URL: https://doi.org/10.1177/1468087411429638 (cit. on p. 98).

[112] R. A. Varella, G. Duarte, P. Baptista, P. Mendoza Villafuerte, and L. Sousa. "Analysis of the Influence of Outdoor Temperature in Vehicle Cold-Start Operation Following EU Real Driving Emission Test Procedure". *SAE International Journal of Commercial Vehicles* 10(2) (2017), pp. 596–697. ISSN: 1946-391X. DOI: https://doi.org/10.4271/2017-24-0140. URL: https://doi.org/10.4271/2017-24-0140 (cit. on p. 99).

[113] D. Engelmann, Y. Zimmerli, J. Czerwinski, and P. Bonsack. "Real Driving Emissions in Extended Driving Conditions". *Energies* 14(21) (2021). ISSN: 1996-1073. DOI: 10.3390/en14217310. URL: https://www.mdpi.com/1996-1073/14/21/7310 (cit. on p. 99).

[114] V. Bermúdez, J. R. Serrano, P. Piqueras, and B. Diesel. "Fuel consumption and aftertreatment thermal management synergy in compression ignition engines at variable altitude and ambient temperature". *International Journal of Engine Research* 0(0) (0), p. 14680874211035015. DOI: 10.1177/14680874211035015. eprint: https://doi.org/10.1177/14680874211035015. URL: https://doi.org/10.1177/14680874211035015 (cit. on p. 99).

[115] S. Funk. "Real World NOx Sensor Accuracy Assessment and Implications for REAL NOx Tracking". In: *SAE WCX Digital Summit*. SAE International, 2021. DOI: https://doi.org/10.4271/2021-01-0593. URL: https://doi.org/10.4271/2021-01-0593 (cit. on p. 99).

[116] Y. Wang, Y. Ge, J. Wang, X. Wang, H. Yin, L. Hao, and J. Tan. "Impact of altitude on the real driving emission (RDE) results calculated in accordance to moving averaging window (MAW) method". *Fuel* 277 (2020), p. 117929. ISSN: 0016-2361. DOI: https://doi.org/10.1016/j.fuel.2020.117929. URL: https://www.sciencedirect.com/science/article/pii/S001623612030925X (cit. on p. 99).

[117] H. Wang et al. "The real driving emission characteristics of light-duty diesel vehicle at various altitudes". *Atmospheric Environment* 191 (2018), pp. 126–131. ISSN: 1352-2310. DOI: https://doi.org/10.1016/j.atmosenv.2018.07.060. URL: https://www.sciencedirect.com/science/article/pii/S1352231018305132 (cit. on p. 99).

[118] J. Serrano, P. Piqueras, E. Sanchis, and B. Diesel. "A modelling tool for engine and exhaust aftertreatment performance analysis in altitude operation". *Results in Engineering* 4 (2019), p. 100054. ISSN: 2590-1230. DOI: https://doi.org/10.1016/j.rineng.2019.100054. URL: https://www.sciencedirect.com/science/article/pii/S2590123019300544 (cit. on p. 99).

[119] P. Bielaczyc, J. Woodburn, J. Merkisz, and J. Pielecha. "RDE Testing of Passenger Cars: The Effect of the Cold Start on the Emissions Results" (2019). ISSN: 0148-7191. DOI: https://doi.org/10.4271/2019-01-0747. URL: https://doi.org/10.4271/2019-01-0747 (cit. on p. 99).

[120] B. Du, L. Zhang, Y. Geng, Y. Zhang, H. Xu, and G. Xiang. "Testing and evaluation of cold-start emissions in a real driving emissions test". *Transportation Research Part D: Transport and Environment* 86 (2020), p. 102447. ISSN: 1361-9209. DOI: https://doi.org/10.

1016/j.trd.2020.102447. URL: https://www.sciencedirect.com/science/article/pii/S1361920920306349 (cit. on p. 99).

[121] D. Engelmann, Y. Zimmerli, J. Czerwinski, and P. Bonsack. "Real Driving Emissions in Extended Driving Conditions". *Energies* 14(21) (2021). ISSN: 1996-1073. DOI: 10.3390/en14217310. URL: https://www.mdpi.com/1996-1073/14/21/7310 (cit. on p. 99).

[122] B. Giechaskiel, D. Komnos, and G. Fontaras. "Impacts of Extreme Ambient Temperatures and Road Gradient on Energy Consumption and CO2 Emissions of a Euro 6d-Temp Gasoline Vehicle". *Energies* 14(19) (2021). ISSN: 1996-1073. DOI: 10.3390/en14196195. URL: https://www.mdpi.com/1996-1073/14/19/6195 (cit. on p. 99).

[123] R. García-Contreras, A. Gómez, P. Fernández-Yáñez, and O. Armas. "Estimation of thermal loads in a climatic chamber for vehicle testing". *Transportation Research Part D: Transport and Environment* 65 (2018), pp. 761–771. ISSN: 1361-9209. DOI: https://doi.org/10.1016/j.trd.2017.11.010. URL: https://www.sciencedirect.com/science/article/pii/S136192091730771X (cit. on p. 99).

[124] J. Ko, D. Jin, W. Jang, C.-L. Myung, S. Kwon, and S. Park. "Comparative investigation of NOx emission characteristics from a Euro 6-compliant diesel passenger car over the NEDC and WLTC at various ambient temperatures". *Applied Energy* 187 (2017), pp. 652–662. ISSN: 0306-2619. DOI: https://doi.org/10.1016/j.apenergy.2016.11.105. URL: https://www.sciencedirect.com/science/article/pii/S0306261916317366 (cit. on p. 99).

[125] A Calle-Asensio, J. Hernández, J Rodríguez-Fernández, M Lapuerta, A Ramos, and J Barba. "Effect of advanced biofuels on WLTC emissions of a Euro 6 diesel vehicle with SCR under different climatic conditions". *International Journal of Engine Research* 22(12) (2021), pp. 3433–3446. DOI: 10.1177/14680874211001256. eprint: https://doi.org/10.1177/14680874211001256. URL: https://doi.org/10.1177/14680874211001256 (cit. on p. 99).

[126] X. Wang et al. "Proceedings of Real Driving Emission (RDE) Measurement in China" (2018). ISSN: 0148-7191. DOI: https://doi.org/10.4271/2018-01-0653. URL: https://doi.org/10.4271/2018-01-0653 (cit. on p. 99).

[127] L. Ciferri. "SUVs, crossovers continue to grow market share in Europe, ANE's segment-by-segment analysis shows." *Automotive News Europe.* (2020). DOI: https://europe.autonews.com/sales-segment/suvs-crossovers-continue-grow-market-share-europe-anes-segment-segment-analysis-shows (cit. on p. 100).

[128] J. M. Luján, H. Climent, L. M. García-Cuevas, and A. Moratal. "Volumetric efficiency modelling of internal combustion engines based on a novel adaptive learning algorithm of artificial neural networks". *Applied Thermal Engineering* 123 (2017), pp. 625–634. ISSN: 1359-4311. DOI: https://doi.org/10.1016/j.applthermaleng.2017.05.087. URL: https://www.sciencedirect.com/science/article/pii/S1359431116319573 (cit. on p. 103).

[129] C. A. Idicheria and L. M. Pickett. "Ignition, soot formation, and end-of-combustion transients in diesel combustion under high-EGR conditions". *International Journal of Engine Research* 12(4) (2011), pp. 376–392. DOI: 10.1177/1468087411399505 (cit. on pp. 107, 108).

[130] T. Donateo and M. Giovinazzi. "Some Repeatability and Reproducibility Issues in Real Driving Emission Tests" (2018). ISSN: 0148-7191. DOI: https://doi.org/10.4271/2018-01-5020. URL: https://doi.org/10.4271/2018-01-5020 (cit. on p. 112).

[131] K. R. Vos, G. M. Shaver, M. C. Joshi, and J. James McCarthy. "Implementing variable valve actuation on a diesel engine at high-speed idle operation for improved aftertreatment warm-up". *International Journal of Engine Research* 21(7) (2020), pp. 1134–1146. DOI: 10.1177/1468087419880639. eprint: https://doi.org/10.1177/1468087419880639. URL: https://doi.org/10.1177/1468087419880639 (cit. on p. 118).

"Never too high, never too low"

Ricky Rubio.